12-2014

HYPOXIA MEDIATED DOWNREGULATION OF MIRNA BIOGENESIS LEADS TO INCREASED TUMOR PROGRESSION

rajesha rupaimoole

HYPOXIA MEDIATED DOWNREGULATION OF MIRNA BIOGENESIS LEADS TO INCREASED TUMOR PROGRESSION

By

Rajesha Rupaimoole, M.S.

APPROVED:

_____
Anil K. Sood, M.D.
Advisory Professor

_____
Gary E. Gallick, Ph.D.

_____
Menashe Bar-Eli, Ph.D.

_____
George A. Calin, M.D., Ph.D.

_____
Eric J. Wagner, Ph.D.

APPROVED:

_____
Dean, The University of Texas
Graduate School of Biomedical Sciences at Houston

HYPOXIA MEDIATED DOWNREGULATION OF MIRNA BIOGENESIS LEADS TO INCREASED TUMOR PROGRESSION

A

DISSERTATION

Presented to the Faculty of

The University of Texas

Health Science Center at Houston

and

The University of Texas

MD Anderson Cancer Center

Graduate School of Biomedical Sciences

in Partial Fulfillment

of the Requirements

for the Degree of

DOCTOR OF PHILOSOPHY

By

Rajesha Rupaimoole, M.S.

Houston, Texas

December, 2014

Dedication

To my parents and sister for all the love and support they have provided

To my first research Guru Dr. Sathyanarayana Dixit for holding my hand and guiding me, while I took baby steps in research

Acknowledgements

It would not have been possible for me to come to this stage of my life without the love, help, and support of the kind people to whom I will be always grateful. I truly appreciate their support, however I am able to mention only a few due to space constraints.

I would like to thank my advisor, Dr. Anil Sood, who has been tremendously supportive, always encouraging throughout my graduate education. I have been fortunate to be a part of his team and I sincerely thank him for all his support and guidance.

I really appreciate and thank my committee members, Dr. Garry E. Gallick, Dr. George A Calin, Dr. Menashe Bar-Eli, and Dr. Eric J. Wagner for all their guidance, help and suggestions during my last five years.

I would like to thank Dr. Mircea Ivan, Dr. Milan Radovich, Dr. Wei Zhang, Dr. Cristina Ivan for help with deep sequencing services, microarray services, and help with bioinformatics analysis.

I would like to thank my current and past lab mates who have always been there to cheer me up when I was upset over experiments not working as expected or even share happiness when the experiments were successful, and all the countless fun moments. I need to mention here a few names of the people who were more than just lab mates; rather they were second family to me in America. First, I would like to thank Dr. Chad Pecot for being a good friend to share all the gossip, conspiracy

theories, and teaching me initial exercises in gym. Dr. Sherry Wu, I am not sure how much energy you have packed-in, always running, helping me with questions, and saying ‘cheers’ for pretty much everything with an Australian accent and I will remember and thank you through my life for all the help you have provided me. Dr. Morgan Taylor is always energetic and throughout the years he has become more than a friend to me. We have discussed endless issues, science and non-science related. Thank you Morgan for what you have added in my journey of learning. I would like to thank Dr. Heather Dalton, Dr. Guillermo Aramiz-Penza for being one of my close friends in lab and for always being there to listen to my stories. One person I am especially thankful to is my “labmom”, Dr. Mangala Selanere. I would like to thank her for keeping my stomach always happy by providing me with her delicious food during lunch, sharing laughs, and being supportive. Three graduate students in lab, Archana, Kshipra and Noura, you three have become more than friends over the years to me. I have always shared, cherished all the happiness and sad moments. You guys were always there for me to listen to my stories of excitement, laughing together. I thank you all from the bottom of my heart for being part of this amazing team last few years. I also thank all other lab members whose names I have not mentioned but have helped me in every way possible. I also like to thank co-graduate student in the lab, Michael McGuire for his friendship and support.

I would like to thank my parents who have always supported me, gave me their hands when I needed them in all these years of studies and my life. I would like to thank my sister Anupama, for being my best friend, with whom I can share all the fun and sad stories. In the early years of my studies, two people have been instrumental

in making my journey possible. They are my uncles Krishna Varanasi and Ishwara Varanasi. With all the love and support they have given me, I have achieved what I am today and I truly thank you. I thank Dr. Nitasha Bhat GM, who even though has entered in my life very recently; has provided support and encouragement with her ever positive outlook in life.

I would like to thank my roommate, friend, and co-graduate student Avinashnarayan for all his support, continued friendship, sharing all the happy, sad, and frustrating moments of graduate student life. I acknowledge the support of my friends Anantha, Vikas, and Bharath, and I thank you for being who you are in my life. Especially, I thank Anantha for her best food delicacies and for sharing them with me and Avinash. Vikas and Bharath have been part of my research journey from undergraduate days and I truly thank you both for all your support.

Hypoxia Mediated Downregulation of miRNA Biogenesis Leads to Increased Tumor Progression

Rajesha Rupaimoole, M.S.

Advisory Professor: Anil K. Sood, M.D.

In recent years, there has been a growing recognition of the importance of tumor associated microenvironment in the initiation and progression of tumors. However, a mechanistic understanding of the complicated biological interplay between the stromal framework and malignant regions of the tumor remains incompletely understood. In this study, we address mechanisms by which hypoxia in the tumor microenvironment leads to attenuation of miRNA biogenesis by downregulation of two key enzymes, Drosha and Dicer in cancer cells. Previous data from our laboratory had shown the clinical relevance of downregulated Dicer and Drosha in ovarian and other cancer types, but a clear mechanistic understanding is needed for future clinical intervention strategies to curb deleterious effect of miRNA biogenesis downregulation. Using several *in vitro* techniques, orthotopic *in vivo* models and clinical patient samples, we demonstrate novel deregulatory mechanisms involved in Dicer and Drosha downregulation under hypoxia. Data from deep sequencing of normoxia and hypoxia treated cells demonstrate clear effect of this downregulation on miRNA maturation. Collectively, we show substantial functional effects of this downregulation on cancer progression under *in vivo* conditions by use of siRNAs incorporated in liposomes mediated gene silencing. Our work will provide the missing links for this mechanistic understanding, with a goal of novel interventions to

rescue the Dicer and Drosha-miRNA biogenesis pathway. The findings described in this thesis have significant clinical implications with respect to understanding mechanisms of tumor growth and metastasis and the design of new therapeutic approaches in cancers.

Table of Contents

List of Figures

List of Tables

Chapter 1: Introduction

1.1: MicroRNAs - small noncoding RNA biogenesis and physiological functions

MicroRNAs (miRNA) are evolutionarily conserved small RNA molecules that are involved in gene regulation by targeting mRNA to suppress gene expression [1-3]. Currently over 1000 miRNAs have been identified and are involved in key cellular functions by regulating several important gene expression *via* controlling their translation [1]. These small RNA molecules are a key component of noncoding RNAs (ncRNA) and are involved in multiple cellular functions. Since the discovery of these short RNA molecules in *C. elegans*, their multi-faceted roles have been recognized to control cellular functions by repressing target genes [3-8].

Mature miRNA biogenesis starts at RNA polymerase II processing of long primary transcripts (>100nts), termed precursor miRNAs [9]. This transcript gets further processed *via* Drosha along with its binding partners such as DGCR8, leading to pri-miRNAs. Upon translocation of this pri-miRNA into the cytoplasm *via* exportin 5, it binds to Dicer and RNA-induced silencing complex (RISC), which includes argonaute proteins. After binding with the RISC complex, the guide strand helps to navigate the complex to the target mRNA and consequently results in downregulation of target genes [9] (Figure 1).

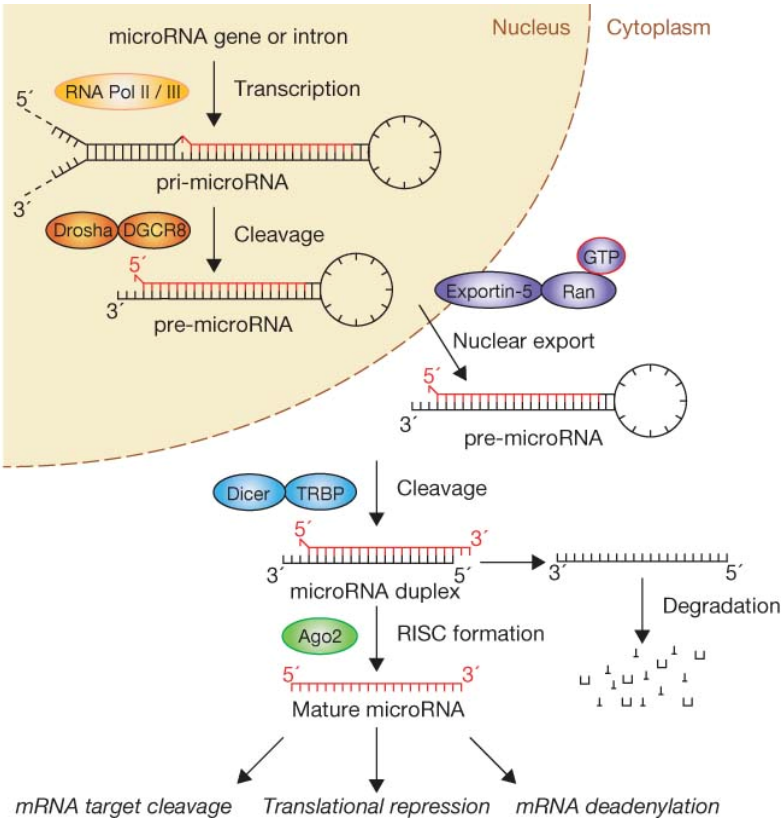

Figure 1: MicroRNA biogenesis, a multistep tightly controlled process. Canonical pathway of biogenesis starts at pri-miRNA produced by RNA polymerase II or III. Next, pri-miRNA is cleaved by Drosha-DGCR8 complex to yield pre-miRNAS, which gets exported into cytoplasm by XPO5-GTP nuclear export system. In cytoplasm, Dicer in conjugation with TRBP cleaves pre-miRNAs to mature duplex miRNAs. Later, Ago2 and RISC come together to select functional strand and silence target mRNAs through mRNA cleavage, translational repression or deadenylation.

(Figure is taken with permission from Winter, S.C., F.M. Buffa, P. Silva, C. Miller, H.R. Valentine, H. Turley, K.A. Shah, G.J. Cox, R.J. Corbridge, J.J. Homer, B. Musgrove, N. Slevin, P. Sloan, P. Price, C.M. West, and A.L. Harris, Relation of a hypoxia metagene derived from head and neck cancer to prognosis of multiple cancers. Cancer Res, 2007. 67(7): p. 3441-9.)

Drosha: DGCR8 microprocessor complex*:* RNA polymerase II or III processed miRNA genes into primary miRNA transcripts (pri-miRNA) in the nucleus [10]. Nuclear processor complex is composed of RNase III enzyme Drosha and binding partner DGCR8 cleaves the pri-miRNA by endonuclease type digestion. This cleavage happens *via* two double-stranded RNA-binding domains present in DGCR8. Human pri-miRNA contains a hairpin stem of 33 base-pairs, a terminal loop and two single-stranded flanking regions on both sides of hairpin towards 3' and 5' prime [1, 11]. Reports have suggested the importance of double-stranded stem and the unpaired flanking regions for cleavage by Drosha and DGCR8 complex. Drosha plays a central role in processing of pri-miRNA at 5' and 3' arms of hairpin. DGCR8 is typically referred as a molecular ruler, which determines precise position at which Drosha cleaves the RNA [12]. The cleavage happens at 11 base pair away from single and double stranded RNA junction at the base of hairpin. Timing of this processing happens co-transcriptionally and precedes splicing events of coding or noncoding RNA that hosts the miRNA in some cases. Upon processing by Drosha/DGCR8 complex, pri-miRNAs are called precursor miRNAs and exported into cytoplasm by Exportin-5 (XPO5) in complex with Ran-GTP [13]. It is recognized that apart from the role as a transporter of pre-miRNA, XPO5 protects pre-miRNAs from nuclease digestion. Recognition of pre-miRNA by XPO5 is sequence independent and predominately by defined length of the double-stranded stem and the 3' overhangs.

RNAi Induced Silencing Complex (RISC) – Dicer and Ago2 - Final players in miRNA function: RISC consists of RNase enzyme Dicer, the double-stranded RNA-

binding domain proteins TRBP and PACT, and the core component Argonaute-2 mediate the miRNA effects on mRNA targets [14-16]. Dicer is the core component of RISC and is involved in cleavage of pre-miRNA to result in mature miRNAs. TRBP and PACT are two proteins which facilitate Dicer mediated cleavage stem loop of pre-miRNA. Also, they are involved in the recruitment of Ago2 to the complex to facilitate the processing of mature miRNA [17]. In some cases with high complementarity along the hairpin loop, an additional Ago2 mediated cleavage of 3' arm of hairpin produces Ago2-cleaved precursor miRNA [17-19]. Dicer is an RNase III type enzyme and cleaves the pre-miRNA at the hairpin loop to generate a 22-nucleotide miRNA duplex. The DExD/H-box helicase domain present in Dicer protein inhibits this cleavage activity. Binding of TRBP to Dicer, helps to facilitate the release of this inhibitory domain via conformational changes. The PAZ (PIWI–AGO–ZWILLE) domain present in Dicer protein is responsible for binding of Dicer to pre-miRNA and, the region between PAZ and RNase III domains functions as a 'molecular ruler' [20, 21]. Upon binding, Dicer cleaves pre-miRNA at 22 nt away from the 5' end following 5' counting rule [15]. Following unwinding and dissociation of Dicer-TRBP complex from miRNA duplex, RISC complex undergoes next step of miRNA function, i.e., duplex unwinding. Several helicases such as p68, p72, RNA helicase A (RHA), RCK/p54, TNRC6B, Gemin3/4 and human Mov10 or its *D. melanogaster* orthologue Armitage have been identified with this function [22]. Some reports have also shown the role of Ago2 in unwinding duplex in the absence of helicases suggesting a dual role of Ago2. Following unwinding, the miRNA strand with thermodynamically less stable base pair at 5' end is loaded into RISC.

Two mechanisms on how miRNAs downregulate gene expression has been identified: (1) mRNA cleavage and (2) translational repression. If mRNA-miRNA binding site has perfect complementarity, mRNA will be cleaved, otherwise miRNA represses translation [1, 23]. In the case of miRNA mediated mRNA cleavage, the site is in between the nucleotides pairing 10 to 11 of miRNA. It is also shown that miRNA gets recycled and can act on other mRNA following base complementarity rules. Regarding the translational repression, process is aided by RISC and miRNA/mRNA binding via cooperative action of multiple miRNA binding sites in the same mRNA.

Physiological functions of miRNAs: Early discoveries of miRNA functions were carried out in classical model organisms such as *C. elegans*. Two key discovered miRNAs in *C. elegans* were lin-4 and let-7 [24, 25]. Both miRs are involved in developmental stages. Loss of lin4 results in significant defects in normal development and early embryonic cells have defective cell division processes [4, 26]. Studies suggest Let7 is well conserved across species and has several developmental roles as well roles in disease physiologies, such as cancer [25]. Loss of Dicer functional studies show that Dicer is essential for normal embryonic development and Dicer-/- animals are embryonically lethal. In a Zebrafish model, loss of Dicer during development results in growth arrest and failure in development of organs [27]. Interestingly, restoration of one miRNA such as miR-430 could reverse this defective brain development in the Dicer-/- Zebrafish model [28]. In Dicer-/- mice, embryos die at embryonic day 8.5 with significant defects in stem cells [27].

One of the well-studied miRNAs, miR-181, has been shown to be important for development of B-lymphocytes [29]. This miRNA has been shown to regulate muscle differentiation by downregulation of HOXA11, which suggests strong roles of miRNAs in developmental physiology [30]. Another important miRNA involved in development of normal tissues is miR-1, which has been shown to play a role in muscle development [31]. Loss of miR-1 during development results in impaired muscle growth and differentiation defects. These effects of miR-1 were reported to be mediated *via* targeting of HDAC4 [32]. In summary, these miRNAs are great examples of the role of ncRNAs in normal physiology of cells and perturbation of their signaling could have profound significant effects on cells, resulting in initiation or progression of different types of diseases.

1.2: MicroRNA dysregulation in cancer

MiRNA biogenesis downregulation and clinical relevance: Downregulation of Drosha, Dicer, Ago2 in cancers: Over 6 years ago, downregulation of Drosha and Dicer, two key enzymes involved in miRNA biogenesis, was reported in many cancers including ovarian, lung and breast cancers [33, 34]. Such changes are functionally relevant since cells with deficient biogenesis have defects in miRNA processing [34]. Since then, several others have shown the importance of Drosha and Dicer in an array of cancer types [35-39]. Possible mechanisms for Drosha downregulation include transcriptional downregulation *via* c-myc [35] or ADARB1 [36] proteins. For Dicer, direct binding of *Tap63* transcription factor to Dicer promoter has been shown and downregulated Dicer due to loss of Tap63 in cancer has been observed [40]. Another study highlighted the mutant p53 dependency on p63

independent Dicer downregulation [41], suggesting layers of complexity in Dicer downregulation in cancer. Another layer of complexity in Dicer downregulation is *via* miRNAs targeting Dicer 3' UTR. Two independent studies shown different miRNAs targeting Dicer, namely miR-103/107 [42] and let-7 [43]. Apart from Drosha and Dicer, other enzymes in the miRNA biogenesis pathway such as TARBP2, AGO2 have also been reported to be downregulated in cancer. In sporadic and hereditary carcinomas, mutations leading to truncated form of TARBP2 protein can lead to impaired Dicer function [44]. Also, downregulation in TARBP2 protein expression in cancer stem cells was shown to be important for cancer pre-metastasis signaling [45]. EGFR dependent Ago2 phosphorylation results in hampering of Ago2 binding to Dicer, resulting in decreased miRNA biogenesis [46]. Even though the downregulation of these key enzymes involved in biogenesis is important for cancer progression, additional alterations in miRNA not related to biogenesis enzymes have been reported. DNA damage induces ATM kinase, which leads to increased processing of selective set of miRNAs [47]. Likewise, Hippo protein sequesters DDX17 and leads to decreased miRNA production [48]. Genetic defect in exportin-5 results in hampering of precursor miRNAs exporting to cytoplasm for processing by Dicer [49]

Key miRNAs deregulated in cancer and implications: One of the main miRNAs downregulated in cancer is the miR-200 family, which is involved in many diverse functions such as induction of EMT *via* downregulation e-cadherin, leading to increased ZEB proteins [50-52]. MiR-200 targets ETS1, and as result of loss of miR-200 repression of ETS1 under hypoxia exposure, cancer cells induce angiogenic

responses [53]. We have demonstrated that miR-200 influences angiogenesis directly via downregulation of CXCL1 and IL8, two major cytokines in tumor microenvironment [54]. The Let-7 family members were shown to regulate cancer stem cells by targeting H-RAS and HMGA2 [55, 56]. Additional roles of Let-7 relate to regulation of several cell cycle regulators and proliferation [57]. Using *in-silico* and tumor samples' analyses, master regulatory network of miRNAs involved in mesenchymal phenotype of cancer cells have been reported [58]. Some of the key miRNAs identified were miR-506, miR-200, and miR-25 [58]. MiR-10b is another important miRNA induced by Twsit1 protein, which targets homeobox D10, leading to increased RHOC protein and has been suggested to have a role in initiation of metastasis [59].

1.3: Hypoxia as a tumor microenvironment factor: significantly influences tumor biology

During cancer growth, tumors develop significant hypoxia and have been attributed to tumor promoting effects and resistance to therapy [60, 61]. Direct assessment of tumor hypoxia in clinical patient samples has shown worse patient outcome in the cohort of patients whose tumors are highly hypoxic [62]. Cancer cells evolve to grow under hypoxia conditions by modifying their key cellular metabolisms and gene alterations [60, 61]. During tumor growth and metastasis, cancer cells encounter significant amount of hypoxia due to improperly developed and tortuous blood vessels [62, 63].

Role of hypoxia on miRNAs: In human endothelial cells, Dicer dependent miR-185 was decreased under chronic hypoxia, and resulted in HIF2-α increase [64]. Interestingly, suppression of angiogenesis under complete loss of Dicer has been reported [65]. In tumor from Dicer-/- mice, significant increase in hypoxia due to reduced angiogenesis resulting from de-repression of HIF1 inhibiting factor called FIH1 was observed [65]. Anti-VEGF therapies have also been shown to induce hypoxia and cancers have aggressive tumor recurrence and increased invasiveness but the mechanisms are not clear. An, important protein in the miRNA biogenesis pathway is Ago2, which is part of RNA induced silencing complex (RISC) complex. In cancer cells, under hypoxia exposure, EGFR phosphorylates Ago2 at Tyr 393 results in decreased Ago2 function [46]. Ago2 phosphorylation results in decreased Dicer-Ago2 interaction, leading to decreased miRNA maturation and function [46]. However another study reported that Ago2 protein was increased due to posttranslational changes in hydroxylation under hypoxia exposure [66], suggesting multifaceted role of hypoxia in Ago2 regulation. In summary, the studies suggest a complexity in the miRNA biogenesis regulations and necessitates detailed investigations into tumor microenvrionmental influences on this important cellular machinery.

Hypothesis and specific aims of the study: Hypoxia, a master tumor microenvironment factor influencing tumor progression via altering miRNA biogenesis

Aim 1: To understand the mechanisms of hypoxia induced down regulation of Dicer and Drosha.

Hypothesis: Hypoxia induces down regulation of Dicer1 and Drosha, resulting in global deregulation of miRNA biogenesis.

Rationale: Dicer1 and Drosha – two key components of miRNA processing machinery have been reported to be deregulated in cancer [34, 40]. Preliminary experiments based on mouse models show that Dicer1 and Drosha mRNA expression in tumors is heterogeneous and dynamic. These data suggest the greater influence of microenvironment factors in causing these effects. Our preliminary data show strong down regulation of Dicer1 and Drosha following exposure to hypoxia. Additional mechanistic experiments related to the deregulation of miRNA biogenesis will be carried out in this aim.

Aim 2: To determine the biological significance of the miRNA processing machinery deregulation in tumor progression and metastasis.

Hypothesis: Hypoxia induced deregulation of miRNA biogenesis results in driving EMT, resulting in aggressive tumor growth and progression.

Rationale: Epithelial to mesenchymal transition has a significant contribution to the development of metastasis and aggressive cancer subtype [67, 68]. Our observations suggest that cells under hypoxia resemble fibroblast like structures, indicating EMT-like changes. In addition, molecular data show changes in the expression of gene signatures associated with EMT, suggesting strong induction of EMT upon exposure to hypoxia or treatment of cell lines with siRNA against Dicer or Drosha alone or in combination. However, the biological significance of miRNA deregulation under hypoxia is not known and will be pursued in this aim.

In this thesis study, we shed light on the understanding of tumor microenvironment factor, hypoxia influences on miRNA biogenesis and tumor growth. We show that hypoxia strongly inhibits miRNA biogenesis by downregulating two key enzymes in biogenesis, Dicer and Drosha, through two independent yet converging mechanisms in cancer cells. Drosha is downregulated by transcriptional repression mediated by ETS1/ELK1 through recruitment of methylation and histone de-acetylation related molecules onto promoter region. Dicer is downregulated by miR-630, which is upregulated in hypoxia. MiR-630 is transcriptionally upregulated under exposure to hypoxia by direct binding of STAT1 onto miR-630 promoter region. Further we show biological effects of miRNA downregulation using *in vitro* and *in vivo* models. Increased tumor invasiveness and growth was observed under downregulated miRNAs and we identified novel key miRNA-mRNA networks facilitating this increase in tumor progression.

Chapter 2: Material and Methods

This chapter is based on Rupaimoole, R., S.Y. Wu, S. Pradeep, C. Ivan, C.V. Pecot, K.M. Gharpure, A.S. Nagaraja, G.N. Armaiz-Pena, M. McGuire, B. Zand, H.J. Dalton, J. Filant, J.B. Miller, C. Lu, N.C. Sadaoui, L.S. Mangala, M. Taylor, T. van den Beucken, E. Koch, C. Rodriguez-Aguayo, L. Huang, M. Bar-Eli, B.G. Wouters, M. Radovich, M. Ivan, G.A. Calin, W. Zhang, G. Lopez-Berestein, and A.K. Sood, Hypoxia-mediated downregulation of miRNA biogenesis promotes tumour progression. Nat Commun, 2014. 5: p. 5202.

Cell line maintenance and siRNA and miRNA transfections

All cell lines were maintained in 5% CO_2 at 37℃. Ovarian cancer (A2780, OVCAR3, SKOV3, OVCA432, HeyA8, IGROV, EG) and breast cancer (MDA-MB-231, MCF7, GILM2) cells were obtained from the American Type Culture Collection and were maintained in RPMI 1640 supplemented with 10-15% fetal bovine serum (FBS) and 0.1% gentamicin sulfate (GeminiBioproducts, Calabasas, CA). All cell lines were routinely tested to confirm the absence of Mycoplasma, and all *in vitro* experiments were conducted with 60-80% confluent cultures.

All siRNA transfections (Table 1) were performed using RNAiMAX (Invitrogen Carlsbad, CA) reagent using forward transfection protocol from the manufacturer. Media was changed 5 hours after transfections to minimize toxicity. For all hypoxia treatments, cells were incubated in an oxygen-controlled hypoxia chamber at 1% O_2.

For ectopic expression of Drosha and Dicer, we obtained plasmids from Addgene (IDs 10828, 25851 respectively). Next, we cloned open reading frames into pLKO.1-GFP or Puromycin lentiviral plasmids. We transduced HeyA8 cells with viral particles and then selection using GFP (Drosha) or puromycin (Dicer) was carried out to establish stable cell variants.

In vivo models

Female athymic nude mice were purchased from Taconic Farms (Hudson, NY). These animals were cared for according to guidelines set forth by the American Association for Accreditation of Laboratory Animal Care and the US Public Health Service policy on Human Care and Use of Laboratory Animals. All mouse studies were approved and supervised by The University of Texas MD Anderson Cancer Center Institutional Animal Care and Use Committee. All animals used were 8-12 weeks old at the time of injection.

Orthotopic models of ovarian cancer were developed as described previously [69, 70]. For all animal experiments, cells were harvested using trypsin-EDTA, neutralized with FBS-containing media, washed, and resuspended to the appropriate cell number in Hanks' balanced salt solution (HBSS; Gibco, Carlsbad, CA) prior to injection. For the A2780 model, cells were injected either intraperitoneally (1×10^6 cells in 200 µL of HBSS) or directly into the ovary (0.8×10^6 cells in a 1:1 mixture of BD Matrigel and HBSS with a total volume of 100 µL of HBSS). For the HeyA8 cells and variants expressing Drosha, Dicer, and Drosha+Dicer (0.8×10^6 cells in a 1:1 mixture of BD Matrigel and HBSS with a total volume of 100 µL of HBSS) intra-ovarian injections were performed. For the breast cancer model, MCF7 cells were

injected into the mammary fat pad (5×10^6 cells in a 1:1 mixture of BD Matrigel and HBSS). For the intra-ovary injections, mice were anesthetized with ketamine and xylazine. An incision just above the approximate site of the right ovary was made to visualize the ovary. A 1-mL tuberculin syringe with a 30-gauge needle was used to inject the cell suspension directly into the ovary. After injection, the incision was closed using surgical clips and the mouse was returned to a cage until fully recovered. For the orthotopic breast cancer model, the MCF7 cell mixture was injected into the second mammary fat pad from the top after the mouse was anesthetized with ketamine and xylazine. One week before the injection of breast cancer cells, a 60-day release pellet containing 0.72 mg of 17β-estradiol (Innovative Research of America, Toledo, OH) was implanted subcutaneously into each mouse.

For all therapeutic experiments, a dose of 200 µg siRNA/kg, 200 µg miRNA/kg was used, as described previously [54, 70, 71]. For all models, unless indicated otherwise, twice weekly treatments were started 1 week after cell injection and continued for approximately 4 weeks. For miRNA or siRNA experiments, mice were randomly divided and treated with siRNA incorporated in neutral DOPC nanoliposomes (intraperitoneal administration). For the anti-VEGF therapy experiment, mice were allowed to develop tumors for 2-3 weeks and then 2 treatments of bevacizumab (6.25 mg/kg) were administered. For the Drosha and Dicer rescue experiment, treatment with bevacizumab was started on day 7 after cell implantation and continued until the end of the experiment. In all experiments, once mice in any group became moribund they were killed and necropsied and tumors were harvested. Tumor weight and number and location of tumor nodules were

recorded. Tumor tissue was either fixed in formalin for paraffin embedding, frozen in optimal cutting temperature (OCT) media to prepare frozen slides, or snap-frozen for lysate preparation.

Liposomal nanoparticle preparation

MiRNA or siRNA for *in vivo* intratumor delivery was incorporated into DOPC, as previously described [71]. DOPC and miRNA or siRNA were mixed in the presence of excess tertiary butanol at a ratio of 1:10 (w/w) miRNA or siRNA:DOPC. Tween 20 was added to the mixture in a ratio of 1:19 Tween 20:miRNA/DOPC. The mixture was vortexed, frozen in an acetone/dry ice bath, and lyophilized. Before *in vivo* administration, this preparation was hydrated with phosphate-buffered saline (PBS) at room temperature at a concentration of 200 µg miRNA or siRNA/kg per injection.

Tumor samples

Tumor samples were obtained as per previously approved protocol [34]. We obtained 75 specimens of invasive epithelial ovarian cancer from The University of Texas MD Anderson Cancer Center Tumor Bank. For use as normal control, 15 benign ovarian epithelial samples were also obtained. Frozen tumor samples (approximately 0.2 mg each) were used for total RNA isolation.

TCGA data and bioinformatics analysis

Bioinformatics analysis was performed in R (version 2.14.2; http://www.r-project.org). Statistical significance was set at $p < 0.05$. We downloaded and analyzed publicly available data from the Cancer Genome Atlas Project (TCGA; http://tcga-data.nci.nih.gov/) for patients with ovarian serous cystadenocarcinoma.

Level 3 Illumina RNASeq and miRNASeq were used to measure mRNA and miRNA expression. miRNASeq data were derived from the "isoform_quantification" files from the "reads per million miRNA mapped" values for mature forms of each microRNA. A list of 99 genes that comprised the hypoxia metagene was obtained from Winter et al [72]. Univariate Cox analysis was performed, and 10 genes with hazard ratio >1.1 (*KCTD11*, *TNS4*, *TUBB2A*, *ANGPTL4*, *TEAD4*, *DPM2*, *PYGL*, *TPI1*, *C16orf74*, and *ADORA2B*) were selected for further study. The median of the distribution was calculated for each patient.

For survival analysis, the patients were grouped into percentiles according to the hypoxia metagene signature described above. We checked for an association between hypoxia signature and overall survival by choosing a cutoff to optimally split the samples into 2 groups, and the log-rank test was employed to determine the significance of the association. To examine the association between Drosha and Dicer levels and overall survival, the patients were grouped into sextiles according to *DICER1* and *DROSHA* expression. We compared all groups and obtained the best separation (minimal log-rank test p value) for the groups linked to a positive association: *DICER1* expression last sextile and *DROSHA* expression last sextile with *DICER1* expression first sextile and *DROSHA* expression first sextile. We also compared miRNA levels between 2 additional groups: good responders and bad responders.

MiRNA microarray and deep sequencing

Total RNA was extracted from the A2780 cells under normoxic or hypoxic conditions using the mirVana RNA Isolation kit (Ambion). RNA purity was assessed

using Nanodrop spectrophotometric measurement (Thermo Scientific, Pittsburgh, PA) of the OD260/280 ratio with acceptable values falling between 1.9 and 2.1, as well as using Agilent Bioanalyser (Agilent Technologies, La Jolla, CA) with a RIN number of at least 8. Five hundred nanograms of total RNA was used for labeling and hybridization, according to the manufacturer's protocols (Agilent Technologies). Expression levels of miRNAs in ovarian cancer cells upon exposure to hypoxia (1% O_2) were profiled using miRNA microarray (Agilent v14). Bioinformatic analysis was performed in R (version 2.14.2). Statistical significance was set at $p < 0.05$. The raw intensity for each probe was the median feature pixel intensity with the median background subtracted, and setting an offset 1 ensured that no negative values would appear after log-transforming the data. Data were quantile-normalized and log2 transformed. A 2-sided *t* test was applied to determine significantly different miRNAs between samples. Heat maps were generated using the heat plot function of the library.

Starting with 3 µg of total RNA for each sample, ribosomal RNA was depleted using Ribominus (Invitrogen/Life Technologies, Inc., Carlsbad, CA), following the manufacturer's recommendations. Sequencing libraries were then prepared and barcoded individually using the SOLiD™ Total RNA-Seq Kit for Whole Transcriptome Libraries (Life Technologies), following the manufacturer's recommendations. Prepared samples were then pooled and sequenced using the Life Technology 5500xl sequencer using 75 base forward read only. Data was extracted from XSQ files containing the read sequences, quality values were loaded

onto a compute cluster, and the reads were mapped in colorspace using the Life Technologies LifeScope 2.5.1 software, using default parameters.

Reads were mapped to the human genome (hg19) downloaded from the UCSC Genome Bioinformatics Site (http://genome.ucsc.edu). The hg19 genome was slightly modified by deleting the Y chromosome to make a female genome. An hg19 exon reference file provided by Life Technologies was required by LifeScope to create the exon junction libraries needed to map reads that cross exon boundaries. This file was derived from the refGene database from UCSC. A human filter reference file was required (provided by Life Technologies) that contains the sequences of ribosomal and repetitive regions of the genome to filter reads that mapped to those regions.

Mapped reads were exported in the standard BAM (Binary Alignment/Map) format. BAM files were imported into Partek Genomics Suite 6.6 (Partek Incorporated, St. Louis, MO) for gene expression analysis. Mapped reads contained in the BAM files were cross-referenced against the RefSeq database (downloaded from UCSC Genome Browser) and a small RNA database (UCSC Genome Browser) to generate RPKM (reads per kilobase of exon per million mapped reads) values for each gene. Low-expressing genes were excluded.

Differential expression using the derived RPKM values was performed using analysis of variance. Genes with a false discovery rate <5% were considered significant. Significantly deregulated miRNAs from miRNA array and mRNA data from deep sequencing were uploaded onto ingenuity pathway network analysis (Ingenuity Systems®, www.ingenuity.com) and a network analysis with miRNA-

mRNA target analysis was carried out to identify potential gene deregulation as a result of miRNA changes under hypoxic conditions.

Target gene binding sites, luciferase reporter assays, and Dicer 3' UTR site mutagenesis

The putative miRNA binding sites on Dicer 3' UTR were predicted bioinformatically using several algorithms for predicting miRNA targets. This was done using the following publically available sites: http://www.microrna.org for the miRanda algorithm, http://www.targetscan.org for the TargetScan algorithm, http://genie.weizmann.ac.il/pubs/mir07 for the PITA algorithm, http://cbcsrv.watson.ibm.com for the RNA22 algorithm, http://diana.cslab.ece.ntua.gr/microT for microT algorithm, and http://genome.ucsc.edu/cgi-bin/hgTables?command=start together with http://pictar.mdc-berlin.de/ for the PicTar algorithm. The predicted miRNAs were further shortlisted by cross-referencing with miRNA data from the miRNA array. GoClone pLightSwitch luciferase reporters for the 3' UTR regions of Dicer were obtained from SwitchGear Genomics (Menlo Park, CA).

A2780 and MCF7 cells were transfected with FuGENE HD TFX reagent in a 96-well plate with scrambled control, miR-630 mimics (100nM; Ambion) along with the 3' UTR reporter gene, and Cypridina TK control construct (pTK-Cluc). After 24 hours of transfection, luciferase activity was obtained with the LightSwitch Dual Luciferase assay kits using a microplate luminometer, per manufacturer guidelines (Biotek, VT). Luciferase activity was normalized using the Cypridina TK control construct, and an empty luciferase reporter vector was used as a negative control.

The ratios obtained were further normalized according to the scrambled control. Mutants of the Dicer 3' UTR were generated using the QuikChange Lightning Multi Site-direct Mutagenesis kit (Agilent Technologies), using the primers to mutate 5 base pairs within the miR-630 binding site (**Table 1**). Mutagenesis was confirmed using Sanger DNA sequencing prior to luciferase assays.

Immunoblotting

Lysates from cultured cells were prepared using modified RIPA buffer (50mM Tris-HCl [pH 7.4], 150mM NaCl, 1% Triton, 0.5% deoxycholate) plus 25 µg/mL leupeptin, 10 µg/mL aprotinin, 2mM EDTA, and 1mM sodium orthovandate. The protein concentrations were determined using a BCA Protein Assay Reagent kit (Pierce Biotechnology, Rockford, IL). Lysates were loaded and separated on sodium dodecyl sulfate–polyacrylamide gels. Proteins were transferred to a nitrocellulose membrane by semidry electrophoresis (Bio-Rad Laboratories, Hercules, CA) overnight, blocked with 5% bovine serum albumin for 1 hour, and then incubated at 4℃ overnight with primary antibody (Dicer, Drosha [Littleton, Colorado], ETS1, ELK1, pELK1, STAT1, and pSTAT1 [Danvers, MA]. After washing with tris-buffered saline with Tween 20, the membranes were incubated with horseradish peroxidase (HRP)–conjugated horse anti-Mouse or Rabbit IgG (1:2000, GE Healthcare, UK) for 2 hours. HRP was visualized using an enhanced chemiluminescence detection kit (Pierce Biotechnology). To confirm equal sample loading, the blots were probed with an antibody specific for β-actin (0.1 µg/mL; Sigma).

Immunoprecipitation using antibodies against ETS1 or ELK1 was carried out using the Universal Magnetic Co-IP Kit (Active Motif, Carlsbad, CA)), according to

instructions provided by the company. Samples were processed for Western blotting as described above. Using the antibody against ARID4B (Novus Biologicals) and HDAC1 (Cell Signaling), pull-down samples were probed for interactions.

Quantitative real-time PCR

For mRNA quantification, total RNA was isolated using the Qiagen RNeasy kit (Qiagen). For miRNA quantification, total RNA was isolated using the Trizol/isopropanol total RNA precipitation method. Using 1000 ng of RNA, cDNA was synthesized using a Verso cDNA kit (Thermo Scientific), as per manufacturer instructions. Analysis of mRNA levels was performed on a 7500 Fast Real-Time PCR System (Applied Biosystems) with SYBR Green-based real-time PCR for all genes except the one specified. Dicer and Drosha Taqman assays (Life Technologies) were performed. Specific primers used are described in extended data Table 1. Semi-quantitative real-time PCR was done with reverse-transcribed RNA and 100 ng/μL sense and antisense primers in a total volume of 20 μL. For miRNA quantification, total RNA was isolated using Trizol (Invitrogen) extraction. TaqMan miRNA assays (Life Technologies) were used for reverse transcription and real-time PCR, according to the manufacturer's instructions. RNU6B was used as a housekeeping gene. RNA was isolated from nuclear and cytoplasmic fractionated cells using Paris kit (Life technologies, CA). Fractionation purity was confirmed by running the samples on agarose gel electrophoresis and visualization of precursor rRNA bands, 18s, and 28s rRNA bands. For pri-miRNA and mature miRNA quantifications, taqMan miRNA assays (Life Technologies, CA) were used and reverse transcription, real-time PCR were carried out, according to the

manufacturer's instructions. Precursor miRNAs were quantified using miRscript precursor miRNA assays (Qiagen, CA). RNU6B (for mature miRNAs) or 18S (pri and precursor miRNAs) were used as a housekeeping gene.

Immunostaining

Staining was performed on OCT-embedded frozen tissue sections. Protein blocking of nonspecific epitopes was performed using 4% fish gelatin in tris-buffered saline with Tween 20 for 20 minutes. Slides were incubated with the primary antibody for Dicer, Drosha (Novus Biologicals), E-cadherin (BD Transduction Laboratories) or vimentin (Cell Signaling) overnight at 4℃. For immunofluorescence, secondary antibody staining was performed using either Alexa 594 or Alexa 488 (Molecular Probes). Nuclear staining was performed using Hoechst 33342 (Molecular Probes). Immunofluorescent images were captured using a Zeiss Axioplan 2 microscope and Hamamatsu ORCA-ER digital camera (Zeiss). Bright field light images of hematoxylin and eosin–stained lung tissue sections were obtained using a Nikon Microphot-FXA microscope and Leica DFC320 digital camera (Nikon, Japan; Leica, Germany). From each group, 10 images were taken at random and analyzed for micrometastasis, as well as scored for percentage of micrometastatic nodules.

Migration and invasion assays

Modified Boyden chambers (Coster, Boston, MA) coated with 0.1% gelatin (migration) or extracellular matrix components (invasion) were used. A2780 or MCF7 cells (1×10^5) suspended in 100 μL of serum-free media were added into the upper chamber 24 hours after miRNA/siRNA transfections. Complete media for cells

containing 10% FBS (500 µL) was added to the bottom chamber as a chemo-attractant. The chambers were incubated at 37℃ in 5% CO_2 for 6 hours (migration) or overnight (invasion). After incubation, the cells in the upper chamber were removed with cotton swabs. Cells were fixed and stained and counted using light microscopy. Cells from 5 random fields were counted. Experiments were done in duplicate and performed 3 times.

Methylation specific PCR and Methylation specific restriction enzyme analysis

For methylation-specific PCR, MethPrimer (http://www.urogene.org/methprimer/) software was used for the prediction of the CpG island of the Drosha promoter region and for design of methylation-specific primers **(Table 1)**. Total DNA was isolated from normoxia- and hypoxia-treated cells using Phenol:Chloroform extraction and then treated with bisulphite using a methylation kit (EZ DNA Methylation-Gold; Zymo Research, CA). Using real-time PCR, as described above, quantification of methylation in hypoxia samples was performed by comparing them with normoxia samples. For methylation specific restriction enzyme analysis, primers were designed flanking the CpG island predicted by MethPrimer with at least two CpG islands on primers as suggested by qMethyl Light (Zymo Research, CA). DNA samples from hypoxia and normoxia exposed cancer cells were subjected to MSREs provided in kit. Following MSRE digestion of DNA, quantification of methylation was carried out using real-time PCR. Percentage methylation was calculated by comparing Ct values obtained from test (with MSRE) and reference (no MSRE) reactions as outlines in the kit manual.

Northern blot analysis

RNA from cells treated with normoxia and hypoxia were subjected to Northern blot analysis using non-radioactive biotin-probe method[73]. Briefly, Total RNA from A2780 cells exposed to normoxia and hypoxia was loaded onto 15% Urea gel, electrophoresed and transferred to nylon membranes at 10–15 V (90 min) using Trans-Blot SD Semi-Dry Transfer Cell (Bio-Rad, CA). RNA was cross-linked to the membrane using UV cross linker. For miRNA and U6 probes, pre-synthesized LNA-modified oligonucleotides were purchased from Exiqon (http://www.exiqon.com) with biotin conjugation. Hybridization and washing of the membranes were carried out using Northern max kit (Life Technologies, CA) according to the manufacturer recommended protocol. Membranes were developed using Chemiluminescent Nucleic Acid Detection Module (Pierce Biotechnology, IL).

Actinomycin D mRNA stability assay

Drosha or Dicer mRNA stability under hypoxic and normoxic conditions was assessed using 5 µg/mL actinomycin D. Cells were grown in hypoxic or normoxic conditions for different time periods with or without actinomycin D. At specified time points, RNA was isolated and RNA levels of Drosha and Dicer were measured using real-time PCR, as described above. 18S was used to normalize between the hypoxia and normoxia samples. To assess RNA decay rates, Drosha and Dicer levels under hypoxic conditions after normalization with 18s were compared with Drosha and Dicer levels under normoxic conditions.

Chromatin hybridization and immunoprecipitation assay

Cells were cultured in hypoxic or normoxic conditions for 48 hours and chromatin immunoprecipitation assays were performed using the Chip-it express kit

(Active Motif), as described by the manufacturer. In brief, crosslinked cells were collected, lysed, sonicated, and subjected to immunoprecipitation with the ETS1 or ELK1 antibody or IgG isotype (mIgG) control. Immunocomplexes were collected with protein A/G agarose magnetic beads and eluted. Cross-links were reversed by incubating at 65℃ with high salt concentration. PCR-based quantification of fold enrichment in ETS1 or ELK1 binding on the Drosha promoter region (primers used are listed in **Table 1**) was carried out. The 2500-3000 base upstream region of the ETS1 or ELK1 binding region was used as a control.

Microdissection and RNA isolation

In vivo tumor samples from a previous study [74] injected with Hypoxyprobe (Hypoxyprobe Inc., Burlington, MA) were used for the present study. Frozen sections (10 µm) were affixed onto polyethylene terephthalate slides (Leica), fixed in cold acetone (10 minutes), washed in PBS 3 times, stained for Hypoxyprobe using FITC-conjugated antibody for 1 hour on top of ice, washed, and air-dried; dissection immediately followed. Microdissection was performed using an MD LMD laser microdissecting microscope (Leica). RNA was isolated from some samples using the Cells to Ct Kit (Applied Biosystems), according to the manufacturer instructions. Real-time PCR was carried out to quantify gene expression.

Transcription factor binding analysis, luciferase assays, and mutagenesis

The promoter region of Drosha was analyzed for potential transcription factor binding using Matinspector (Genomatix Inc., Germany), followed by analysis for a potential gene suppression role using LitInspector (Genomatix). The Drosha

promoter luciferase reporter assay was performed in A2780 and MCF7 cells using the Dual Luciferase system (SwitchGear Genomics). Cells were transfected using FuGENE HD TFX reagent in a 96-well plate with empty promoter or Drosha promoter (Switchgear Genomics), along with the Cypridina TK control construct (pTK-Cluc). Cells were treated with hypoxia or normoxia for 48 hours and luciferase activity was measured using the kit as described above. Mutation in the ETS1 or ELK1 binding region in the Drosha promoter was created using the Quick change site-directed mutagenesis kit (Agilent Technologies) and verified by sequencing. Primers used for mutagenesis are listed in extended data Table 1.

Table 1: Primer and siRNA sequences used in the study		
Type	**Gene**	**Sequence**
SiRNA	Dicer Sequence 1	S 5′ CAUUGAUCCUGUCAUGGAU [dT] [dT] 3′
		AS 5′ AUCCAUGACAGGAUCAAUG [dT] [dT] 3′
	Dicer Sequence 2	S 5′ GCAGUUAUGAUUUAGCUAA [dT] [dT] 3′
		AS 5′ UUAGCUAAAUCAUAACUGC [dT] [dT] 3′
	Drosha Sequence 1	S 5′ CAGUAACUGUGACUGUUGU [dT] [dT] 3′
		AS 5′ ACAACAGUCACAGUUACUG [dT] [dT] 3′
	Drosha Sequence 2	S 5′ GGAUUAGCAACCUAUCCGA [dT] [dT] 3′
		AS 5′ UCCGAUAGGUUGCUAAUCC [dT] [dT] 3′
	ETS1 Sequence 1	S 5′ GUGAAACCAUAUCAAGUUA [dT] [dT] 3′
		AS 5′ UAACUUGAUAUGGUUUCAC [dT] [dT] 3′
	ETS1 Sequence 2	S 5′ CAUAUCAAGUUAAUGGAGU [dT] [dT] 3′
		AS 5′ ACUCCAUUAACUUGAUAUG [dT] [dT] 3′
	ELK1 Sequence 1	S 5′ GGGUUUGUGUGCCAGAAACCA [dT] [dT] 3′
		AS 5′ UGGUUUCUGGCACAAACCC [dT] [dT] 3′
	ELK1 Sequence 2	S 5′ CCUUACACGUCUCCUACUU [dT] [dT] 3′
		AS 5′ AAGUAGGAGACGUGUAAGG [dT] [dT] 3′
	HIF1α Sequence	S 5′ CUGAUGACCAGCAACUUGA [dT] [dT] 3′
		AS 5′ UCAAGUUGCUGGUCAUCAG [dT] [dT] 3′
	STAT1 Sequence 1	S 5′ CUCAUUCCGUGGACGAGGU [dT] [dT] 3′
		AS 5′ ACCUCGUCCACGGAAUGAG [dT] [dT] 3′
	STAT1 Sequence 2	S 5′ CCUGAUUAAUGAUGAACUA [dT] [dT] 3′
		AS 5′ UAGUUCAUCAUUAAUCAGG [dT] [dT] 3′
Primers		
	ETS1	F 5′TGGGGACATCTTATGGGAAC3′ R 5′ATTCTGGATAGGCTGGGTTG3′
	ELK1	F 5′GGCCTTGCGGTACTACTATGAC3′ R 5′CCTCAGGGTAGGACACAAAC3′
	E Cadherin	F 5′GACCGGTGCAATCTTCAAA3′ R 5′TTGACGCCGAGAGCTACAC3′
	Vimentin	F 5′ATTCCACTTTGCGTTCAAGG3′ R 5′CTTCAGAGAGAGGAAGCCGA3′
	CA9	F 5′CAGCAACTGCTCATAGGCAC3′ R 5′CTTTGCCAGAGTTGACGAGG3′
	GLUT1	F 5′GGCATTGATGACTCCAGTGTT3′ R 5′ATGGAGCCCAGCAGCAA3′
	Drosha UM	F 5′GTTTTAAAGGGTTTTTTGTTGATGA3′ R 5′AAAACAAAACCAAACTACTACCACA 3′
	Drosha M	F 5′GGTTTTAAAGGGTTTTTTGTTGAC3′ R 5′CAAAACAAAACCAAACTACTACCG3′
	Drosha (qMethyl Light)	F 5′ ACGTAGGGGGAGGGGGCGCG3′ R 5′ACCGCCCGCGCCTCCGGAACA3′
	Drosha ChIP	F 5′ATTCCCTCGGTTTCCTGTTC3′ R 5′TCAGAGCAAAGCCAGGCTAC 3′
	Drosha ChIP -ve control	F 5′GAGCCTTAAATGCCAAGCAC3′ R 5′ACTGCGCCTGACTCCTTATTAC 3′
	Drosha promoter ETS1 mut	F 5′AATTCCCTCGGTTTCCTGTTAAAAAGGCGCGGGCGGTGCCACTGTCTTG 3′ R 5′CAAGACAGTGGCACCGCCCGCGCCTTTTTAACAGGAAACCGAGGGAATT3′
	Drosha promoter ELK1 mut	F 5′GGTTTGCTTTTTAATTCCCTCGGTAAAATGAAAAGGAGGCGCGGGCGGTG3′ R 5′CACCGCCCGCGCCTCCTTTTCATTTTACCGAGGGAATTAAAAAGCAAACC3′
	Dicer 3' UTR mut	F 5′TGATGCAGATAAAGCAGGAAGGACCTCGGGTAAATGTCACTTACATATAAATGCAGCATTCCACGAAGCATCAAGTT3′
	18s	F 5′CGCCGCTAGAGGTGAAATTC3′ R 5′TTGGCAAATGCTTTCGCTC3′
	STAT1	F 5′TGAATATTCCCCGACTGAGC3′ R 5′AGGAAGACCCAATCCAGATGT3′
	RHOB1	F 5′GGGACAGAAGTGCTTCACCT3′ R 5′CGACGTCATTCTCATGTGCT3′
	TAGLN	F 5′CTCATGCCATAGGAAGGACC3′ R 5′GTCCGAACCCAGACACAAGT 3′
	SERTAD2	F 5′AGCCCATCTTCATGCTCATC3′ R 5′CCTCCTGATGCGTTAGTTCC 3′
	TXNIP	F 5′AGGAAGCTCAAAGCCGAACT3′ R 5′ACGCTTCTTCTGGAAGACCA3′
	JAG1	F 5′ACTGTCAGGTTGAACGGTGTC3′ R 5′ATCGTGCTGCCTTTCAGTTT3′
	JUN	F 5′TCTCACAAACCTCCCTCCTG3′ R 5′GAGGGGGTTACAAACTGCAA3′
	CTGF	F 5′TGGAGATTTTGGGAGTACGG3′ R 5′CAGGCTAGAGAAGCAGAGCC3′
	HIF2a	F 5′ CATCCCGGGACTTCTCCT 3′ R 5′ GTCTGAACGTCTCAAAGGGC 3′
	VEGF	F 5′ AGCTGCGCTGATAGACATCC 3′ R 5′ CTACCTCCACCATGCCAAGT 3′

Chapter 3: Hypoxia downregulates miRNA biogenesis

This chapter is based on Rupaimoole, R., S.Y. Wu, S. Pradeep, C. Ivan, C.V. Pecot, K.M. Gharpure, A.S. Nagaraja, G.N. Armaiz-Pena, M. McGuire, B. Zand, H.J. Dalton, J. Filant, J.B. Miller, C. Lu, N.C. Sadaoui, L.S. Mangala, M. Taylor, T. van den Beucken, E. Koch, C. Rodriguez-Aguayo, L. Huang, M. Bar-Eli, B.G. Wouters, M. Radovich, M. Ivan, G.A. Calin, W. Zhang, G. Lopez-Berestein, and A.K. Sood, Hypoxia-mediated downregulation of miRNA biogenesis promotes tumour progression. Nat Commun, 2014. 5: p. 5202.

3.1 MiRNA biogenesis is dynamic in nature under in vivo conditions

First, we determined whether tumors have stable heterogeneity with regard to Drosha and Dicer. We examined single-cell clones of A2780 ovarian cancer cells and found heterogeneous expression of Drosha and Dicer **(Figure 2a)**. To understand the functional implications of this heterogeneity, we expanded and injected 2 single-cell clones of A2780 cells into the peritoneal cavity of mice (Clones 2 and 4). Upon analysis of individual tumor samples, we observed that each sample had varying Drosha and Dicer expression levels compared with the expression of clones at the time of injection **(Figure 2b)**.

This prompted us to consider whether changes in expression levels of Drosha and Dicer could be dynamic and potentially affected by the tumor microenvironment. Considering the critical role of hypoxia in the tumor microenvironment[60-62], we

tested levels of hypoxia in the clones with low Drosha and Dicer, also A2780 tumor samples using a hypoxia marker, carbonic anhydrase 9 (CA9). In the cell clones, *in vitro*, we observed variable levels of CA9 with small magnitude of changes **(Figure 2c)**. In contrast, the tumor samples with low Drosha and Dicer levels displayed significantly increased expression of CA9, which was inversely correlated with Drosha **(Figure 2d)** and Dicer **(Figure 2e)** levels. This suggests possibility that hypoxia and miRNA biogenesis is linked together.

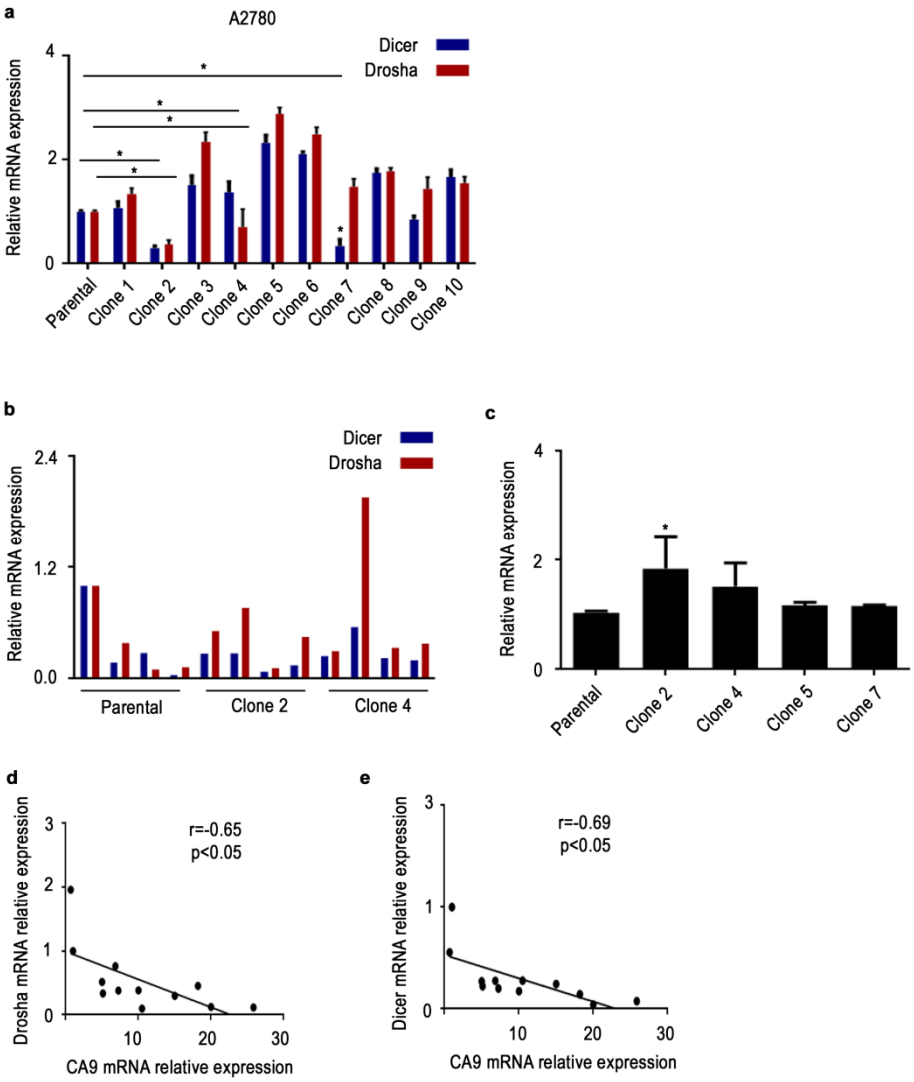

Figure 2: (a) mRNA expression levels of Drosha and Dicer in single-cell clones derived from A2780 cells. (b) mRNA expression levels of Drosha and Dicer in individual tumor samples from mice injected with A2780 clones (n = 4 per group). (c) Expression of CA9 (hypoxia marker) in single cells clones of A2780 cell line, compared to parental cells. (d-e) Spearman correlation between mRNA expression levels of Dicer and Drosha with carbonic anhydrase 9 (CA9) levels in individual tumor samples from mice injected with parental cells and single-cell clones. Data are presented as mean ± standard error of the mean of n ≥ 3 independent experimental groups. *p < 0.05 (Student t test).

We next tested the effect of hypoxia on Drosha and Dicer levels using various cancer cell lines. In multiple cell lines exposed to hypoxia, we observed marked reductions in Drosha and Dicer mRNA and protein levels **(Figure 3a-g)**. This observed downregulation was consistent across several time points **(Figure 3e)**; the 48-hour time point was selected for all subsequent experiments. Drosha and Dicer levels were significantly increased after cells were restored to normoxic conditions, demonstrating the dynamic nature of the regulation **(Figure 3h)**. To test the possibility of HIF1α dependency in Drosha and Dicer downregulation, we examined Drosha and Dicer expression levels in mouse embryonic fibroblasts (MEFs) with wild-type HIF1α or HIF1α-knockout cultured under normoxic or hypoxic conditions. HIF1α-knockout MEFs showed complete abrogation in Drosha downregulation under hypoxia exposure and partial abrogation in Dicer downregulation **(Figure 4a)**, suggesting that Drosha downregulation is highly dependent on HIF1α. Additionally, siHIF1α significantly rescued Drosha levels in hypoxia exposed A2780 cells and Dicer levels were partially rescued **(Figure 4b)**. These data were further supported by stabilization of HIFα by $CoCl_2$ in A2780 cells under normoxia. Increased CA9 was observed, followed by Drosha and Dicer downregulation in $CoCl_2$-treated samples compared to control cells **(Figure 4c)**.

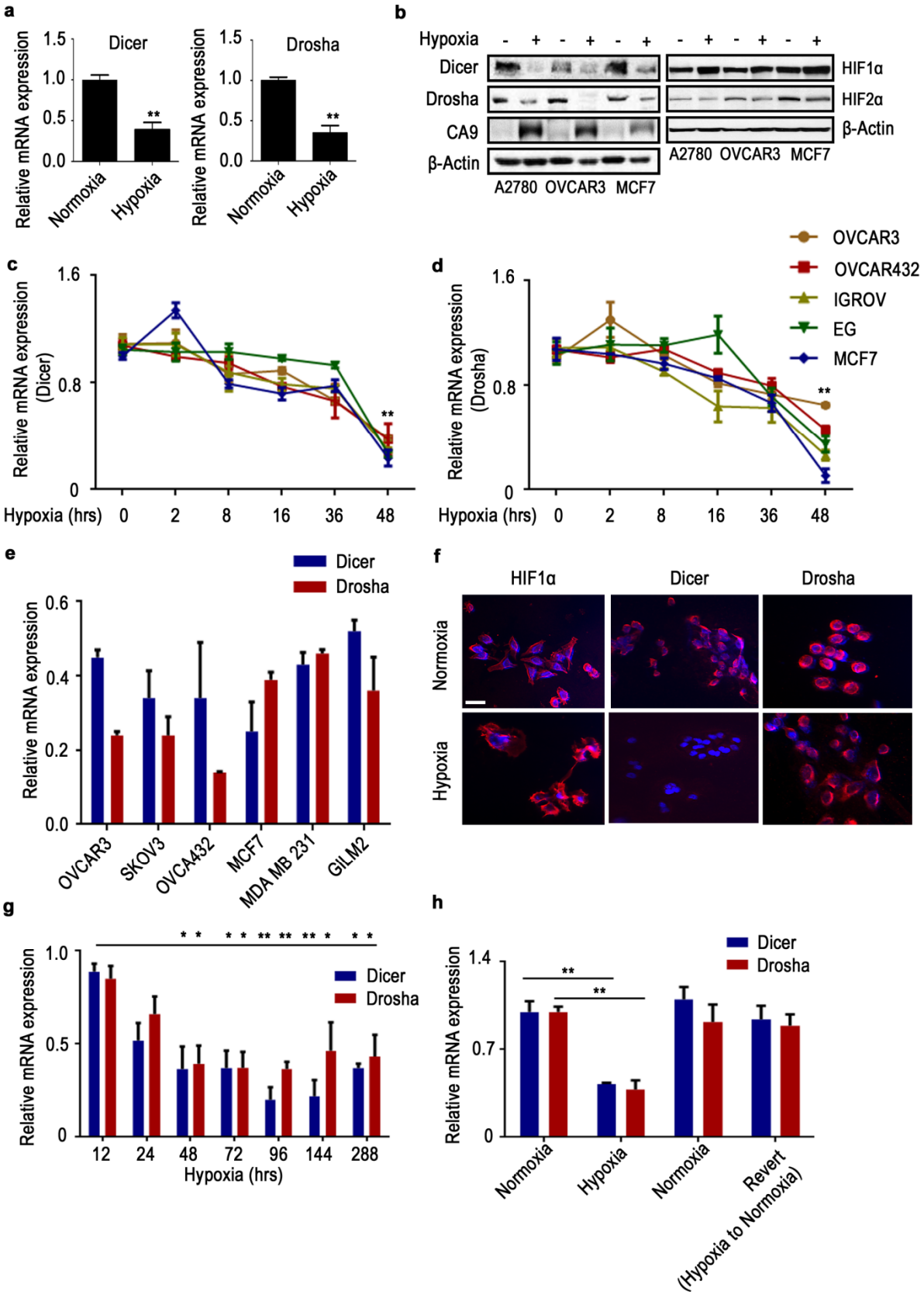
a
Dicer
Drosha
Relative mRNA expression
1.5
1.0
0.5
0.0
**
Normoxia
Hypoxia
b
Hypoxia
Dicer
Drosha
CA9
β-Actin
HIF1α
HIF2α
β-Actin
A2780 OVCAR3 MCF7
c
Relative mRNA expression (Dicer)
1.6
0.8
0
Hypoxia (hrs) 0 2 8 16 36 48
d
OVCAR3
OVCAR432
IGROV
EG
MCF7
Relative mRNA expression (Drosha)
e
Dicer
Drosha
Relative mRNA expression
0.6
0.4
0.2
0.0
OVCAR3
SKOV3
OVCA432
MCF7
MDA MB 231
GILM2
f
HIF1α
Dicer
Drosha
Normoxia
Hypoxia
g
Relative mRNA expression
1.0
0.5
0
12 24 48 72 96 144 288
Hypoxia (hrs)
h
Relative mRNA expression
1.4
0.7
0
Normoxia
Hypoxia
Normoxia
Revert
(Hypoxia to Normoxia)

Figure 3: (a) Drosha and Dicer mRNA expression levels under hypoxic conditions (1% oxygen, 48 hr) in A2780 cells. (b) Protein expression of Dicer, Drosha, hypoxia marker carbonic anhydrase 9 (CA9), HIF1α, HIF2α under hypoxic conditions in A2780, OVCAR3, and MCF7 cells. (c and d) Drosha and Dicer mRNA expression levels under hypoxic conditions for several ovarian and breast cancer cell lines at different time points. (e) Drosha and Dicer mRNA expression levels in several ovarian and breast cancer cell lines 48 hrs following hypoxia treatment. Data are normalized to normoxic conditions. (f) Protein levels of HIF1α, Dicer, and Drosha in OVCAR3 cells under hypoxic and normoxic conditions at 48 hr time point. Scale bar: 200 μm. (g) mRNA expression levels of Drosha and Dicer in A2780 cells after long durations of hypoxic conditions. Data are normalized to normoxic conditions. (h) mRNA expression levels of Drosha and Dicer in A2780 cells after 48 hr of hypoxia treatment and reversal to normoxic condition. Data are presented as mean ± standard error of the mean of $n \geq 3$ independent experimental groups. *$p < 0.05$, **$p < 0.01$ (Student t test).

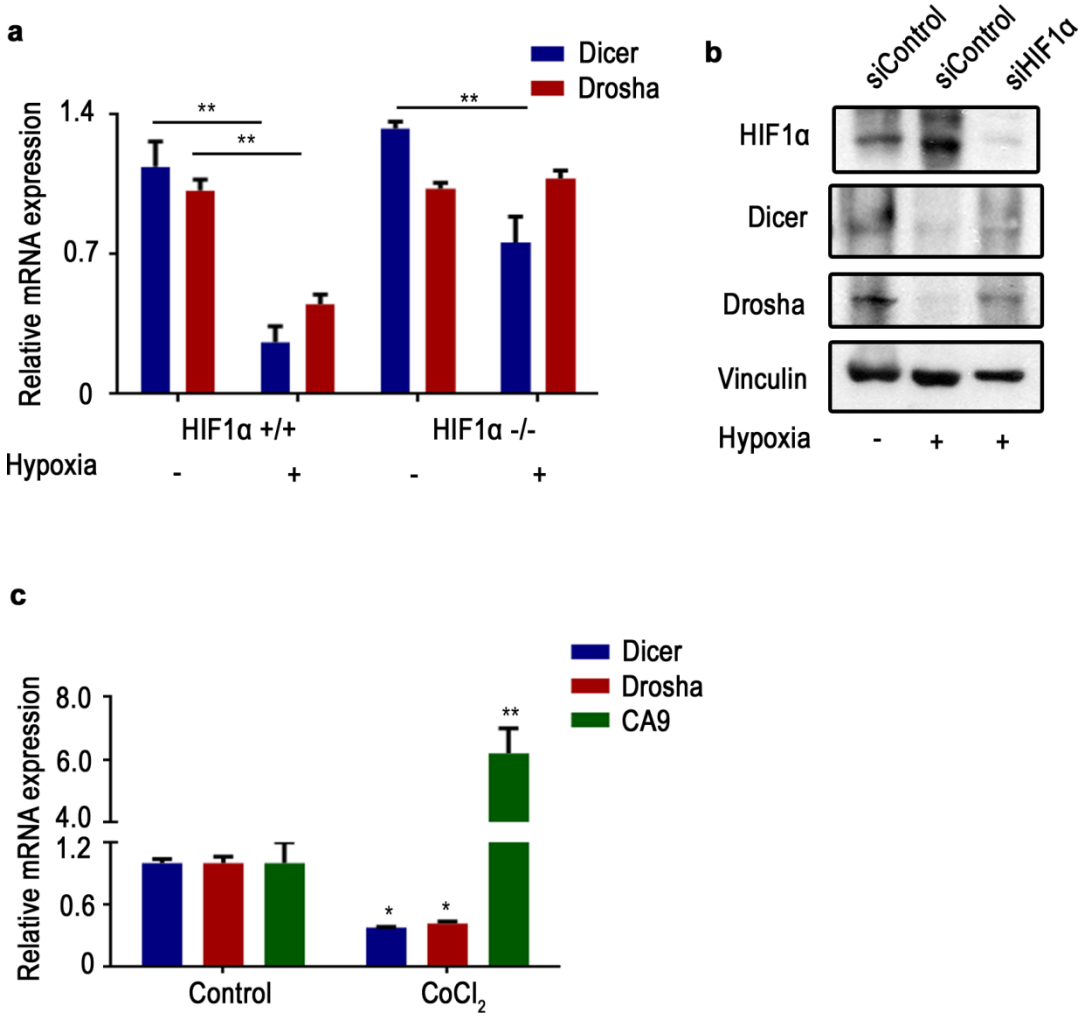

Figure 4: (a) Drosha and Dicer levels in mouse embryonic fibroblasts with wild-type HIF1α (+/+) or HIF1α-knockout (-/-) mouse embryonic fibroblasts under normoxic and hypoxic conditions for 48 hrs. (b) Western blot analysis of the protein expression of HIF1α, Drosha, and Dicer in cells treated with siControl or siHIF1α in normoxic or hypoxic conditions (48 hr). Vinculin used as loading control. (c) Drosha, Dicer, and CA9 levels in $CoCl_2$ treated A2780 cells under normoxia. Data are presented as mean ± standard error of the mean of n ≥ 3 independent experimental groups. *p < 0.05, **p < 0.01 (Student t test).

In RNA samples isolated from microdissected hypoxic regions of A2780 tumor samples, we observed significantly increased expression of hypoxia markers, CA9 and GLUT1. In the same RNA samples, we observed 60% downregulation of Drosha and Dicer **(Figure 5a, b)**. These data support our finding that hypoxia is an important regulator of Drosha and Dicer downregulation in cancer. As previous studies have shown that anti-VEGF therapies can increase hypoxia[75], we assessed Drosha and Dicer levels in mouse tumor samples following treatment with bevacizumab, an anti-VEGF agent. We observed increased CA9 expression and, consequently, significantly decreased Drosha and Dicer expression levels in tumors treated with bevacizumab compared with untreated controls **(Figure 5c, d)**. To determine whether similar findings extend to clinical samples, we analyzed expression levels of Drosha, Dicer, and CA9 in human tumor samples (n=30). Results showed a significant inverse correlation between CA9 and Drosha and Dicer levels **(Figure 5e)**.

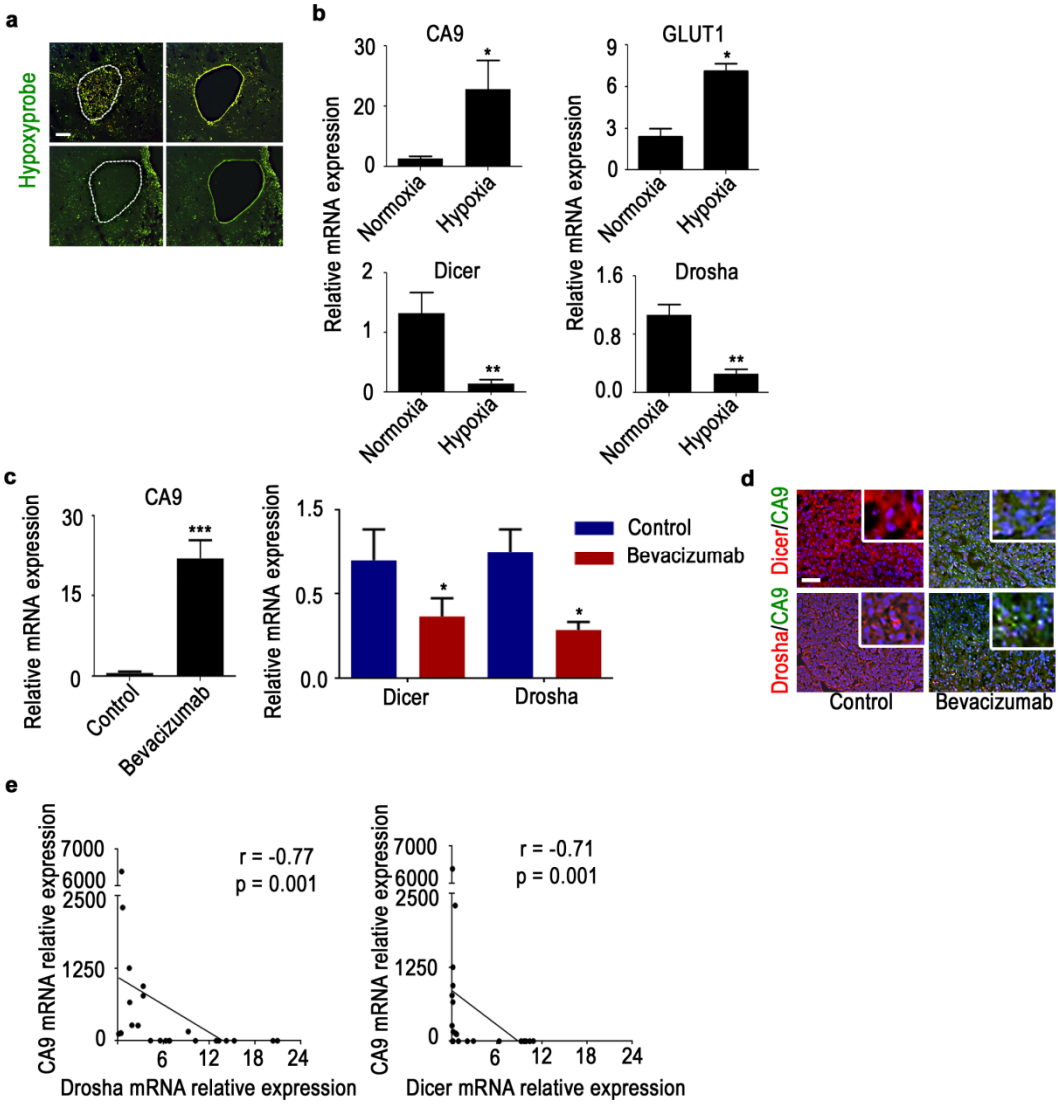
a
Hypoxyprobe
b
CA9
GLUT1
Dicer
Drosha
Relative mRNA expression
Normoxia
Hypoxia
c
CA9
Relative mRNA expression
Control
Bevacizumab
Dicer
Drosha
d
Dicer/CA9
Drosha/CA9
Control
Bevacizumab
e
CA9 mRNA relative expression
r = -0.77
p = 0.001
Drosha mRNA relative expression
r = -0.71
p = 0.001
Dicer mRNA relative expression

Figure 5: (a) Laser microdissection of hypoxic areas of tumors, guided by Hypoxyprobe staining (green). Scale bar: 500 µm. (b) mRNA expression levels of hypoxia markers CA9 and GLUT1, as well as Dicer and Drosha expression levels, in normoxic and hypoxic regions of tumors isolated using microdissection. (c) mRNA expression levels of CA9, Drosha, and Dicer in A2780 mouse tumors treated with bevacizumab. (d) Protein expression levels of Dicer (red), Drosha (red), and CA9 (green) in A2780 mouse tumor samples treated with bevacizumab compared with untreated controls. Nucleus indicated as Blue. Scale bar: 200 µm. (e) Pearson correlation between Dicer and Drosha mRNA expression levels and hypoxia marker CA9 levels (n=30). All images shown are representative and data are presented as mean ± standard error of the mean of $n \geq 3$ experimental groups. *$p < 0.05$, **$p < 0.01$, ***$p < 0.001$ (Student t test).

3.2: Effect of hypoxia on miRNA levels and clinical outcomes

We next considered whether Drosha or Dicer downregulation leads to impaired miRNA biogenesis by carrying out miRNA microarray analysis of samples exposed to hypoxia or normoxia. Upon analysis of mature miRNA array data, we observed significant global miRNA downregulation following exposure to hypoxia **(Figure 6a; Table 2)**. Analysis of precursor and mature miRNA levels from deep sequencing data revealed significant downregulation of mature miRNAs, compared to their precursors **(Figure 6b; Table 2)**. Using qRT-PCR, we analyzed expression of seven significantly downregulated miRNAs from **Figure 6a,** in cells exposed to normoxia or hypoxia. There was a significant increase in pri-miRNA levels of six of seven miRNAs that were tested **(Figure 6c)**. There was also significant downregulation of corresponding mature miRNA levels in response to hypoxia **(Figure 6d)**, suggesting defective processing machinery under hypoxic conditions. Next, to understand the individual contribution of Drosha and Dicer downregulation in the miRNA processing downregulation, we carried out quantification of pri, precursor, and mature miRNAs in RNA from nuclear and cytoplasmic fractionated A2780 cells exposed to normoxia or hypoxia. RNA from nuclear fractionated samples had significantly upregulated pri-miRNA levels **(Figure 6e)**, consistent with the total RNA data in **Fig. 6c**. Interestingly, we noted >40% reduction in precursor miRNA levels in hypoxia treated samples compared to normoxia **(Figure 6f)**. Additionally, samples from hypoxia exposed cells had >60% reduction in mature miRNA levels compared to normoxia in the cytoplasmic fraction **(Figure 6g)**. This

data was further validated by northern blot analysis of miR-16a and 27a in cancer cells exposed to normoxia and hypoxia **(Figure 6h)**.

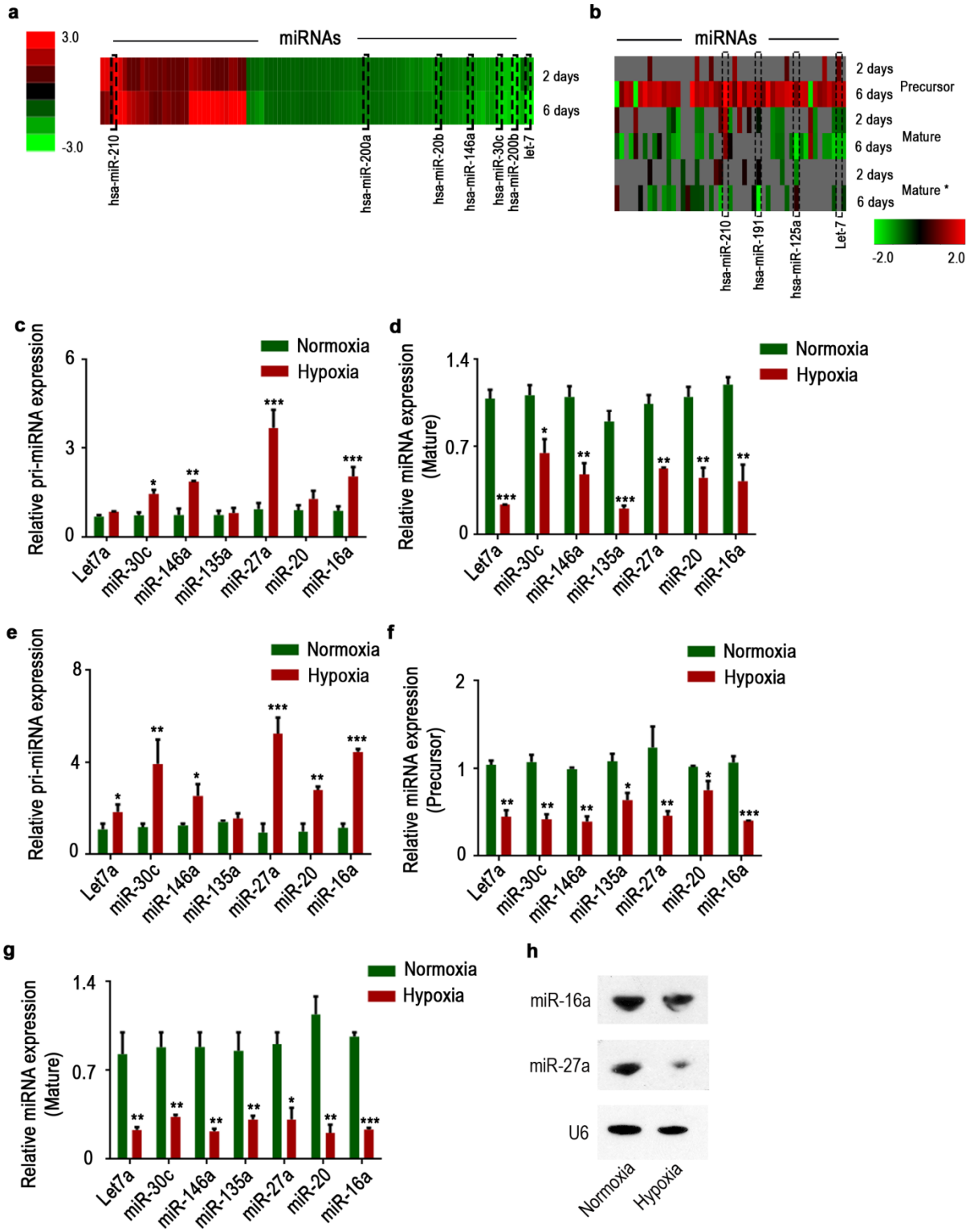
a
3.0
-3.0
miRNAs
2 days
6 days
hsa-miR-210
hsa-miR-200a
hsa-miR-20b
hsa-miR-146a
hsa-miR-30c
hsa-miR-200b
let-7
b
miRNAs
2 days
6 days
Precursor
2 days
6 days
Mature
2 days
6 days
Mature *
hsa-miR-210
hsa-miR-191
hsa-miR-125a
Let-7
-2.0
2.0
c
Relative pri-miRNA expression
Normoxia
Hypoxia
Let7a
miR-30c
miR-146a
miR-135a
miR-27a
miR-20
miR-16a
d
Relative miRNA expression (Mature)
Normoxia
Hypoxia
e
Relative pri-miRNA expression
Normoxia
Hypoxia
f
Relative miRNA expression (Precursor)
Normoxia
Hypoxia
g
Relative miRNA expression (Mature)
Normoxia
Hypoxia
h
miR-16a
miR-27a
U6
Normoxia
Hypoxia

Figure 6: Hypoxia mediated downregulation in Drosha and Dicer results in decreased miRNA levels. (a), Heat map showing mature microRNA (miRNA) levels under hypoxic conditions, assessed using miRNA array data. (b), Heat map showing precursor miRNA levels under hypoxic conditions, along with the corresponding mature sense (mature) and antisense (mature*) levels. (c-d), Pri-miRNA and mature miRNA expression levels of significantly altered miRNAs under hypoxia exposure in A2780 cells. (e), Pri-miRNA levels in RNA extracted from nuclear fractionated A2780 cells treated with normoxia and hypoxia. (f-g), Precursor and mature miRNA levels in RNA extracted from cytoplasmic fraction of A2780 cells treated with normoxia and hypoxia. (h) Northern blot data showing expression of mature miRNAs in RNA samples from normoxia and hypoxia exposed A2780 cells. Probing for U6 used as loading control. Data are presented as mean ± standard error of the mean of $n \geq 3$ experimental groups. *$p < 0.05$, **$p < 0.01$, ***$p < 0.001$ (Student t test).

Table 2: Mature miRNAs dysregulated under Hypoxia
p<0.05

miRNA ID	Day6 Foldchange	48hr Foldchange	miRNA ID	Day6 Foldchange	48hr Foldchange
hsa-let-7i	-2.742508197	-2.829567113	hsa-miR-98	-1.176388117	-1.199518249
hsa-miR-9*	-2.690184339	-10.24266995	hsa-miR-140-5p	-1.175849416	-1.161892363
hsa-miR-30a	-2.644615882	-2.326619088	hsa-miR-517*	-1.170811187	-1.132741854
hsa-miR-125b	-2.270582922	-2.551576201	hsa-miR-1305	-1.167470006	-2.001669795
hsa-miR-100	-2.267068806	-2.36137412	hsa-miR-96	-1.167351881	-1.267240124
hsa-let-7b	-2.129702753	-3.908353872	hsa-miR-299-3p	-1.159194003	-1.458417562
hsa-miR-27a	-2.097821392	-2.479997154	hsa-miR-486-5p	-1.15788961	-1.205542643
hsa-miR-31	-1.968774583	-2.007136093	hsa-miR-1264	-1.149540713	-1.189899698
hsa-miR-31*	-1.888714827	-2.209072083	hsa-miR-146b-5p	-1.138480932	-1.115721533
hsa-miR-200b	-1.78976662	-1.792176796	hsa-miR-515-3p	-1.136561598	-1.158293317
hsa-miR-542-5p	-1.775066709	-1.670069854	hsa-miR-518c	-1.116722796	-1.162794513
hsa-miR-520h	-1.767397699	-2.044013715	hsa-miR-520g	-1.106358167	-1.170564172
hsa-miR-30c	-1.74196543	-1.793198297	hsa-miR-330-3p	-1.105840739	-1.213753059
hsa-miR-24	-1.6928636	-1.942200002	hsa-miR-371-3p	-1.105182258	-1.196428388
hsa-miR-93	-1.676595317	-1.949694415	hsa-miR-1288	-1.100533631	-1.43017636
hsa-miR-16	-1.666807038	-1.471543424	hsa-miR-27a*	-1.100153618	-1.112555192
hsa-miR-15a	-1.661775493	-1.49459517	hsa-miR-610	1.100190438	4.203800569
hsa-miR-200a	-1.657756364	-1.606516942	hsa-miR-375	1.112101345	2.707847267
hsa-miR-886-3p	-1.611754993	-1.87259647	hsa-miR-125b-2*	1.116288978	6.594530507
hsa-miR-29a	-1.548162542	-1.475958582	hsa-miR-1471	1.125857934	1.854067578
hsa-let-7g	-1.500426367	-1.686143944	hsa-miR-1224-5p	1.127285824	6.443831556
hsa-miR-10a	-1.489859719	-1.384002157	hsa-miR-150*	1.142220252	3.576234723
hsa-miR-30a*	-1.488715897	-1.642941851	hsa-miR-32*	1.144058247	2.062073969
hsa-let-7a	-1.488217701	-2.820468382	hsa-miR-513b	1.147868403	2.861590839
hsa-miR-135b	-1.463770738	-1.419250371	hsa-miR-498	1.168354947	1.335445056
hsa-miR-20b	-1.459306715	-1.527387427	hsa-miR-874	1.1687466	2.289391073
hsa-miR-29c	-1.440108354	-1.301947459	hsa-miR-1271	1.176632868	1.257995801
hsa-miR-629	-1.415085172	-1.595407965	hsa-miR-574-5p	1.193871933	1.474406697
hsa-miR-362-5p	-1.409702516	-1.556115654	hsa-miR-1183	1.20318063	1.184566667
hsa-miR-146a	-1.396753784	-1.367158207	hsa-miR-877	1.205997119	1.291386016
hsa-let-7d	-1.339397752	-1.816463617	hsa-miR-557	1.256494927	1.396654312
hsa-miR-518b	-1.330385452	-1.481544743	hsa-miR-1249	1.331526245	1.151704523
hsa-miR-20a	-1.328038667	-1.368878326	hsa-miR-671-5p	1.35489568	1.840529572
hsa-miR-649	-1.321493598	-1.430821614	hsa-miR-483-5p	1.364133971	1.289377056
hsa-miR-429	-1.315922846	-1.306045767	hsa-miR-371-5p	1.367226431	1.608692658
hsa-miR-524-3p	-1.294552998	-1.456300094	hsa-miR-939	1.403214966	3.723865561
hsa-miR-1276	-1.277696658	-1.389806363	hsa-miR-1915	1.44341231	4.28587659
hsa-miR-618	-1.268366749	-1.446796168	hsa-miR-513a-5p	1.598552614	5.811211783
hsa-miR-10b	-1.265876457	-1.313808682	hsa-miR-1268	1.631604275	6.770729661
hsa-miR-224	-1.248397784	-1.354770001	hsa-miR-188-5p	1.687380507	4.107325135
hsa-miR-95	-1.241775156	-1.21944233	hsa-miR-134	1.721336264	1.857328175
hsa-miR-181c	-1.236420382	-1.287217957	hsa-miR-1275	1.751670277	2.892611566
hsa-miR-218	-1.231406206	-1.128194836	hsa-miR-638	1.78424914	4.247522675
hsa-miR-181a	-1.230330348	-1.255042229	hsa-miR-630	1.952545232	33.0688801
hsa-miR-551b	-1.221553333	-1.232784473	hsa-miR-663	2.143502737	1.351287052
hsa-miR-1263	-1.214632288	-1.351541081	hsa-miR-1207-5p	2.525174009	2.919258618
hsa-miR-516a-3p	-1.193289078	-1.165840922	hsa-miR-210	2.714002547	1.645007164
hsa-miR-101	-1.186547008	-1.156438162	hsa-miR-1202	2.722874918	1.29920483
hsa-miR-1287	-1.186535846	-1.63703979	hsa-miR-1225-5p	3.451773543	4.284229745
hsa-let-7c*	-1.180929264	-1.320213748			

Table 3: Mature vs Precursor miRNA levels under hypoxia exposure.										
	Deep Seq.Precursor miRNA data		Mature miRNA array data							
	Hypoxia vs Normoxia, 48hrs		Hypoxia vs Normoxia, 48hrs			* = passive strand				
			Downregulated		Upregulated		Downregulated*		Upregulated*	
Probeset ID	p-value	Fold Change	p-value	Fold Change	p-value	Fold Change	p-value	Fold Change	p-value	Fold Change
hsa-mir-210	9.19E-06	NA			2.21E-15	2.714002547				
hsa-mir-200c	0.00377362	2.69938								
hsa-let-7a-2	0.00701313	1.98452								
hsa-mir-425	0.00719504	2.26324								
hsa-mir-103-2	0.0201067	2.28532								
hsa-mir-30b	0.0336866	NA								
hsa-mir-151	0.0341427	1.75112								
hsa-mir-27a	0.036819	2.70892	8.24E-05	-2.097821392			0.040169608	-1.100153618		
hsa-mir-23a	0.0476355	2.75066								
hsa-mir-675	0.0625298	3.98128								
hsa-mir-10a	0.065216	3.19398	0.004438425	-1.489859719						
hsa-mir-183	0.0680151	2.229								
hsa-mir-877	0.0794451	1.92006			2.11E-05	1.205997119				
hsa-mir-107	0.0870375	3.55507								
hsa-mir-16-1	0.0941606	5.23084	0.006340296	-1.666807038						
hsa-mir-182	0.0947654	1.74618								
hsa-mir-30d	0.106034	5.2826								
hsa-mir-222	0.114635	-2.57618								
hsa-mir-663	0.150519	1.74293			4.04E-09	2.143502737				
hsa-mir-1244-1	0.159374	-1.32261								
hsa-mir-874	0.175368	15.1447			2.32E-06	1.1687466				
hsa-mir-106b	0.17551	-1.75781	0.032047429	-1.310714792						
hsa-mir-1296	0.176266	1.63677								
hsa-mir-130b	0.182715	3.71282	0.012904142	-1.189241135						
hsa-let-7c	0.20251	1.6611								
hsa-mir-181a-1	0.212706	3.49771	5.19E-06	-1.230330348						
hsa-mir-130a	0.228627	-1.94281								
hsa-mir-125a	0.236088	1.32252					3.27E-07	-1.285392254		
hsa-mir-212	0.251686	2.62749								
hsa-let-7f-1	0.301391	1.86383							2.46E-10	1.244570953
hsa-mir-15b	0.306757	2.33668								
hsa-mir-1307	0.30902	1.4513								
hsa-mir-1291	0.310613	2.27083								
hsa-mir-1236	0.311357	1.81147								
hsa-mir-342	0.314769	4.59126								
hsa-mir-1306	0.320843	1.30847								
hsa-mir-191	0.324294	1.50147							8.13E-11	1.293707523
hsa-mir-505	0.329782	2.23796			0.0079331	1.15119627				
hsa-mir-25	0.335277	-2.13563								
hsa-mir-23b	0.343157	1.39226								
hsa-mir-664	0.358022	2.25443								
hsa-mir-103-1	0.365926	1.46508								
hsa-mir-3175	0.383318	2.16874								
hsa-mir-1244-2	0.386042	-1.12761								
hsa-mir-21	0.389891	2.89661	2.88E-05	-1.628401554						
hsa-mir-1259	0.407209	-1.45442								
hsa-mir-1979	0.410974	-1.68805								
hsa-mir-24-1	0.413434	1.6039	1.08E-08	-1.6928636						
hsa-mir-196a-1	0.428592	-2.11393								
hsa-mir-16-2	0.431148	4.07798								
hsa-mir-361	0.444002	2.04947								
hsa-mir-24-2	0.468925	NA								
hsa-mir-663b	0.472549	1.5933								
Note: Missing columns indicate those miRNAs are not present in sequening data due to low sequence reads or failing p value cut off.										

Table 3: Mature vs Precursor miRNA levels under hypoxia exposure.										
	Deep Seq.Precursor miRNA data		Mature miRNA array data							
	Hypoxia vs Normoxia, 48hrs		Hypoxia vs Normoxia, 48hrs				* = passive strand			
			Downregulated		Upregulated		Downregulated*		Upregulated*	
Probeset ID	p-value	Fold Change	p-value	Fold Change	p-value	Fold Change	p-value	Fold Change	p-value	Fold Change
hsa-mir-1201	0.48261	-1.49743								
hsa-mir-181b-1	0.49382	-2.01493								
hsa-mir-27b	0.517068	1.17709								
hsa-mir-621	0.526467	1.26764								
hsa-mir-331	0.534977	1.64511								
hsa-let-7g	0.536318	1.51467	0.001062757	-1.500426367						
hsa-mir-29b-2	0.587664	-2.01291								
hsa-mir-423	0.595498	1.30036								
hsa-mir-1248	0.599322	-1.14076								
hsa-mir-199a-2	0.613624	1.62418			0.02574314	1.281458279				
hsa-mir-218-1	0.624416	-1.24153	0.000254545	-1.231406206						
hsa-mir-92a-2	0.627743	-1.24148								
hsa-mir-199b	0.629279	2.10035			0.00438815	1.307500312				
hsa-mir-320a	0.630662	-1.19158			0.00560733	1.154260446				
hsa-mir-615	0.632953	1.25278								
hsa-mir-671	0.650737	-1.1317								
hsa-mir-744	0.651109	-1.37244			3.33E-07	1.26355013				
hsa-mir-93	0.656194	1.13276	0.014252374	-1.676595317						
hsa-let-7a-3	0.670021	1.07895								
hsa-mir-17	0.682833	1.27394								
hsa-mir-31	0.683234	1.42907	1.09E-06	-1.968774583			0.000831437	-1.888714827		
hsa-let-7d	0.683974	-1.09396	0.00377375	-1.339397752						
hsa-mir-34a	0.684139	-1.94894								
hsa-mir-1244-3	0.685263	-1.03937								
hsa-mir-92a-1	0.724657	1.22876								
hsa-mir-1301	0.732593	-1.27183								
hsa-mir-99a	0.735518	NA								
hsa-mir-1181	0.736216	1.07897								
hsa-mir-1226	0.763447	1.13419								
hsa-mir-193b	0.78722	1.1236								
hsa-mir-1975	0.791036	-1.10512								
hsa-let-7b	0.796986	-1.12866	3.75E-11	-2.129702753					5.81E-09	1.204464042
hsa-mir-181b-2	0.800815	1.54035								
hsa-mir-339	0.834129	-1.16261								
hsa-mir-1246	0.857537	1.06741								
hsa-mir-152	0.866218	NA								
hsa-mir-181d	0.87316	1.37052			0.04478281	1.109669522				
hsa-mir-214	0.873929	1.05291			4.47E-05	2.005934044			0.000126923	1.402334689
hsa-let-7a-1	0.880772	-1.08405	0.003742473	-1.488217701						
hsa-mir-92b	0.885569	1.05844			8.17E-06	1.220500926				
hsa-mir-29b-1	0.885884	-1.1642								
hsa-mir-1826	0.889362	1.05088								
hsa-mir-1229	0.914338	1.03578								
hsa-mir-197	0.920659	-1.61106								
hsa-mir-532	0.924274	-1.18268								
hsa-mir-886	0.925564	1.0199								
hsa-mir-196a-2	0.939169	-1.0549								
hsa-mir-1308	0.956811	-1.02314								
hsa-mir-99b	0.957883	1.02831			0.0065096	1.2821829				
hsa-mir-141	0.959128	-1.18268								
hsa-mir-221	0.967854	1.04538								
hsa-mir-324	0.987644	-1.01068							4.34E-10	1.230492249
hsa-mir-30c-1	0.992256	1.01159	0.001042768	-1.74196543						
hsa-mir-1207	0.999766	-1.00024								
Note: Missing columns indicate those miRNAs are not present in sequening data due to low sequence reads or failing p value cut off.										

Using the ovarian cancer data from the Cancer Genome Atlas project (TCGA), we investigated the effect of low Drosha and Dicer levels on mature miRNA levels and observed that most miRNAs (>80%) were affected by downregulation of Drosha and Dicer **(Figure 7a)**. In the TCGA dataset, we observed significantly worse median overall survival with low Drosha and Dicer levels **(Figure 7b)**. Using a hypoxia metagene signature [72], we examined the survival difference between patients with high vs. low hypoxia levels in their tumors, according to TCGA data. We observed significantly worse survival rates in patients whose tumors had high levels of hypoxia **(Figure 7c)**.

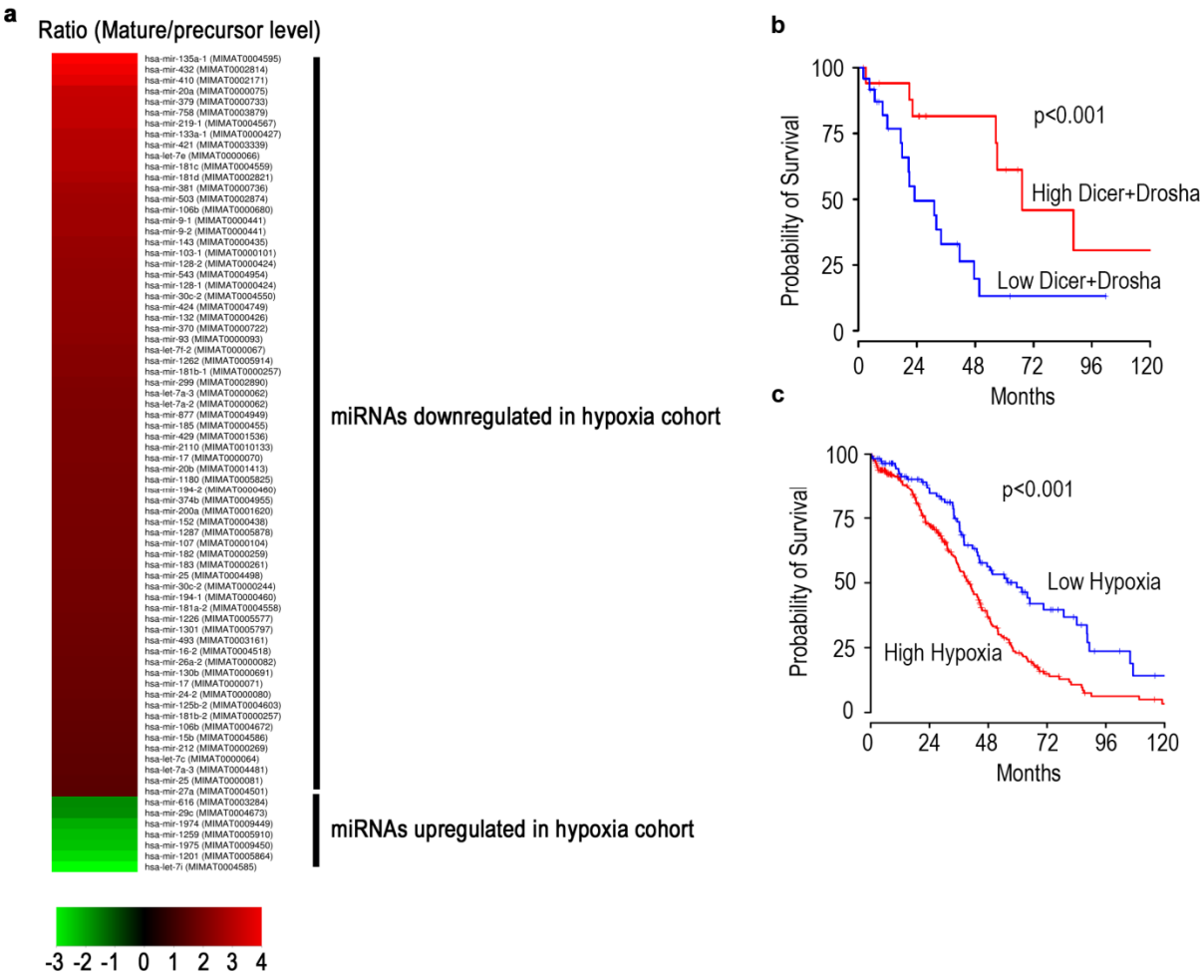

Figure 7: (a) Heat map depicting the ratio of mature miRNAs to precursor miRNAs in cells with high or low Drosha and Dicer expression levels. (b) Kaplan-Meier overall survival curves for Cancer Genome Atlas project (TCGA) samples analyzed for low and high Drosha and Dicer expression levels ($p < 0.001$). (c) Analysis of TCGA samples for hypoxia levels and correlation with overall survival duration plotted using the Kaplan-Meier method ($p < 0.001$).

Chapter 4: Drosha downregulation under hypoxia exposure is mediated *via* ETS1/ELK1 transcription factors

This chapter is based on Rupaimoole, R., S.Y. Wu, S. Pradeep, C. Ivan, C.V. Pecot, K.M. Gharpure, A.S. Nagaraja, G.N. Armaiz-Pena, M. McGuire, B. Zand, H.J. Dalton, J. Filant, J.B. Miller, C. Lu, N.C. Sadaoui, L.S. Mangala, M. Taylor, T. van den Beucken, E. Koch, C. Rodriguez-Aguayo, L. Huang, M. Bar-Eli, B.G. Wouters, M. Radovich, M. Ivan, G.A. Calin, W. Zhang, G. Lopez-Berestein, and A.K. Sood, Hypoxia-mediated downregulation of miRNA biogenesis promotes tumour progression. Nat Commun, 2014. 5: p. 5202.

Next, we investigated the mechanism by which hypoxia could regulate Drosha expression. There was no significant change in Drosha mRNA half-life under hypoxic conditions **(Figure 8a)**, pointing to transcriptional regulation of Drosha. Luciferase activity for the Drosha and Dicer promoters showed a significant decrease in Drosha promoter luciferase activity after exposure to hypoxia in A2780 cancer cells **(Figure 8b)**. Additionally, there was no significant change in Drosha protein half-life with hypoxia, suggesting that the mechanism is likely to be transcriptional **(Figure 8c)**. To identify potential regulatory transcription factors, we carried out bioinformatics analyses using Matinspector and Matbase (Genomatix Inc.). In addition, we tested the role of previously reported transcription factors in the hypoxia mediated downregulation of Drosha [35, 76, 77]. There was no significant

change in Drosha following siRNA mediated silencing of Myc, NF-kB or SP-1 transcription factors **(Figure 8d)**. From the bioinformatics analysis, ETS1 and ELK1 were found to have binding sites on opposite strands at very close proximity to the transcription initiation site **(Figure 8e, Table 4)**, and a previous study demonstrated transcriptional downregulation of downstream genes when ETS1/ELK1 bind to regions with very close proximity to the transcription initiation site [78]. Consistent with these findings, we observed an increase in both mRNA and protein levels of ETS1 and ELK1 under hypoxic conditions **(Figure 8f-h)**. Of note, we also observed an increase in pELK1 levels, suggesting that ELK1 is activated under hypoxic conditions **(Figure 8f)**.

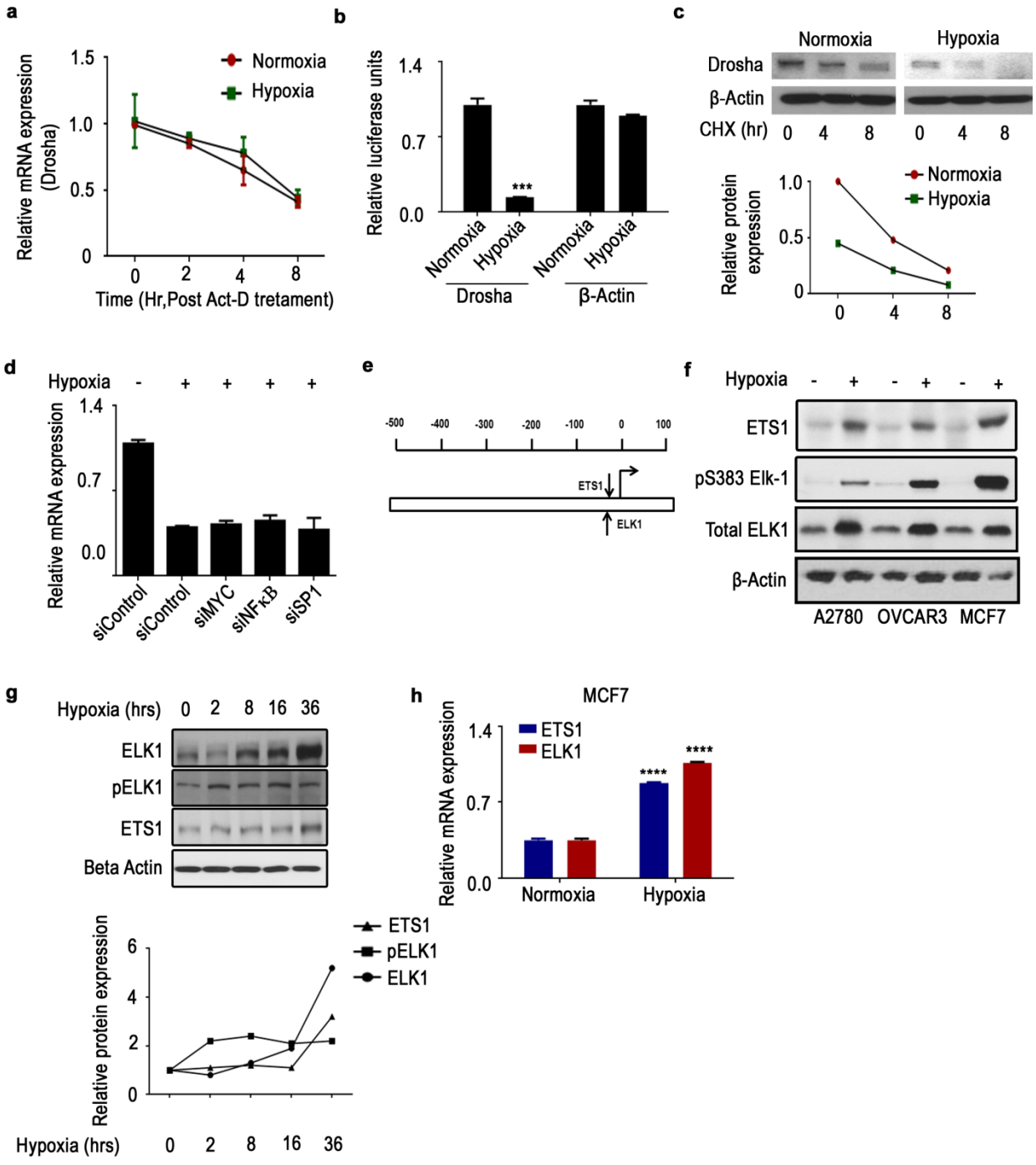
a
Relative mRNA expression (Drosha)
1.5
1.0
0.5
0
Normoxia
Hypoxia
0
2
4
8
Time (Hr,Post Act-D tretament)
b
Relative luciferase units
1.4
0.7
0.0
***
Normoxia
Hypoxia
Normoxia
Hypoxia
Drosha
β-Actin
c
Normoxia
Hypoxia
Drosha
β-Actin
CHX (hr)
0
4
8
0
4
8
Relative protein expression
1.0
0.5
0
Normoxia
Hypoxia
0
4
8
d
Hypoxia
-
+
+
+
+
Relative mRNA expression
1.4
0.7
0.0
siControl
siControl
siMYC
siNFκB
siSP1
e
-500
-400
-300
-200
-100
0
100
ETS1
ELK1
f
Hypoxia
-
+
-
+
-
+
ETS1
pS383 Elk-1
Total ELK1
β-Actin
A2780
OVCAR3
MCF7
g
Hypoxia (hrs)
0
2
8
16
36
ELK1
pELK1
ETS1
Beta Actin
Relative protein expression
6
4
2
0
ETS1
pELK1
ELK1
Hypoxia (hrs)
0
2
8
16
36
h
MCF7
Relative mRNA expression
1.4
0.7
0.0
ETS1
ELK1
****
****
Normoxia
Hypoxia

Figure 8: (a) Drosha mRNA half-life in A2780 cells exposed to normoxia and hypoxia in A2780 cells. (b), Relative luciferase reporter activity for the Drosha promoter region under hypoxic conditions. β-actin was used as a control. (c) Stability of Drosha protein in A2780 cells exposed to normoxia and hypoxia. Cycloheximide at 100ug/ml was used to block protein synthesis. (d) Drosha mRNA expression after siRNA mediated silencing of Myc, NF-kB, and SP-1 transcription factors under hypoxia exposure in A2780 cells. (e) Graphical representation of ETS1 and ELK1 binding sites on the Drosha promoter region. (f) Protein expression of ETS1 and ELK1 under hypoxic conditions in various cell lines. (g) ETS, ELK1, and pELK1 expression in A2780 cells across several time points. Quantitative data from Western blot are shown. (h) ETS1 and ELK1 mRNA expression levels under hypoxic conditions compared to normoxic conditions in MCF7 cells. Data are presented as mean ± standard error of the mean of n ≥ 3 independent experimental groups. ***p<0.001, ****p<0.0001 (Student t test).

We observed rescue of Drosha promoter activity in cells with mutations at the ETS1 or ELK1 binding sites under hypoxic conditions **(Figure 9a-b)**. Previous studies have demonstrated HIF1α-dependent increase in ETS1 [79] and ELK1 *via* MAPK signaling [80] under hypoxia exposure. Nevertheless, we tested the potential role of loss of miRNA repression under hypoxia exposure resulting in increased ETS1 and ELK1. In siDicer + siDrosha treated cells, we did not observe any significant changes in ETS1 or ELK1 expression **(Figure 9c)**. Also, we tested for CA9 and VEGF changes in siDicer + siDrosha treated cells and observed no significant changes in their expression **(Figure 9c),** ruling out the possibility miRNA repression loss as a mechanism for CA9 or VEGF increase under hypoxia exposure. Next, we knocked down ETS1 and/or ELK1 to study the eff ect of these 2 proteins on Drosha levels **(Figure 9d)**. Drosha expression was rescued after silencing ETS1, ELK1, or both, suggesting that ETS1 and ELK1 serve as transcriptional repressors for Drosha **(Figure 9e)**. Chromatin immunoprecipitation (ChIP) assays with anti-ETS1, anti-ELK1 were performed to confirm definitive binding of these elements in the promoter region. Compared with IgG or normoxic controls, significant enrichment in the binding of ETS1 and ELK1 to the promoter region of Drosha was observed in A2780 **(Figure 9f)** and MCF7 cells **(Figure 9g)** under hypoxic conditions. Additionally, we observed a significant reduction in polymerase II occupancy at the Drosha promoter region under hypoxia conditions **(Figure 9f)**.

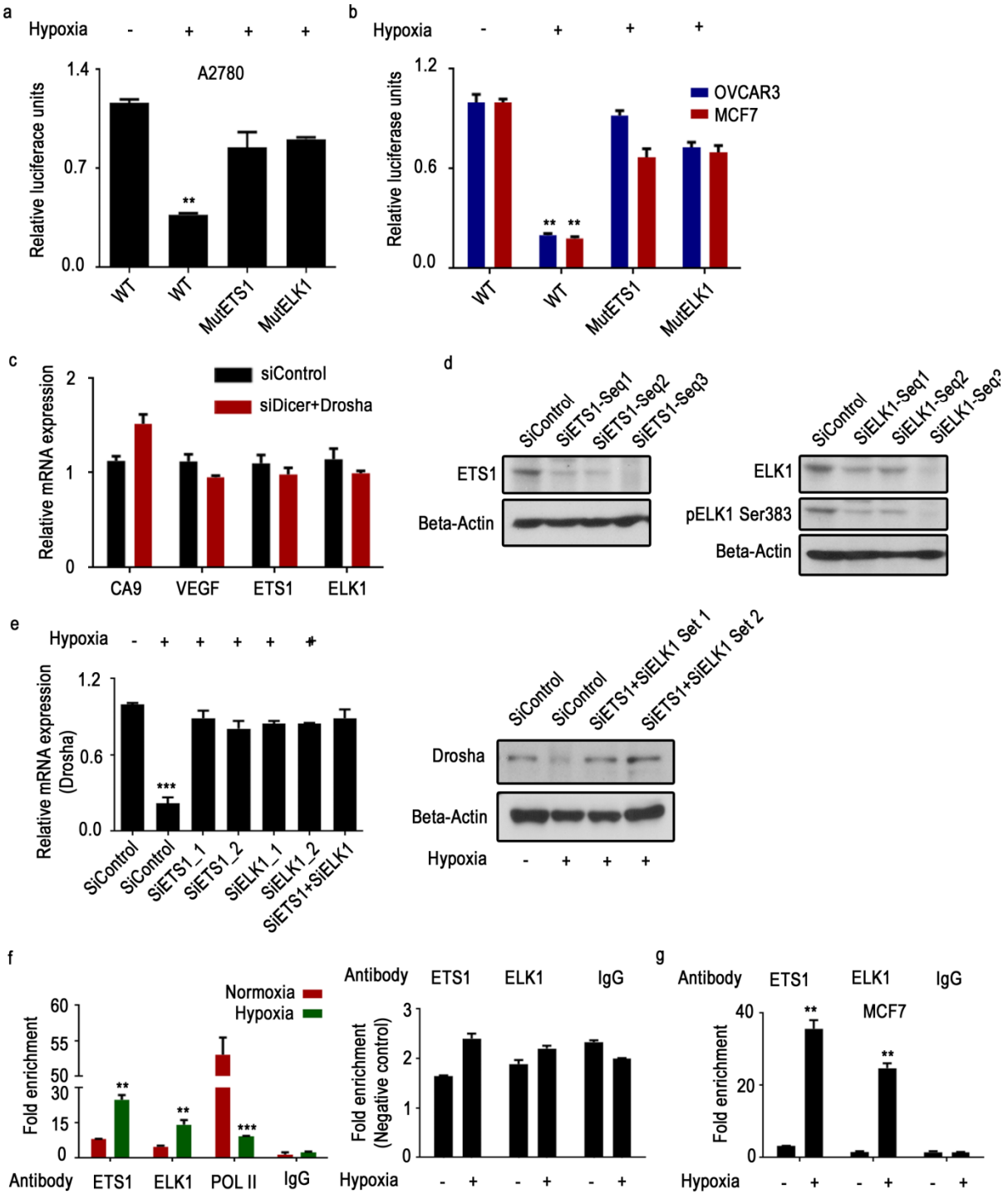
a
Hypoxia - + + +
A2780
Relative luciferace units
1.4
0.7
0.0
**
WT
WT
MutETS1
MutELK1
b
Hypoxia - + + +
OVCAR3
MCF7
Relative luciferase units
1.2
0.6
0.0
** **
WT
WT
MutETS1
MutELK1
c
siControl
siDicer+Drosha
Relative mRNA expression
2
1
0
CA9
VEGF
ETS1
ELK1
d
SiControl
SiETS1-Seq1
SiETS1-Seq2
SiETS1-Seq3
ETS1
Beta-Actin
SiControl
SiELK1-Seq1
SiELK1-Seq2
SiELK1-Seq3
ELK1
pELK1 Ser383
Beta-Actin
e
Hypoxia - + + + + +
Relative mRNA expression (Drosha)
1.2
0.6
0.0
***
SiControl
SiControl
SiETS1_1
SiETS1_2
SiELK1_1
SiELK1_2
SiETS1+SiELK1
SiControl
SiControl
SiETS1+SiELK1 Set 1
SiETS1+SiELK1 Set 2
Drosha
Beta-Actin
Hypoxia - + + +
f
Normoxia
Hypoxia
Fold enrichment
60
55
50
30
15
0
** ** ***
Antibody ETS1 ELK1 POL II IgG
Antibody ETS1 ELK1 IgG
Fold enrichment (Negative control)
3
2
1
0
Hypoxia - + - + - +
g
Antibody ETS1 ELK1 IgG
MCF7
Fold enrichment
40
20
0
** **
Hypoxia - + - + - +

Figure 9: (a, b), Luciferase reporter activity for the wild-type (WT) Drosha promoter region and the ETS1 or ELK1 binding site–mutant Drosha promoter region under hypoxic conditions in (a), A2780 cells and (b), OVCAR3, MCF7 MRNA and protein expression levels of ETS1 (a) and ELK1 (b) after siRNA-mediated silencing of respective genes using 3 different sequences of siRNA in A2780 cells. (c), Expression of CA9, VEGF, ETS1, and ELK1 in A2780 cells treated with siRNA against Dicer and Drosha. (d) Protein expression levels of ETS1 and ELK1 after siRNA-mediated silencing of respective genes using 3 different sequences of siRNA in A2780 cells. (e) Drosha expression under hypoxic conditions, after ETS1 and ELK1 gene knockdown with 2 independent siRNA sequences in A2780 cells. (f) Anti-ETS1, anti-ELK1, anti-POL II chromatin immunoprecipitation assay results showing fold enrichment of ETS1, ELK1, POL II binding to the Drosha promoter region in A2780 cells. Rabbit IgG was used as a control and real-time polymerase chain reaction (PCR) was used to quantitate the fold enrichment. Fold enrichment 1000 base pair upstream of ETS1 and ELK1 binding region at the Drosha promoter under hypoxia conditions in A2780 cells, used as negative control. (g) Fold enrichment of ETS1 and ELK1 binding at the Drosha promoter region under hypoxic conditions (MCF7), assessed using chromatin immunoprecipitation assays. Data are presented as mean ± standard error of the mean of n ≥ 3 independent experimental groups. **$p<0.01$, ***$p<0.001$ (Student t test).

To elucidate potential mechanisms by which ETS family members transcriptionally repress Drosha levels, we performed ingenuity pathway network analysis. This analysis revealed that ETS1 could bind to the histone de-acetylation-related molecule HDAC1 and that ELK1 could bind to the DNA methylation-related molecule ARID4B [81, 82] **(Figure 10a)**. A concentrated CpG island was observed near the Drosha promoter region where ETS1 and ELK1 bind **(Figure 10b)**. We performed methylation-specific polymerase chain reaction (MSP) reaction following treatment of DNA samples with bisulphite to study the impact of hypoxia on Drosha promoter methylation. Analysis of data revealed a significant increase in methylation at the ETS1 and ELK1 binding regions **(Figure 10c, d)** in DNA from cells exposed to hypoxia compared to normoxia cultured cells. Methylation specific restriction enzyme (MSRE) treatment and PCR analysis showed significant methylation at the CpG islands at the Drosha promoter region following *in vitro* hypoxia exposure or in bevacizumab treated *in vivo* tumor samples **(Figure 10e)**. In addition, cells treated with siRNAs against ETS1 or ELK1 under hypoxia showed significant reversal of Drosha promoter methylation compared to cells treated with control siRNA (**Figure 10f)**.

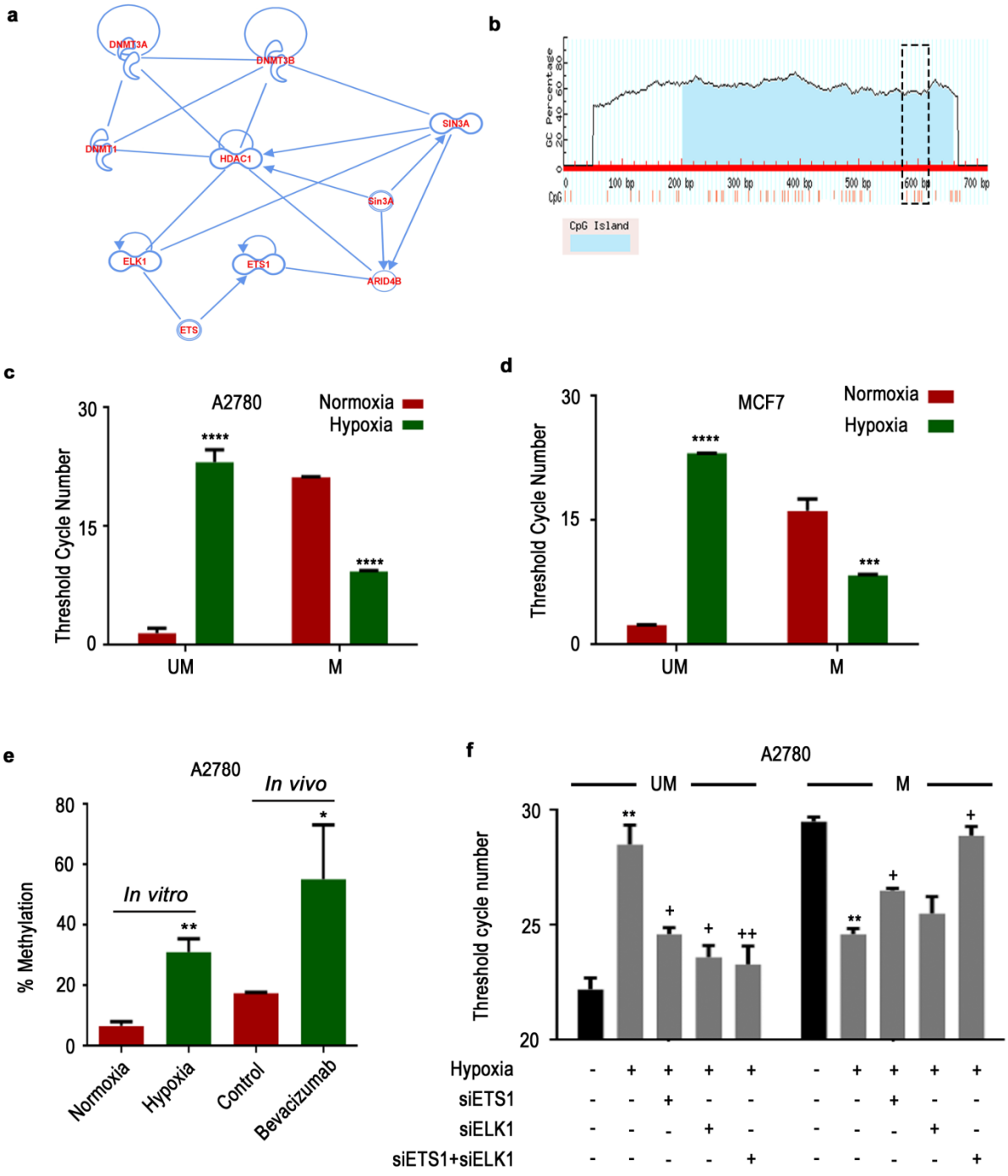
a
DNMT3A
DNMT3B
SIN3A
DNMT1
HDAC1
Sin3A
ELK1
ETS1
ARID4B
ETS
b
GC Percentage
0
20
40
60
80
0
100 bp
200 bp
300 bp
400 bp
500 bp
600 bp
700 bp
CpG
CpG Island
c
A2780
Normoxia
Hypoxia
Threshold Cycle Number
30
15
0
****
****
UM
M
d
MCF7
Normoxia
Hypoxia
Threshold Cycle Number
30
15
0
****
***
UM
M
e
A2780
In vivo
In vitro
% Methylation
80
60
40
20
0
**
*
Normoxia
Hypoxia
Control
Bevacizumab
f
A2780
UM
M
Threshold cycle number
30
25
20
Hypoxia
siETS1
siELK1
siETS1+siELK1

Figure 10: (a and b) Ingenuity pathway network analysis of possible interacting molecules of ETS1 and ELK1 and graphical representation of the CpG island in the Drosha promoter region. Dotted box highlights the area covered by methylation-specific primers. (c-d) Threshold cycle number of unmethylated (UM) and methylated (M) targeting primers under normoxic and hypoxic conditions in A2780 and MCF7 cells. (e) Percentage methylation in Drosha promoter region CpG island measured using methylation specific restriction enzyme analysis. DNA from A2780 cells exposed normoxia and hypoxia were used. (f) Threshold cycle number of unmethylated (UM) and methylated (M) targeting primers under normoxic and hypoxic conditions in A2780 cells treated with hypoxia and siETS1, siELK1 or combinations. Data are presented as mean ± standard error of the mean of $n \geq 3$ independent experimental groups. *$p<0.05$, **$p<0.01$, ***$p<0.001$ compared to normoxia control, +$p<0.05$, ++$p<0.01$, compared to hypoxia control. (Student t test).

Treatment of cells with the methylation inhibitor, azacitidine, or the HDAC1 inhibitor, valproic acid, under hypoxic conditions rescued Drosha levels, which was consistent with MSP or MSRE data (**Figure 11a**). In addition, *in vivo* tumor samples treated with azacitidine showed significant rescue of Drosha even under hypoxic conditions induced by anti-VEGF therapy (VEGF targeted antibody, B-20), with a corresponding increase in ETS1 and ELK1 levels **(Figure 11b)**. Cells treated with the HIF1α antagonist topotecan [83] under hypoxic conditions showed rescue of Drosha by suppressing ETS1 across several time points **(Figure 11c)**, confirming the role of HIF1α-mediated signaling in ETS1 expression. Importantly, immunoprecipitation of ETS1 and ELK1 from hypoxia-treated cells showed clear binding of ARID4B and HDAC1, respectively; this binding was abrogated by treatment of cells with siETS1 + siELK1 under hypoxia **(Figure 11d)**.

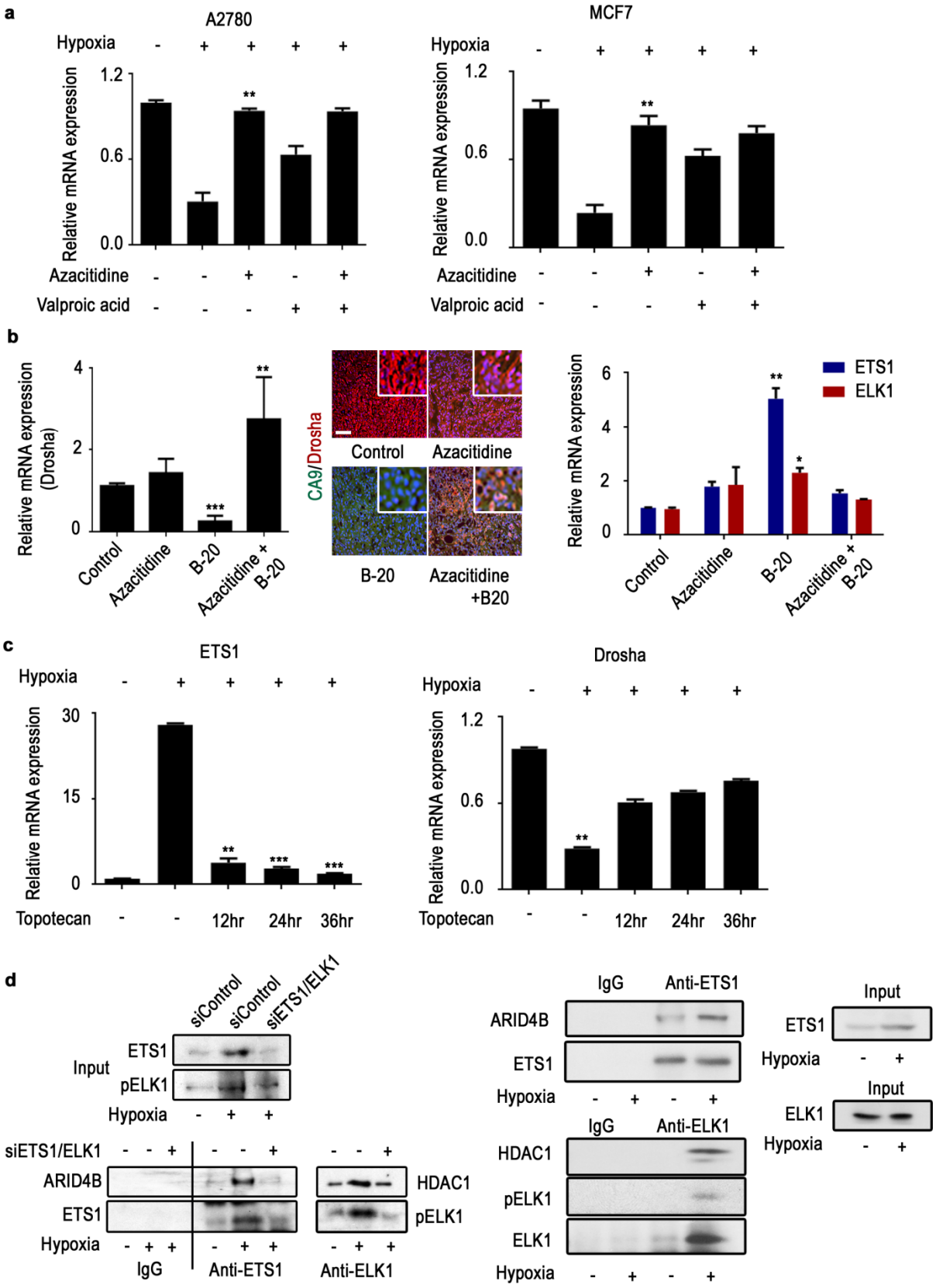
a
A2780
Hypoxia
Relative mRNA expression
Azacitidine
Valproic acid
MCF7
b
Relative mRNA expression (Drosha)
Control
Azacitidine
B-20
Azacitidine + B-20
CA9/Drosha
Azacitidine +B20
ETS1
ELK1
c
ETS1
Drosha
Topotecan
12hr
24hr
36hr
d
siControl
siETS1/ELK1
Input
pELK1
ARID4B
HDAC1
IgG
Anti-ETS1
Anti-ELK1
Anti-ELK1

Figure 11: (a) Drosha expression under hypoxic conditions in A2780 and MCF7 cells exposed to azacitidine and valproic acid either individually or in combination. (b) Drosha, ETS1 and ELK1 expression levels in tumor samples treated with B-20, azacitidine, or both in a A2780 mouse model of ovarian cancer. (c) ETS1 and Drosha expression in A2780 cells treated with the HIF1α inhibitor topotecan under hypoxic conditions. (d) Anti-ARID4B and anti-HDAC1 chromatin immunoprecipitation assay results showing fold enrichment of ARID4B and HDAC1 binding to the Drosha promoter region in A2780 cells. Data are presented as mean ± standard error of the mean of $n \geq 3$ independent experimental groups. *$p < 0.05$, **$p < 0.01$, ***$p < 0.001$ (Student t test).

In the A2780 mouse model of ovarian cancer, using DOPC nanoliposomes to deliver siRNAs against ETS1, ELK1, or both, we observed significant tumor reduction in the tumors treated with siETS1 and siELK1; the lowest tumor weight was observed in the combination treatment group **(Figure 12a)**. Tumors from all 3 treatment groups showed increased expression of Drosha compared with the control group, and a significant reduction in ETS1 and ELK1 was observed in the treatment groups **(Figure 12b)**. In the MCF7 orthotopic breast cancer model, treatment with the combination of siETS1-DOPC and siELK1-DOPC resulted in similar biological effects, suggesting that ETS1- and ELK1-mediated Drosha deregulation is not limited to one particular cancer type **(Figure 12c)**. To understand the clinical relevance to ETS1/ELK1 expression, we next examined the correlation of ETS1 and ELK1 with patient survival by analyzing mRNA expression of ETS1 and ELK1 in human ovarian tumor samples (n=74). Patients with high tumoral ETS1 or ELK1 expression had significantly lower survival compared to those with low ETS1 or ELK1 expression **(Figure 12d)**.

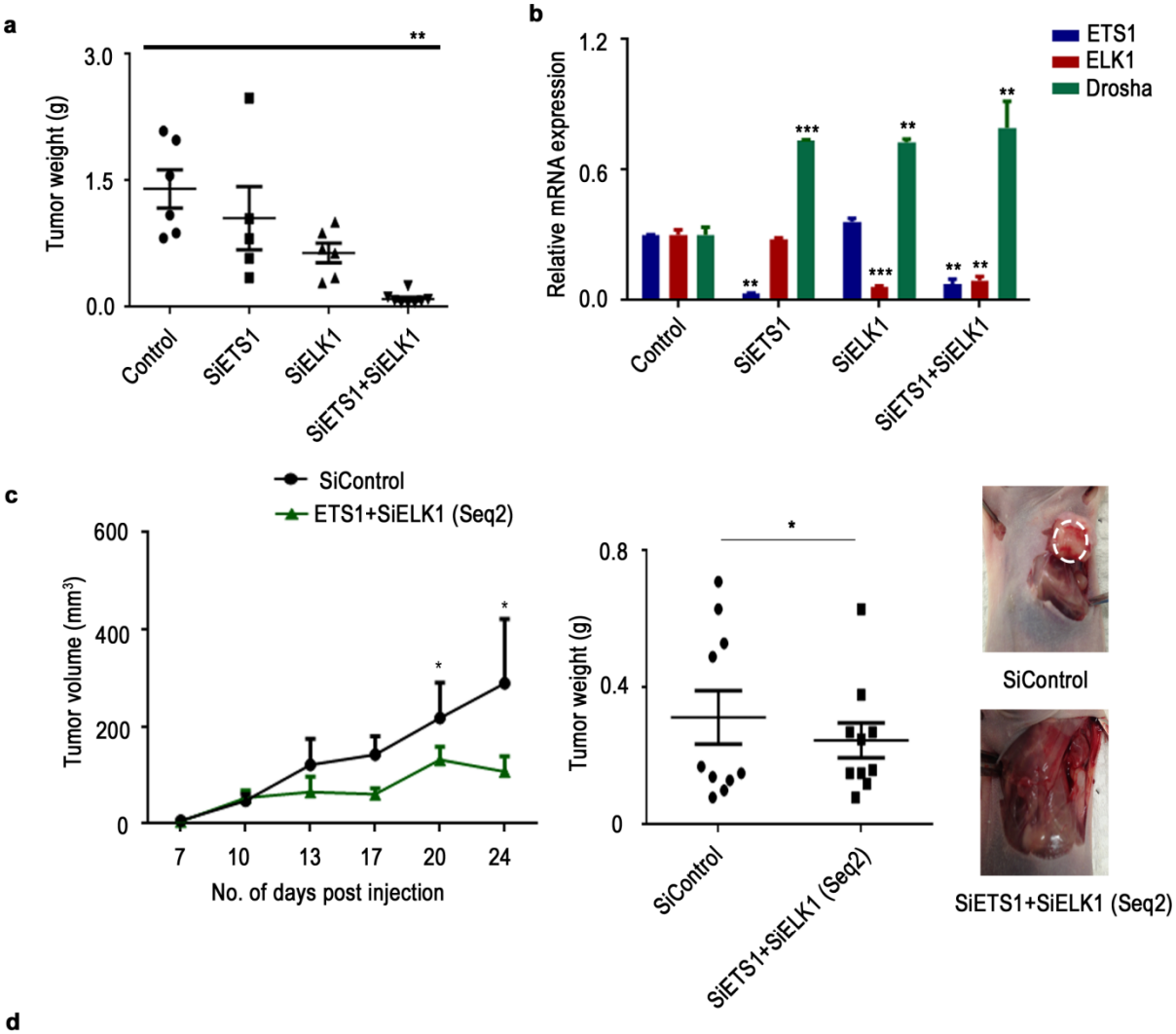
a
Tumor weight (g)
3.0
1.5
0.0
**
Control
SiETS1
SiELK1
SiETS1+SiELK1
b
Relative mRNA expression
1.2
0.6
0.0
ETS1
ELK1
Drosha
**
***
Control
SiETS1
SiELK1
SiETS1+SiELK1
c
SiControl
ETS1+SiELK1 (Seq2)
Tumor volume (mm³)
600
400
200
0
7
10
13
17
20
24
No. of days post injection
*
Tumor weight (g)
0.8
0.4
0
SiControl
SiETS1+SiELK1 (Seq2)
SiControl
SiETS1+SiELK1 (Seq2)
d
Probability of Survival
100
75
50
25
0
p<0.001
Low ETS1
High ETS1
0
24
48
72
96
120
Months
p<0.05
Low ELK1
High ELK1

Figure 12: (a) Aggregate tumor mass from tumors in the mouse orthotopic ovarian cancer model treated with control, ETS1, ELK1, and combination siRNAs. (b) Average mRNA expression of Drosha, ETS1, and ELK1 in the same tumor samples. All images shown are representative and data are presented as mean ± standard error of the mean of n ≥ 3 experimental groups. (c) Effect of silencing ETS1 and ELK1 using siRNAs (Seq2) in the MCF7 mouse model of breast cancer. Tumor volume and aggregate tumor weight across 2 groups. Representative pictures showing tumor burden in two groups. (d) Overall disease specific survival of patients with human high grade serous ovarian cancer (n=74) based on tumoral ETS1 (a) and ELK1 (b) mRNA expression levels. Kaplan-Meier curves shown; differences in survival were calculated using log rank method. *$p < 0.05$, **$p < 0.01$, ***$p < 0.001$ (Student t test).

Chapter 5: Hypoxia upregulated miR-630 mediates Dicer downregulation in hypoxia

In contrast to Drosha, Dicer expression was not affected by actinomycin D-mediated inhibition of mRNA transcription under hypoxic conditions **(Figure 13a**). This prompted us to examine potential 3' UTR-mediated Dicer mRNA degradation under hypoxic conditions. Dicer 3' UTR luciferase reporter assays showed significant reduction in reporter activity after cells were exposed to hypoxia **(Figure 13b)**. Also, Dicer promoter luciferase assay showed modest decrease in reporter activity under hypoxia exposure **(Figure 13b)**. To determine the specific miRNAs that are potentially involved in the downregulation of Dicer, we performed an integrative analysis using publicly available miRNA target prediction software and a miRNA array that compares miRNA expression in normoxic conditions with hypoxic conditions **(Table 4)**. Among the list of most significantly upregulated miRNAs, we found that miR-630 was validated to be one of the highly upregulated in hypoxia **(Figure 13c)** and it is also predicted to target Dicer. Transfection of miR-630 into cells resulted in significant downregulation of mRNA and protein expression levels of Dicer in A2780 cells **(Figure 13d)** and additional cell lines **(Figure 13e).** Treatment with anti-miR-630 under hypoxic conditions significantly rescued mRNA and protein expression of Dicer **(Figure 13d)**. To address the definitive role of miR-630-mediated downregulation of Dicer, we performed the Dicer 3' UTR assay. There was a significant reduction in luciferase reporter activity in cells treated with miR-630 compared with cells treated with control miRNA **(Figure 13f)**. A mutation in the Dicer

3’ UTR region that corresponds to the miR-630 binding region resulted in abrogation of the effect of miR-630 on Dicer 3’ UTR luciferase reporter activity **(Figure 13g)**.

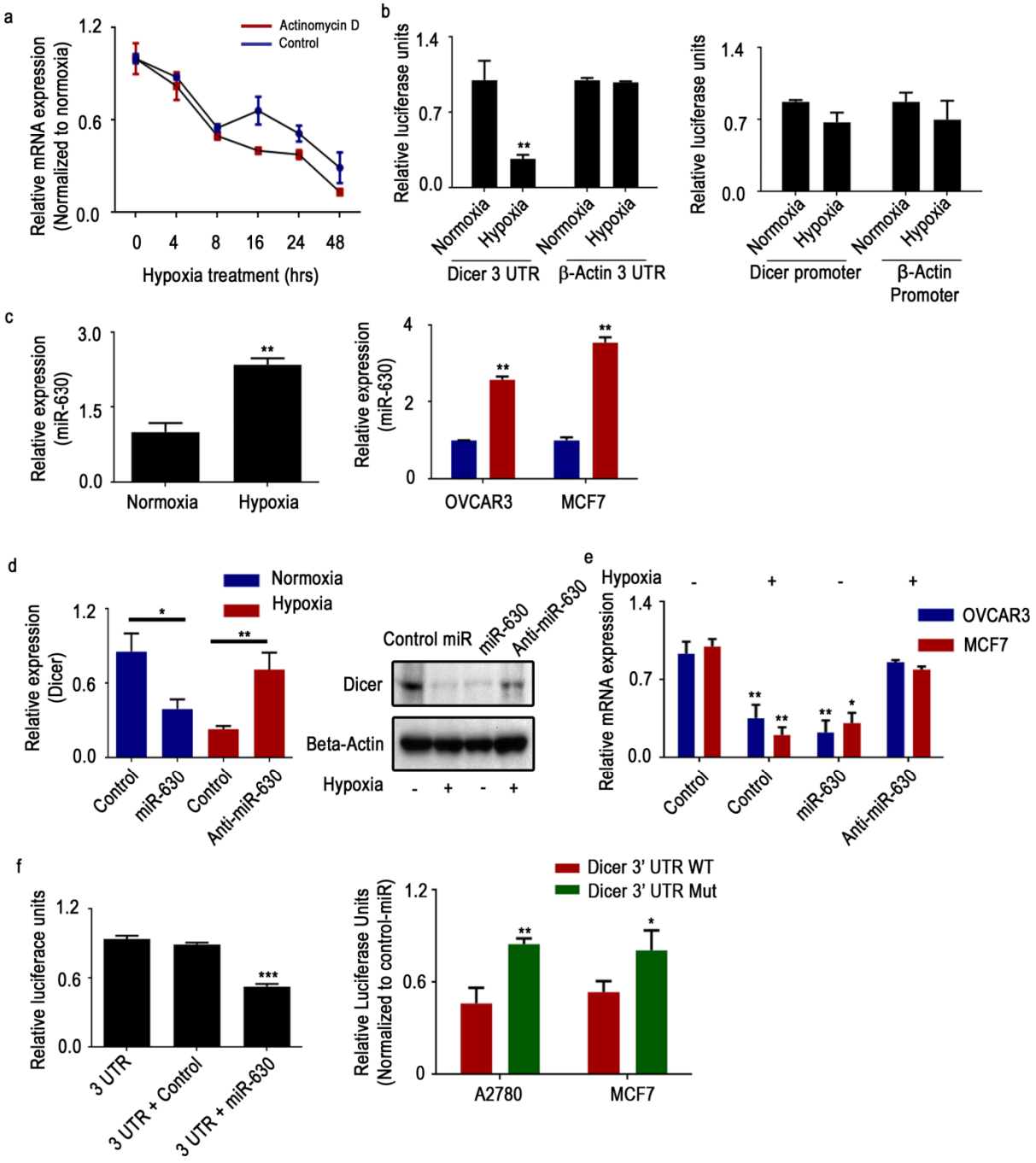
a
Relative mRNA expression (Normalized to normoxia)
Actinomycin D
Control
Hypoxia treatment (hrs)
b
Relative luciferase units
Normoxia
Hypoxia
Dicer 3 UTR
β-Actin 3 UTR
Dicer promoter
β-Actin Promoter
c
Relative expression (miR-630)
OVCAR3
MCF7
d
Relative expression (Dicer)
Control miR
miR-630
Anti-miR-630
Dicer
Beta-Actin
e
Relative mRNA expression
f
Relative luciferace units
3 UTR
3 UTR + Control
3 UTR + miR-630
Dicer 3' UTR WT
Dicer 3' UTR Mut
Relative Luciferase Units (Normalized to control-miR)
A2780

Figure 13: (a) Dicer mRNA decay under hypoxic conditions (relative to normoxic conditions) in A2780 cells with and without treatment with actinomycin D. (b) Relative Dicer 3' UTR and promoter luciferase reporter activity under hypoxic conditions. β-actin 3' UTR or promoter was used as a control. (c) Expression of miR-630 under hypoxic and normoxic conditions in A2780, OVCAR3, and MCF7 cells. (d) mRNA and protein expression of Dicer after transfecting cells with miR-630 under normoxic conditions or with anti-miR-630 under hypoxic conditions in A2780 cells (right panel) and additional cells (left panel). (e) Dicer 3' UTR luciferase reporter activity with and without miR-630 in A2780 cell line (left panel). Dicer 3' UTR wild type (WT) and mir-630 binding site mutant (mut) luciferase activity under hypoxia conditions in the A2780 and MCF7 cells (right panel). Data are presented as mean ± standard error of the mean of $n \geq 3$ independent experimental groups. *$p < 0.05$, **$p < 0.01$, ***$p < 0.001$ (Student t test).

Table 4: miRNAs predicted to target Dicer and upregulated under hypoxia condition		
miRNA name	**Number of algorithms**	**Name/s of Algorithm**
miR-150*	1	miRanda
miR-188-5p	1	miRanda
miR-32*	1	miRanda
miR-1271	2	PITA|RNA22
miR-1275	2	PITA|RNA22
miR-134	2	PITA|RNA22
miR-574-5p	2	miRanda|PITA
miR-671-5p	2	PITA|RNA22
miR-939	2	PITA|RNA22
miR-1224-5p	3	miRanda|PITA|RNA22
miR-125b-2*	3	TargetScan||miRandaRNA23
miR-371-5p	3	miRanda|microT|PITA
miR-1183	4	TargetScan|miRanda|PITA|RNA22
miR-1202	4	TargetScan|miRanda|PITA|RNA22
miR-1207-5p	4	TargetScan|miRanda|PITA|RNA22
miR-210	4	TargetScan|miRanda|PITA|RNA22
miR-513b	4	TargetScan|miRanda|PITA|RNA22
miR-557	4	TargetScan|miRanda|PITA|RNA22
miR-638	4	TargetScan|miRanda|PITA|RNA22
miR-630	5	TargetScan|miRanda|PITA|RNA22|microT
miR-375	5	TargetScan|miRanda|PITA|RNA22|microT
miR-498	5	TargetScan|miRanda|PITA|RNA22|microT
miR-513a-5p	5	TargetScan|miRanda|PITA|RNA22|microT
miR-610	5	TargetScan|miRanda|PITA|RNA22|microT
miR-877	5	TargetScan|miRanda|PITA|RNA22|PicTar

Quantification of precursor miR-630 showed increased expression of pri-miR-630 under hypoxic conditions, suggesting that miR-630 is transcriptionally upregulated **(Figure 14a)**. Consistent with *in vitro* findings, in A2780 model tumor samples treated with bevacizumab, we found a substantial increase in miR-630 expression both at mature and precursor levels **(Figure 14b)**. Deep sequencing mRNA array data cross-referenced with miR-630 promoter analysis for potential transcription factor binding, suggested that STAT1 binding to the promoter region potentially leads to increased precursor levels of miR-630. Under hypoxic conditions, STAT1 and pSTAT1 levels were increased significantly at the mRNA and protein levels **(Figure 14c)**. Use of siRNA-mediated gene silencing led to significant STAT1 gene knockdown **(Figure 14d)**. Expression of Dicer was significantly rescued under hypoxic conditions by treating cells with siSTAT1, and a corresponding reduction in miR-630 expression levels **(Figure 14e)** was also observed.

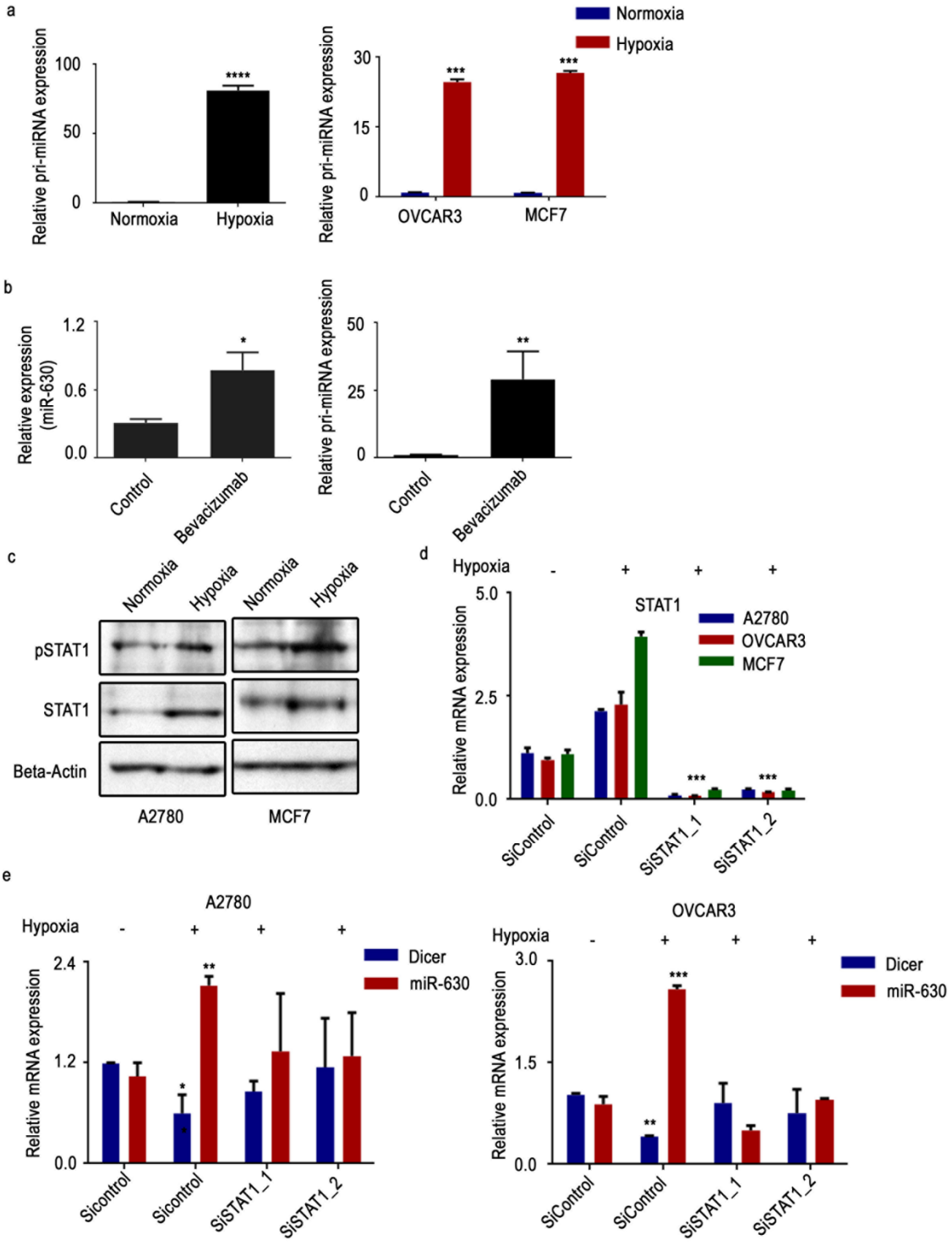
a
Relative pri-miRNA expression
100
50
0
****
Normoxia
Hypoxia
Normoxia
Hypoxia
30
15
0
***
***
OVCAR3
MCF7
b
Relative expression (miR-630)
1.2
0.6
0.0
*
Control
Bevacizumab
Relative pri-miRNA expression
50
25
0
**
Control
Bevacizumab
c
Normoxia
Hypoxia
Normoxia
Hypoxia
pSTAT1
STAT1
Beta-Actin
A2780
MCF7
d
Hypoxia
-
+
+
+
Relative mRNA expression
5.0
2.5
0.0
STAT1
A2780
OVCAR3
MCF7
***
***
SiControl
SiControl
SiSTAT1_1
SiSTAT1_2
e
A2780
Hypoxia
-
+
+
+
Relative mRNA expression
2.4
1.2
0.0
Dicer
miR-630
**
*
Sicontrol
Sicontrol
SiSTAT1_1
SiSTAT1_2
OVCAR3
Hypoxia
-
+
+
+
Relative mRNA expression
3.0
1.5
0.0
Dicer
miR-630
***
**
SiControl
SiControl
SiSTAT1_1
SiSTAT1_2

Figure 14: (a) Expression of Pri-miRNA-630 levels in A2780, OVCAR3, and MCF7 cells exposed to hypoxia. (b) Mature and pri-miRNA-630 levels in A2780 mouse tumor samples treated with bevacizumab, a VEGF antibody. (c) Western blot data showing protein expression of STAT1 (total STAT1 and phospoSTAT1) under hypoxic conditions in A2780 and MCF7 cells. (d) Efficiency of siRNAs targeting the STAT1 gene, as well as STAT1 mRNA expression under hypoxic conditions. (e) mRNA levels of miR-630 and Dicer in the hypoxia-treated cells with or without STAT1 gene knockdown using siRNAs. Data are presented as mean ± standard error of the mean of n ≥ 3 independent experimental groups. *p < 0.05, **p < 0.01, ***p < 0.001, ****p<0.0001 (Student t test).

To understand the biological implications of miR-630 mediated Dicer downregulation under hypoxic conditions, we delivered miR-630 to A2780 tumors *in vivo*. There was significantly increased tumor burden and metastasis following treatment with miR-630-DOPC **(Figure 15a-d)**. We observed metastases in several organs such as omentum, liver in miR-630 treated group while no metastasis was observed in control miRNA treated group **(Figure 15d)**. Importantly, decreased Dicer expression was observed in tumors from mice treated with miR-630 **(Figure 15e)**. We also examined 30 human epithelial ovarian cancer samples, which showed an inverse correlation between Dicer and miR-630 expression **(Figure 15f)**. In addition, we observed a significant positive correlation between miR-630 expression and CA9 levels in these clinical samples **(Figure 15f)**.

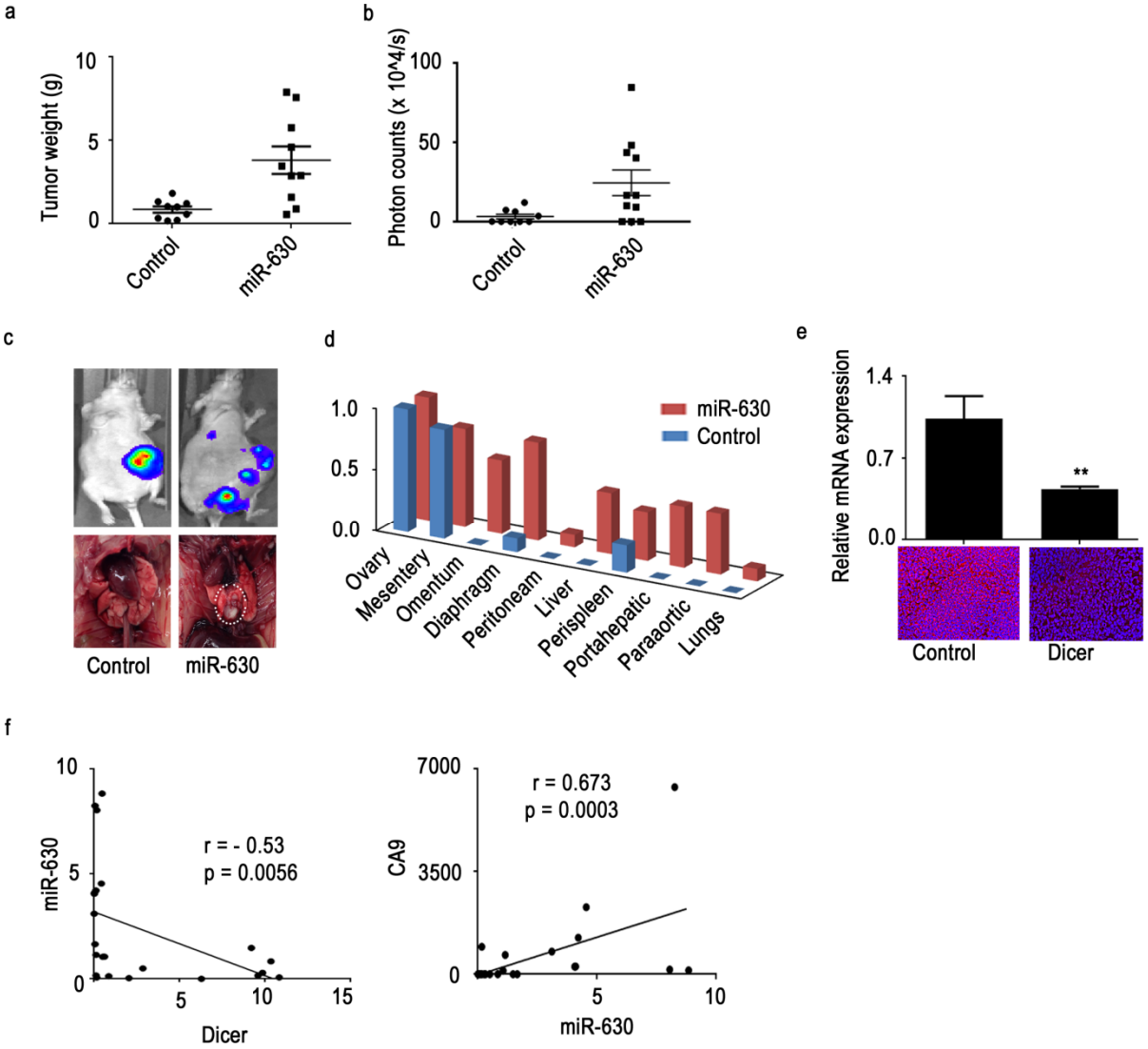
a
Tumor weight (g)
10
5
0
Control
miR-630
b
Photon counts (x 10^4/s)
100
50
0
Control
miR-630
c
Control
miR-630
d
miR-630
Control
1.0
0.5
0.0
Ovary
Mesentery
Omentum
Diaphragm
Peritoneam
Liver
Perispleen
Portahepatic
Paraaortic
Lungs
e
Relative mRNA expression
1.4
0.7
0.0
**
Control
Dicer
f
miR-630
10
5
0
r = - 0.53
p = 0.0056
5
10
15
Dicer
CA9
7000
3500
0
r = 0.673
p = 0.0003
5
10
miR-630

Figure 15: (a-b) Aggregate tumor mass and photon counts from tumors in the mouse orthotopic ovarian cancer model treated with control microRNA and miR-630 (n = 10 per group). (c) Representative pictures showing tumor burden using luminescence from the tumors (top) and gross tumor mass in the lung, showing a rare metastasis nodule in the miR-630 group (bottom). (d) Pattern of metastatic spread in mice treated with control microRNA and miR-630. (e) mRNA and protein expression levels of Dicer in A2780 mouse tumor samples treated with control microRNA or miR-630. (f) Pearson correlation graphs showing Dicer vs miR-630, miR-630 vs CA9 expression level correlation in clinical tumor samples. All images shown are representative and data are presented as mean ± standard error of the mean of n ≥ 3 experimental groups. **$p < 0.01$ (Student t test).

Chapter 6: Hypoxia downregulation of Drosha and Dicer leads to increased tumor progression

This chapter is based on Rupaimoole, R., S.Y. Wu, S. Pradeep, C. Ivan, C.V. Pecot, K.M. Gharpure, A.S. Nagaraja, G.N. Armaiz-Pena, M. McGuire, B. Zand, H.J. Dalton, J. Filant, J.B. Miller, C. Lu, N.C. Sadaoui, L.S. Mangala, M. Taylor, T. van den Beucken, E. Koch, C. Rodriguez-Aguayo, L. Huang, M. Bar-Eli, B.G. Wouters, M. Radovich, M. Ivan, G.A. Calin, W. Zhang, G. Lopez-Berestein, and A.K. Sood, Hypoxia-mediated downregulation of miRNA biogenesis promotes tumour progression. Nat Commun, 2014. 5: p. 5202.

To identify potential tumor promoting pathways affected by hypoxia, we analyzed mRNA expression data from deep sequencing coupled with miRNA expression data from miRNA array analysis of A2780 cells exposed to hypoxia and normoxia. Ingenuity pathway network analysis of mRNA and miRNA data from deep sequencing identified key novel miRNA-mRNA interactions that could potentially lead to enhanced tumor progression under hypoxic conditions **(Table 5)**. MiR-200, a well-studied miRNA to play role in cancer growth and metastasis, was one among the hypoxia activated networks identified. Pathway enrichment analyses revealed that cell adhesion, migration, and growth networks were the most significantly upregulated pathways under hypoxic conditions **(Figure 16a)**. Cells under hypoxic conditions had consistent upregulation of RHOB1, TAGLN, SRTAD1, TXNIP, JAG1,

CTGF, and JUN, while corresponding miRNAs let7a, miR-135a, miR-146a, and miR-30c were significantly downregulated under hypoxic conditions (**Figure 6, 16b**). Dicer, and Drosha silencing under normoxia resulted in similar downregulation of the aforementioned miRNAs and corresponding upregulation of genes (**Figure 6, 16b)**. Ectopic expression of Dicer and Drosha under hypoxia exposure resulted in rescue of the miRNAs and corresponding downregulation of mRNA targets (**Figure 6, 16b)**. In addition, we tested the known miR-185 and HIF2α axis [64] in the A2780 cancer cells following exposure to hypoxia. MiR-185 was significantly downregulated along with corresponding upregulation of HIF2α **(Figure 16c)**. Additionally, rescue of miR-185 by Drosha and Dicer ectopic expression or delivery of miR-185 mimics under hypoxia exposure resulted in significant downregulation of HIF2α **(Figure 16c)**. These data further support the role of hypoxia-mediated Dicer and Drosha deregulation in hypoxia signaling and tumor progression. Consistent with the altered pathways described above, enhanced epithelial-to-mesenchymal transition (EMT) features were observed in cells under hypoxic conditions in A2780 and several additional cell lines **(Figure 16d, e)**.

a

mRNA data (Normoxia vs Hypoxia)

Molecular function	p Value
Cellular Development	3.91E-15 to 1.35E-04
Cellular Growth and Proliferation	3.94E-15 to 1.35E-04
Cell Death	1.39E-14 to 1.42E-04
Cellular Movement	1.78E-14 to 1.40E-04
Cell Cycle	7.21E-13 to1.35E-04

miRNA data (Normoxia vs Hypoxia)

Molecular function	p Value
Cellular Movement	1.37E-06 to 4.27E-02
Cellular Growth and Proliferation	3.76E-05 to 4.83E-02
Cell Cycle	5.08E-05 to 4.55E-02
Cell Death	6.21E-05 to 3.71E-02
Cellular Development	8.23E-05 to 4.83E-02

b

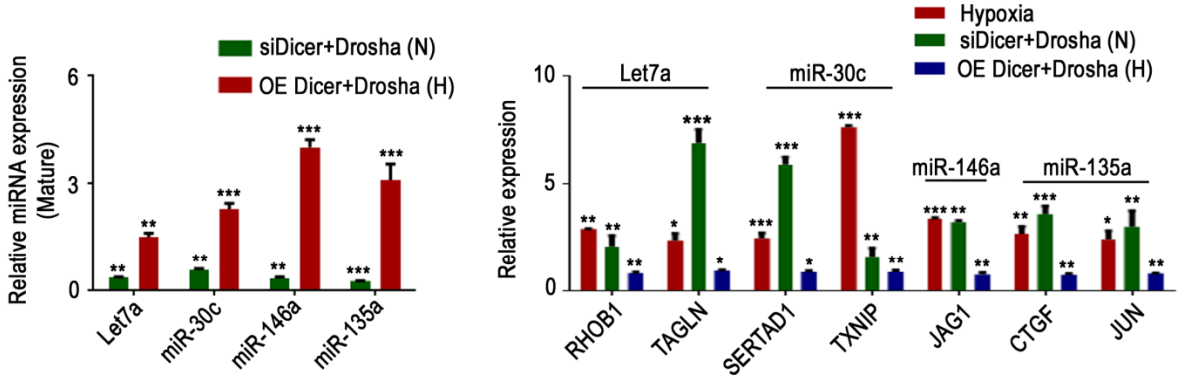

c

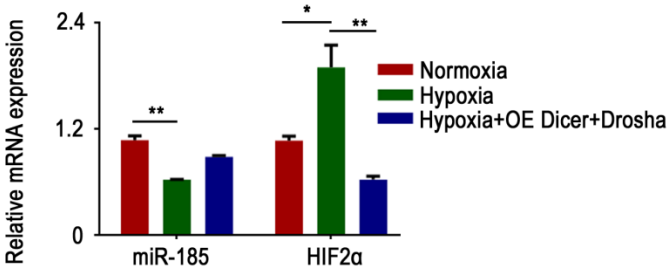

d

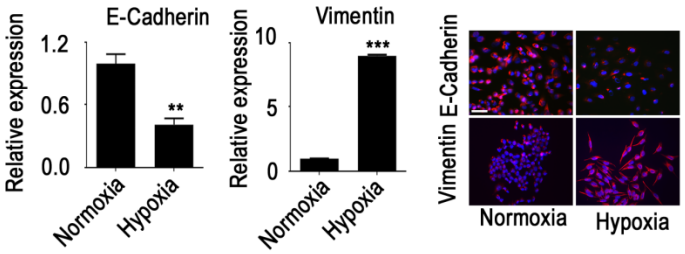

e

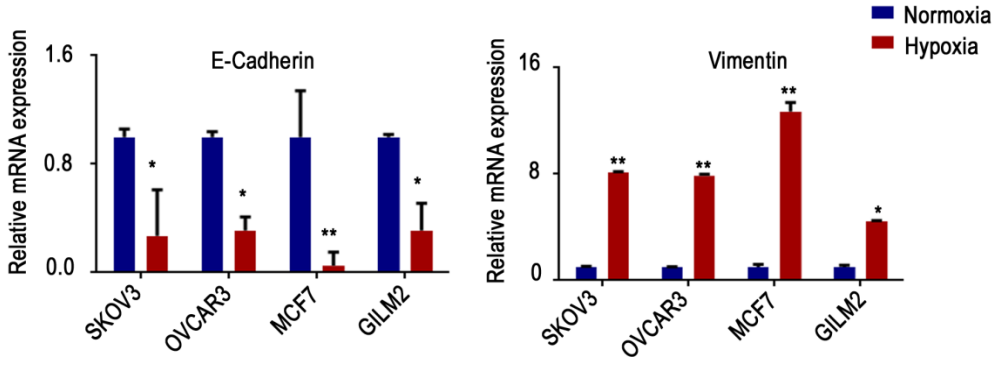

Figure 16: (a) Top 5 molecular functions that are significantly altered as result of mRNAs (left) or miRNAs (right) deregulated under hypoxic condition. Data are from RNA deep sequencing and miRNA arrays from cells exposed to hypoxia and normoxia. Data were analyzed using ingenuity pathway network analysis. (b) Expression of significantly altered pro-miRNAs (a) and metastatic genes (b) in Dicer and Drosha knocked down A2780 cells under normoxia (data shown normalized to siControl) or ectopic expression of Dicer and Drosha under hypoxia (data shown normalized to control), N - normoxia and H - hypoxia. (c) Expression of miR-185 and HIF2α in A2780 cells exposed normoxia, hypoxia, and cells ectopically expressing Dicer and Drosha exposed hypoxia. (d-e) E-cadherin, vimentin expression levels under hypoxic exposure in A2780 cells (d) and additional cell lines (e). Blue - Nucleus, Scale bar: 200 μm. Data are presented as mean ± standard error of the mean of n ≥ 3 independent experimental groups. *p<0.05, **p<0.01, ***p<0.001 (Student t test).

Table 5: Ingenuity miRNA-mRNA target analysis of upregulated mRNAs and downregulated miRNA data from cells exposed to hypoxia for 48hrs			
miRNA Symbol	**Fold Change**	**Target Symbol**	**Fold Change**
let-7a-5p (and other miRNAs w/seed GAGGUAG)	-2.743	ADAMTS1	1.282
let-7a-5p (and other miRNAs w/seed GAGGUAG)	-2.743	APBB3	1.132
let-7a-5p (and other miRNAs w/seed GAGGUAG)	-2.743	BLOC1S6	1.049
let-7a-5p (and other miRNAs w/seed GAGGUAG)	-2.743	BTG2	1.410
let-7a-5p (and other miRNAs w/seed GAGGUAG)	-2.743	C8orf58	1.036
let-7a-5p (and other miRNAs w/seed GAGGUAG)	-2.743	CACNA1I	1.662
let-7a-5p (and other miRNAs w/seed GAGGUAG)	-2.743	CDKN1A	2.696
let-7a-5p (and other miRNAs w/seed GAGGUAG)	-2.743	DUSP1	1.039
let-7a-5p (and other miRNAs w/seed GAGGUAG)	-2.743	ERGIC1	1.176
let-7a-5p (and other miRNAs w/seed GAGGUAG)	-2.743	ERO1L	1.770
let-7a-5p (and other miRNAs w/seed GAGGUAG)	-2.743	FAM43A	1.004
let-7a-5p (and other miRNAs w/seed GAGGUAG)	-2.743	FAM84B	2.062
let-7a-5p (and other miRNAs w/seed GAGGUAG)	-2.743	FGF11	1.348
let-7a-5p (and other miRNAs w/seed GAGGUAG)	-2.743	GLRX	1.667
let-7a-5p (and other miRNAs w/seed GAGGUAG)	-2.743	HAND1	1.299
let-7a-5p (and other miRNAs w/seed GAGGUAG)	-2.743	HK2	1.760
let-7a-5p (and other miRNAs w/seed GAGGUAG)	-2.743	HMOX1	1.615
let-7a-5p (and other miRNAs w/seed GAGGUAG)	-2.743	KIAA1244	1.781
let-7a-5p (and other miRNAs w/seed GAGGUAG)	-2.743	LAMP2	1.465
let-7a-5p (and other miRNAs w/seed GAGGUAG)	-2.743	LCOR	1.124
let-7a-5p (and other miRNAs w/seed GAGGUAG)	-2.743	MEF2D	1.467
let-7a-5p (and other miRNAs w/seed GAGGUAG)	-2.743	MGAT3	1.248
let-7a-5p (and other miRNAs w/seed GAGGUAG)	-2.743	NIPA1	1.111
let-7a-5p (and other miRNAs w/seed GAGGUAG)	-2.743	NSD1	1.049
let-7a-5p (and other miRNAs w/seed GAGGUAG)	-2.743	OPA3	1.089
let-7a-5p (and other miRNAs w/seed GAGGUAG)	-2.743	PANX2	2.065
let-7a-5p (and other miRNAs w/seed GAGGUAG)	-2.743	PIK3IP1	1.162
let-7a-5p (and other miRNAs w/seed GAGGUAG)	-2.743	PLD3	1.173
let-7a-5p (and other miRNAs w/seed GAGGUAG)	-2.743	PTP4A2	1.349
let-7a-5p (and other miRNAs w/seed GAGGUAG)	-2.743	PTPRU	1.168
let-7a-5p (and other miRNAs w/seed GAGGUAG)	-2.743	RBM38	1.055
let-7a-5p (and other miRNAs w/seed GAGGUAG)	-2.743	RGS16	1.133
let-7a-5p (and other miRNAs w/seed GAGGUAG)	-2.743	RHOB	2.088
let-7a-5p (and other miRNAs w/seed GAGGUAG)	-2.743	RIMKLA	1.216
let-7a-5p (and other miRNAs w/seed GAGGUAG)	-2.743	RIOK3	1.137
let-7a-5p (and other miRNAs w/seed GAGGUAG)	-2.743	RNF165	1.396
let-7a-5p (and other miRNAs w/seed GAGGUAG)	-2.743	RRAGD	2.537
let-7a-5p (and other miRNAs w/seed GAGGUAG)	-2.743	SBK1	1.336
let-7a-5p (and other miRNAs w/seed GAGGUAG)	-2.743	SEC14L5	1.227
let-7a-5p (and other miRNAs w/seed GAGGUAG)	-2.743	SLC25A4	1.245
let-7a-5p (and other miRNAs w/seed GAGGUAG)	-2.743	SULF2	1.185
let-7a-5p (and other miRNAs w/seed GAGGUAG)	-2.743	SYT11	1.129
let-7a-5p (and other miRNAs w/seed GAGGUAG)	-2.743	TAGLN	3.009
let-7a-5p (and other miRNAs w/seed GAGGUAG)	-2.743	TEAD3	1.352
let-7a-5p (and other miRNAs w/seed GAGGUAG)	-2.743	TMEM194A	1.019
let-7a-5p (and other miRNAs w/seed GAGGUAG)	-2.743	ZBTB5	1.316
let-7a-5p (and other miRNAs w/seed GAGGUAG)	-2.743	ZMAT3	1.827
let-7a-5p (and other miRNAs w/seed GAGGUAG)	-2.743	ZNF275	1.185
let-7a-5p (and other miRNAs w/seed GAGGUAG)	-2.743	ZNF652	1.135
let-7a-5p (and other miRNAs w/seed GAGGUAG)	-2.743	ZSWIM4	1.474
miR-100-5p (and other miRNAs w/seed ACCCGUA)	-2.267	FGFR3	1.093
miR-100-5p (and other miRNAs w/seed ACCCGUA)	-2.267	RRAGD	2.537
miR-100-5p (and other miRNAs w/seed ACCCGUA)	-2.267	ZNF483	1.449
miR-101-3p (and other miRNAs w/seed ACAGUAC)	-1.187	ABCA1	1.079
miR-101-3p (and other miRNAs w/seed ACAGUAC)	-1.187	ANKRD44	1.184
miR-101-3p (and other miRNAs w/seed ACAGUAC)	-1.187	ANXA2	1.210

miR-101-3p (and other miRNAs w/seed ACAGUAC)	-1.187	BLOC1S6	1.049
miR-101-3p (and other miRNAs w/seed ACAGUAC)	-1.187	C3orf58	1.041
miR-101-3p (and other miRNAs w/seed ACAGUAC)	-1.187	CCNG2	1.522
miR-101-3p (and other miRNAs w/seed ACAGUAC)	-1.187	CEBPA	1.103
miR-101-3p (and other miRNAs w/seed ACAGUAC)	-1.187	CGGBP1	1.049
miR-101-3p (and other miRNAs w/seed ACAGUAC)	-1.187	CREB1	1.133
miR-101-3p (and other miRNAs w/seed ACAGUAC)	-1.187	CSRNP2	1.827
miR-101-3p (and other miRNAs w/seed ACAGUAC)	-1.187	CSRP2	1.708
miR-101-3p (and other miRNAs w/seed ACAGUAC)	-1.187	DDIT4	1.032
miR-101-3p (and other miRNAs w/seed ACAGUAC)	-1.187	DUSP1	1.039
miR-101-3p (and other miRNAs w/seed ACAGUAC)	-1.187	DUSP5	1.262
miR-101-3p (and other miRNAs w/seed ACAGUAC)	-1.187	FAM73A	1.318
miR-101-3p (and other miRNAs w/seed ACAGUAC)	-1.187	FAM84B	2.062
miR-101-3p (and other miRNAs w/seed ACAGUAC)	-1.187	FGFR3	1.093
miR-101-3p (and other miRNAs w/seed ACAGUAC)	-1.187	FOS	1.838
miR-101-3p (and other miRNAs w/seed ACAGUAC)	-1.187	HNRNPU	1.486
miR-101-3p (and other miRNAs w/seed ACAGUAC)	-1.187	JUNB	1.051
miR-101-3p (and other miRNAs w/seed ACAGUAC)	-1.187	KIAA1244	1.781
miR-101-3p (and other miRNAs w/seed ACAGUAC)	-1.187	LCOR	1.124
miR-101-3p (and other miRNAs w/seed ACAGUAC)	-1.187	MCL1	1.009
miR-101-3p (and other miRNAs w/seed ACAGUAC)	-1.187	MEF2D	1.467
miR-101-3p (and other miRNAs w/seed ACAGUAC)	-1.187	N4BP2	1.143
miR-101-3p (and other miRNAs w/seed ACAGUAC)	-1.187	NDRG4	2.087
miR-101-3p (and other miRNAs w/seed ACAGUAC)	-1.187	NSD1	1.049
miR-101-3p (and other miRNAs w/seed ACAGUAC)	-1.187	PCDH7	1.417
miR-101-3p (and other miRNAs w/seed ACAGUAC)	-1.187	PHLDA1	2.392
miR-101-3p (and other miRNAs w/seed ACAGUAC)	-1.187	POLH	1.072
miR-101-3p (and other miRNAs w/seed ACAGUAC)	-1.187	PPFIA4	1.955
miR-101-3p (and other miRNAs w/seed ACAGUAC)	-1.187	SCN2A	1.391
miR-101-3p (and other miRNAs w/seed ACAGUAC)	-1.187	SYT11	1.129
miR-101-3p (and other miRNAs w/seed ACAGUAC)	-1.187	TEAD3	1.352
miR-101-3p (and other miRNAs w/seed ACAGUAC)	-1.187	TP53INP1	2.279
miR-101-3p (and other miRNAs w/seed ACAGUAC)	-1.187	TRIM9	2.268
miR-101-3p (and other miRNAs w/seed ACAGUAC)	-1.187	UNKL	1.007
miR-101-3p (and other miRNAs w/seed ACAGUAC)	-1.187	WSB1	1.697
miR-101-3p (and other miRNAs w/seed ACAGUAC)	-1.187	ZBTB5	1.316
miR-101-3p (and other miRNAs w/seed ACAGUAC)	-1.187	ZMAT3	1.827
miR-10a-5p (and other miRNAs w/seed ACCCUGU)	-1.490	CREB1	1.133
miR-10a-5p (and other miRNAs w/seed ACCCUGU)	-1.490	E2F7	1.181
miR-10a-5p (and other miRNAs w/seed ACCCUGU)	-1.490	ELAVL3	2.393
miR-10a-5p (and other miRNAs w/seed ACCCUGU)	-1.490	EPHA2	1.001
miR-10a-5p (and other miRNAs w/seed ACCCUGU)	-1.490	LCOR	1.124
miR-10a-5p (and other miRNAs w/seed ACCCUGU)	-1.490	LRRFIP1	1.351
miR-10a-5p (and other miRNAs w/seed ACCCUGU)	-1.490	POLH	1.072
miR-10a-5p (and other miRNAs w/seed ACCCUGU)	-1.490	PTP4A2	1.349
miR-10a-5p (and other miRNAs w/seed ACCCUGU)	-1.490	RAP2A	1.052
miR-10a-5p (and other miRNAs w/seed ACCCUGU)	-1.490	RNF165	1.396
miR-10a-5p (and other miRNAs w/seed ACCCUGU)	-1.490	SCARB2	1.076
miR-10a-5p (and other miRNAs w/seed ACCCUGU)	-1.490	SSPN	1.003
miR-10a-5p (and other miRNAs w/seed ACCCUGU)	-1.490	WDR26	1.935
miR-125b-5p (and other miRNAs w/seed CCCUGAG)	-2.271	ADAMTS1	1.282
miR-125b-5p (and other miRNAs w/seed CCCUGAG)	-2.271	ANKRD44	1.184
miR-125b-5p (and other miRNAs w/seed CCCUGAG)	-2.271	CACNB3	1.353
miR-125b-5p (and other miRNAs w/seed CCCUGAG)	-2.271	CREB1	1.133
miR-125b-5p (and other miRNAs w/seed CCCUGAG)	-2.271	CYTH2	1.322
miR-125b-5p (and other miRNAs w/seed CCCUGAG)	-2.271	DNAJB2	1.439
miR-125b-5p (and other miRNAs w/seed CCCUGAG)	-2.271	DPYSL4	2.528
miR-125b-5p (and other miRNAs w/seed CCCUGAG)	-2.271	DUSP3	1.718
miR-125b-5p (and other miRNAs w/seed CCCUGAG)	-2.271	EXO5	1.247

miR-125b-5p (and other miRNAs w/seed CCCUGAG)	-2.271	FAM73A	1.318
miR-125b-5p (and other miRNAs w/seed CCCUGAG)	-2.271	GLTP	1.437
miR-125b-5p (and other miRNAs w/seed CCCUGAG)	-2.271	GPR160	1.030
miR-125b-5p (and other miRNAs w/seed CCCUGAG)	-2.271	HK2	1.760
miR-125b-5p (and other miRNAs w/seed CCCUGAG)	-2.271	ID2	1.682
miR-125b-5p (and other miRNAs w/seed CCCUGAG)	-2.271	KIAA1244	1.781
miR-125b-5p (and other miRNAs w/seed CCCUGAG)	-2.271	LCOR	1.124
miR-125b-5p (and other miRNAs w/seed CCCUGAG)	-2.271	MCL1	1.009
miR-125b-5p (and other miRNAs w/seed CCCUGAG)	-2.271	MEF2D	1.467
miR-125b-5p (and other miRNAs w/seed CCCUGAG)	-2.271	MXD4	1.829
miR-125b-5p (and other miRNAs w/seed CCCUGAG)	-2.271	NIPA1	1.111
miR-125b-5p (and other miRNAs w/seed CCCUGAG)	-2.271	PERP	1.026
miR-125b-5p (and other miRNAs w/seed CCCUGAG)	-2.271	PPME1	1.186
miR-125b-5p (and other miRNAs w/seed CCCUGAG)	-2.271	PSTPIP2	1.485
miR-125b-5p (and other miRNAs w/seed CCCUGAG)	-2.271	RAPGEFL1	1.031
miR-125b-5p (and other miRNAs w/seed CCCUGAG)	-2.271	RBM38	1.055
miR-125b-5p (and other miRNAs w/seed CCCUGAG)	-2.271	RIMKLA	1.216
miR-125b-5p (and other miRNAs w/seed CCCUGAG)	-2.271	RYBP	1.208
miR-125b-5p (and other miRNAs w/seed CCCUGAG)	-2.271	SCARB2	1.076
miR-125b-5p (and other miRNAs w/seed CCCUGAG)	-2.271	SCARF2	1.021
miR-125b-5p (and other miRNAs w/seed CCCUGAG)	-2.271	STAT3	2.118
miR-125b-5p (and other miRNAs w/seed CCCUGAG)	-2.271	STX6	1.220
miR-125b-5p (and other miRNAs w/seed CCCUGAG)	-2.271	SUN1	1.178
miR-125b-5p (and other miRNAs w/seed CCCUGAG)	-2.271	TMEM194A	1.019
miR-125b-5p (and other miRNAs w/seed CCCUGAG)	-2.271	TP53INP1	2.279
miR-125b-5p (and other miRNAs w/seed CCCUGAG)	-2.271	WDR1	1.065
miR-125b-5p (and other miRNAs w/seed CCCUGAG)	-2.271	ZNF652	1.135
miR-125b-5p (and other miRNAs w/seed CCCUGAG)	-2.271	ZSWIM4	1.474
miR-1263 (miRNAs w/seed UGGUACC)	-1.215	CSRNP1	2.331
miR-1263 (miRNAs w/seed UGGUACC)	-1.215	GBE1	1.498
miR-1276 (miRNAs w/seed AAAGAGC)	-1.278	LAMP2	1.465
miR-1287-5p (miRNAs w/seed GCUGGAU)	-1.187	TEAD3	1.352
miR-1288-3p (miRNAs w/seed GGACUGC)	-1.101	EXO5	1.247
miR-1288-3p (miRNAs w/seed GGACUGC)	-1.101	LAMP2	1.465
miR-1288-3p (miRNAs w/seed GGACUGC)	-1.101	SMAD7	1.135
miR-1288-3p (miRNAs w/seed GGACUGC)	-1.101	ZYX	1.635
miR-1305 (miRNAs w/seed UUUCAAC)	-1.167	GALNT3	1.021
miR-135a-5p (and other miRNAs w/seed AUGGCUU)	-1.464	CCNG2	1.522
miR-135a-5p (and other miRNAs w/seed AUGGCUU)	-1.464	CNTNAP1	1.190
miR-135a-5p (and other miRNAs w/seed AUGGCUU)	-1.464	DUSP5	1.262
miR-135a-5p (and other miRNAs w/seed AUGGCUU)	-1.464	HNRNPU	1.486
miR-135a-5p (and other miRNAs w/seed AUGGCUU)	-1.464	JADE1	1.702
miR-135a-5p (and other miRNAs w/seed AUGGCUU)	-1.464	KDM5B	1.270
miR-135a-5p (and other miRNAs w/seed AUGGCUU)	-1.464	KIAA1244	1.781
miR-135a-5p (and other miRNAs w/seed AUGGCUU)	-1.464	KLHL28	1.155
miR-135a-5p (and other miRNAs w/seed AUGGCUU)	-1.464	LRRFIP1	1.351
miR-135a-5p (and other miRNAs w/seed AUGGCUU)	-1.464	MCL1	1.009
miR-135a-5p (and other miRNAs w/seed AUGGCUU)	-1.464	MTURN	1.126
miR-135a-5p (and other miRNAs w/seed AUGGCUU)	-1.464	NCKIPSD	1.502
miR-135a-5p (and other miRNAs w/seed AUGGCUU)	-1.464	NDRG4	2.087
miR-135a-5p (and other miRNAs w/seed AUGGCUU)	-1.464	PLEKHA2	2.391
miR-135a-5p (and other miRNAs w/seed AUGGCUU)	-1.464	PTPRF	1.930
miR-135a-5p (and other miRNAs w/seed AUGGCUU)	-1.464	RAP2A	1.052
miR-135a-5p (and other miRNAs w/seed AUGGCUU)	-1.464	RIMKLA	1.216
miR-135a-5p (and other miRNAs w/seed AUGGCUU)	-1.464	RRBP1	1.139
miR-135a-5p (and other miRNAs w/seed AUGGCUU)	-1.464	RYBP	1.208
miR-135a-5p (and other miRNAs w/seed AUGGCUU)	-1.464	SCN2A	1.391
miR-135a-5p (and other miRNAs w/seed AUGGCUU)	-1.464	SERTAD2	1.719
miR-135a-5p (and other miRNAs w/seed AUGGCUU)	-1.464	STX6	1.220

miR-135a-5p (and other miRNAs w/seed AUGGCUU)	-1.464	TXNIP	1.918
miR-135a-5p (and other miRNAs w/seed AUGGCUU)	-1.464	VGLL4	1.395
miR-135a-5p (and other miRNAs w/seed AUGGCUU)	-1.464	VLDLR	1.193
miR-135a-5p (and other miRNAs w/seed AUGGCUU)	-1.464	WDR45B	1.383
miR-135a-5p (and other miRNAs w/seed AUGGCUU)	-1.464	ZNF275	1.185
miR-135a-5p (and other miRNAs w/seed AUGGCUU)	-1.464	ZNF652	1.135
miR-135a-5p (and other miRNAs w/seed AUGGCUU)	-1.464	ZSWIM4	1.474
miR-140-5p (and other miRNAs w/seed AGUGGUU)	-1.176	ABCA1	1.079
miR-140-5p (and other miRNAs w/seed AGUGGUU)	-1.176	CREB1	1.133
miR-140-5p (and other miRNAs w/seed AGUGGUU)	-1.176	CYTH2	1.322
miR-140-5p (and other miRNAs w/seed AGUGGUU)	-1.176	DCLRE1C	1.132
miR-140-5p (and other miRNAs w/seed AGUGGUU)	-1.176	HEY1	1.133
miR-140-5p (and other miRNAs w/seed AGUGGUU)	-1.176	IGSF3	1.003
miR-140-5p (and other miRNAs w/seed AGUGGUU)	-1.176	LAMP2	1.465
miR-140-5p (and other miRNAs w/seed AGUGGUU)	-1.176	LCOR	1.124
miR-140-5p (and other miRNAs w/seed AGUGGUU)	-1.176	MEF2D	1.467
miR-140-5p (and other miRNAs w/seed AGUGGUU)	-1.176	MYH9	1.022
miR-140-5p (and other miRNAs w/seed AGUGGUU)	-1.176	PLOD1	1.088
miR-140-5p (and other miRNAs w/seed AGUGGUU)	-1.176	PTP4A2	1.349
miR-140-5p (and other miRNAs w/seed AGUGGUU)	-1.176	RIOK3	1.137
miR-140-5p (and other miRNAs w/seed AGUGGUU)	-1.176	SCARB2	1.076
miR-140-5p (and other miRNAs w/seed AGUGGUU)	-1.176	SLC2A1	1.583
miR-140-5p (and other miRNAs w/seed AGUGGUU)	-1.176	SMAD3	1.013
miR-140-5p (and other miRNAs w/seed AGUGGUU)	-1.176	STC2	1.551
miR-140-5p (and other miRNAs w/seed AGUGGUU)	-1.176	SULF2	1.185
miR-140-5p (and other miRNAs w/seed AGUGGUU)	-1.176	TP53INP1	2.279
miR-140-5p (and other miRNAs w/seed AGUGGUU)	-1.176	ZNF652	1.135
miR-141-3p (and other miRNAs w/seed AACACUG)	-1.658	ANKRD44	1.184
miR-141-3p (and other miRNAs w/seed AACACUG)	-1.658	ARL4A	1.065
miR-141-3p (and other miRNAs w/seed AACACUG)	-1.658	ATRN	1.085
miR-141-3p (and other miRNAs w/seed AACACUG)	-1.658	BHLHE40	1.610
miR-141-3p (and other miRNAs w/seed AACACUG)	-1.658	CACNA1I	1.662
miR-141-3p (and other miRNAs w/seed AACACUG)	-1.658	CGGBP1	1.049
miR-141-3p (and other miRNAs w/seed AACACUG)	-1.658	DUSP3	1.718
miR-141-3p (and other miRNAs w/seed AACACUG)	-1.658	EGLN1	1.478
miR-141-3p (and other miRNAs w/seed AACACUG)	-1.658	EPHA2	1.001
miR-141-3p (and other miRNAs w/seed AACACUG)	-1.658	EXOC7	1.178
miR-141-3p (and other miRNAs w/seed AACACUG)	-1.658	FAM84B	2.062
miR-141-3p (and other miRNAs w/seed AACACUG)	-1.658	GLRX	1.667
miR-141-3p (and other miRNAs w/seed AACACUG)	-1.658	GPRC5C	2.499
miR-141-3p (and other miRNAs w/seed AACACUG)	-1.658	IRF2BPL	1.501
miR-141-3p (and other miRNAs w/seed AACACUG)	-1.658	KIAA0408	1.050
miR-141-3p (and other miRNAs w/seed AACACUG)	-1.658	KIAA1715	1.239
miR-141-3p (and other miRNAs w/seed AACACUG)	-1.658	MBTD1	1.374
miR-141-3p (and other miRNAs w/seed AACACUG)	-1.658	NRIP3	1.307
miR-141-3p (and other miRNAs w/seed AACACUG)	-1.658	PAQR7	1.135
miR-141-3p (and other miRNAs w/seed AACACUG)	-1.658	PDCD4	1.269
miR-141-3p (and other miRNAs w/seed AACACUG)	-1.658	PDXP	1.048
miR-141-3p (and other miRNAs w/seed AACACUG)	-1.658	PRKAR1A	1.012
miR-141-3p (and other miRNAs w/seed AACACUG)	-1.658	RYBP	1.208
miR-141-3p (and other miRNAs w/seed AACACUG)	-1.658	SCARB2	1.076
miR-141-3p (and other miRNAs w/seed AACACUG)	-1.658	SHROOM4	1.366
miR-141-3p (and other miRNAs w/seed AACACUG)	-1.658	SIDT2	1.420
miR-141-3p (and other miRNAs w/seed AACACUG)	-1.658	TP53INP1	2.279
miR-141-3p (and other miRNAs w/seed AACACUG)	-1.658	YPEL5	1.866
miR-141-3p (and other miRNAs w/seed AACACUG)	-1.658	ZMAT3	1.827
miR-146a-5p (and other miRNAs w/seed GAGAACU)	-1.397	BTG2	1.410
miR-146a-5p (and other miRNAs w/seed GAGAACU)	-1.397	CNTFR	1.302
miR-146a-5p (and other miRNAs w/seed GAGAACU)	-1.397	FAM43A	1.004

miR-146a-5p (and other miRNAs w/seed GAGAACU)	-1.397	LCOR	1.124
miR-146a-5p (and other miRNAs w/seed GAGAACU)	-1.397	NRIP3	1.307
miR-146a-5p (and other miRNAs w/seed GAGAACU)	-1.397	NSD1	1.049
miR-146a-5p (and other miRNAs w/seed GAGAACU)	-1.397	RRM2B	1.367
miR-146a-5p (and other miRNAs w/seed GAGAACU)	-1.397	SLC2A3	1.781
miR-146a-5p (and other miRNAs w/seed GAGAACU)	-1.397	STAT1	1.423
miR-146a-5p (and other miRNAs w/seed GAGAACU)	-1.397	TMEM194A	1.019
miR-146a-5p (and other miRNAs w/seed GAGAACU)	-1.397	TPM1	1.385
miR-146a-5p (and other miRNAs w/seed GAGAACU)	-1.397	VASN	1.865
miR-146a-5p (and other miRNAs w/seed GAGAACU)	-1.397	VWCE	1.179
miR-146a-5p (and other miRNAs w/seed GAGAACU)	-1.397	ZNF652	1.135
miR-16-5p (and other miRNAs w/seed AGCAGCA)	-1.667	ADAMTS1	1.282
miR-16-5p (and other miRNAs w/seed AGCAGCA)	-1.667	AHNAK2	1.604
miR-16-5p (and other miRNAs w/seed AGCAGCA)	-1.667	AK4	1.350
miR-16-5p (and other miRNAs w/seed AGCAGCA)	-1.667	BTG2	1.410
miR-16-5p (and other miRNAs w/seed AGCAGCA)	-1.667	C8orf58	1.036
miR-16-5p (and other miRNAs w/seed AGCAGCA)	-1.667	CNTNAP1	1.190
miR-16-5p (and other miRNAs w/seed AGCAGCA)	-1.667	CSRNP1	2.331
miR-16-5p (and other miRNAs w/seed AGCAGCA)	-1.667	CSRNP2	1.827
miR-16-5p (and other miRNAs w/seed AGCAGCA)	-1.667	E2F7	1.181
miR-16-5p (and other miRNAs w/seed AGCAGCA)	-1.667	EGLN1	1.478
miR-16-5p (and other miRNAs w/seed AGCAGCA)	-1.667	FAM73A	1.318
miR-16-5p (and other miRNAs w/seed AGCAGCA)	-1.667	GLRX	1.667
miR-16-5p (and other miRNAs w/seed AGCAGCA)	-1.667	GLS2	1.156
miR-16-5p (and other miRNAs w/seed AGCAGCA)	-1.667	HMOX1	1.615
miR-16-5p (and other miRNAs w/seed AGCAGCA)	-1.667	HPCAL4	1.720
miR-16-5p (and other miRNAs w/seed AGCAGCA)	-1.667	IRF2BPL	1.501
miR-16-5p (and other miRNAs w/seed AGCAGCA)	-1.667	JUN	2.508
miR-16-5p (and other miRNAs w/seed AGCAGCA)	-1.667	LAMP2	1.465
miR-16-5p (and other miRNAs w/seed AGCAGCA)	-1.667	LCOR	1.124
miR-16-5p (and other miRNAs w/seed AGCAGCA)	-1.667	MCL1	1.009
miR-16-5p (and other miRNAs w/seed AGCAGCA)	-1.667	NCKIPSD	1.502
miR-16-5p (and other miRNAs w/seed AGCAGCA)	-1.667	NFE2L1	1.418
miR-16-5p (and other miRNAs w/seed AGCAGCA)	-1.667	NISCH	1.496
miR-16-5p (and other miRNAs w/seed AGCAGCA)	-1.667	PAM	1.554
miR-16-5p (and other miRNAs w/seed AGCAGCA)	-1.667	PDCD4	1.269
miR-16-5p (and other miRNAs w/seed AGCAGCA)	-1.667	PFKFB4	2.462
miR-16-5p (and other miRNAs w/seed AGCAGCA)	-1.667	PHLDA3	1.593
miR-16-5p (and other miRNAs w/seed AGCAGCA)	-1.667	PLEKHA1	1.476
miR-16-5p (and other miRNAs w/seed AGCAGCA)	-1.667	PPM1D	1.536
miR-16-5p (and other miRNAs w/seed AGCAGCA)	-1.667	RAB11FIP5	1.155
miR-16-5p (and other miRNAs w/seed AGCAGCA)	-1.667	RAPGEFL1	1.031
miR-16-5p (and other miRNAs w/seed AGCAGCA)	-1.667	RNF24	1.347
miR-16-5p (and other miRNAs w/seed AGCAGCA)	-1.667	SESN1	2.178
miR-16-5p (and other miRNAs w/seed AGCAGCA)	-1.667	SHROOM4	1.366
miR-16-5p (and other miRNAs w/seed AGCAGCA)	-1.667	SIDT2	1.420
miR-16-5p (and other miRNAs w/seed AGCAGCA)	-1.667	SLC16A3	1.081
miR-16-5p (and other miRNAs w/seed AGCAGCA)	-1.667	SLC22A17	1.103
miR-16-5p (and other miRNAs w/seed AGCAGCA)	-1.667	SLC2A14	1.169
miR-16-5p (and other miRNAs w/seed AGCAGCA)	-1.667	SLC2A3	1.781
miR-16-5p (and other miRNAs w/seed AGCAGCA)	-1.667	SMAD3	1.013
miR-16-5p (and other miRNAs w/seed AGCAGCA)	-1.667	SMAD7	1.135
miR-16-5p (and other miRNAs w/seed AGCAGCA)	-1.667	SQSTM1	1.301
miR-16-5p (and other miRNAs w/seed AGCAGCA)	-1.667	SYDE1	1.791
miR-16-5p (and other miRNAs w/seed AGCAGCA)	-1.667	TMEM41B	1.076
miR-16-5p (and other miRNAs w/seed AGCAGCA)	-1.667	TMEM74B	1.796
miR-16-5p (and other miRNAs w/seed AGCAGCA)	-1.667	TXNIP	1.918
miR-16-5p (and other miRNAs w/seed AGCAGCA)	-1.667	WSB1	1.697
miR-16-5p (and other miRNAs w/seed AGCAGCA)	-1.667	ZMAT3	1.827

miR-16-5p (and other miRNAs w/seed AGCAGCA)	-1.667	ZNF275	1.185
miR-16-5p (and other miRNAs w/seed AGCAGCA)	-1.667	ZNF652	1.135
miR-16-5p (and other miRNAs w/seed AGCAGCA)	-1.667	ZYX	1.635
miR-17-5p (and other miRNAs w/seed AAAGUGC)	-1.677	ABCA1	1.079
miR-17-5p (and other miRNAs w/seed AAAGUGC)	-1.677	AHNAK	2.181
miR-17-5p (and other miRNAs w/seed AAAGUGC)	-1.677	AK4	1.350
miR-17-5p (and other miRNAs w/seed AAAGUGC)	-1.677	ARL4A	1.065
miR-17-5p (and other miRNAs w/seed AAAGUGC)	-1.677	BNIP3L	2.633
miR-17-5p (and other miRNAs w/seed AAAGUGC)	-1.677	C2orf69	1.023
miR-17-5p (and other miRNAs w/seed AAAGUGC)	-1.677	CALD1	2.292
miR-17-5p (and other miRNAs w/seed AAAGUGC)	-1.677	CCNG2	1.522
miR-17-5p (and other miRNAs w/seed AAAGUGC)	-1.677	CDKN1A	2.696
miR-17-5p (and other miRNAs w/seed AAAGUGC)	-1.677	CITED4	1.154
miR-17-5p (and other miRNAs w/seed AAAGUGC)	-1.677	CREB1	1.133
miR-17-5p (and other miRNAs w/seed AAAGUGC)	-1.677	EGLN1	1.478
miR-17-5p (and other miRNAs w/seed AAAGUGC)	-1.677	FAM13A	1.877
miR-17-5p (and other miRNAs w/seed AAAGUGC)	-1.677	GPR137B	1.176
miR-17-5p (and other miRNAs w/seed AAAGUGC)	-1.677	IL17RD	1.007
miR-17-5p (and other miRNAs w/seed AAAGUGC)	-1.677	IRF1	1.183
miR-17-5p (and other miRNAs w/seed AAAGUGC)	-1.677	KIAA1191	1.452
miR-17-5p (and other miRNAs w/seed AAAGUGC)	-1.677	KLHL28	1.155
miR-17-5p (and other miRNAs w/seed AAAGUGC)	-1.677	LCOR	1.124
miR-17-5p (and other miRNAs w/seed AAAGUGC)	-1.677	MCL1	1.009
miR-17-5p (and other miRNAs w/seed AAAGUGC)	-1.677	MEF2D	1.467
miR-17-5p (and other miRNAs w/seed AAAGUGC)	-1.677	MTURN	1.126
miR-17-5p (and other miRNAs w/seed AAAGUGC)	-1.677	NRIP3	1.307
miR-17-5p (and other miRNAs w/seed AAAGUGC)	-1.677	PAM	1.554
miR-17-5p (and other miRNAs w/seed AAAGUGC)	-1.677	PANX2	2.065
miR-17-5p (and other miRNAs w/seed AAAGUGC)	-1.677	PFKFB3	2.352
miR-17-5p (and other miRNAs w/seed AAAGUGC)	-1.677	PFKP	1.390
miR-17-5p (and other miRNAs w/seed AAAGUGC)	-1.677	PTP4A2	1.349
miR-17-5p (and other miRNAs w/seed AAAGUGC)	-1.677	RAB11FIP1	1.382
miR-17-5p (and other miRNAs w/seed AAAGUGC)	-1.677	RAB11FIP5	1.155
miR-17-5p (and other miRNAs w/seed AAAGUGC)	-1.677	RAPGEFL1	1.031
miR-17-5p (and other miRNAs w/seed AAAGUGC)	-1.677	RASD1	1.248
miR-17-5p (and other miRNAs w/seed AAAGUGC)	-1.677	RIMKLA	1.216
miR-17-5p (and other miRNAs w/seed AAAGUGC)	-1.677	RRAGD	2.537
miR-17-5p (and other miRNAs w/seed AAAGUGC)	-1.677	RUNDC1	1.386
miR-17-5p (and other miRNAs w/seed AAAGUGC)	-1.677	RYBP	1.208
miR-17-5p (and other miRNAs w/seed AAAGUGC)	-1.677	SCN2A	1.391
miR-17-5p (and other miRNAs w/seed AAAGUGC)	-1.677	SERTAD2	1.719
miR-17-5p (and other miRNAs w/seed AAAGUGC)	-1.677	SLC25A36	1.011
miR-17-5p (and other miRNAs w/seed AAAGUGC)	-1.677	SLC41A1	1.067
miR-17-5p (and other miRNAs w/seed AAAGUGC)	-1.677	SMAD7	1.135
miR-17-5p (and other miRNAs w/seed AAAGUGC)	-1.677	SQSTM1	1.301
miR-17-5p (and other miRNAs w/seed AAAGUGC)	-1.677	STAT3	2.118
miR-17-5p (and other miRNAs w/seed AAAGUGC)	-1.677	STRIP2	1.321
miR-17-5p (and other miRNAs w/seed AAAGUGC)	-1.677	STX6	1.220
miR-17-5p (and other miRNAs w/seed AAAGUGC)	-1.677	SYAP1	1.464
miR-17-5p (and other miRNAs w/seed AAAGUGC)	-1.677	TP53INP1	2.279
miR-17-5p (and other miRNAs w/seed AAAGUGC)	-1.677	TRIM8	1.201
miR-17-5p (and other miRNAs w/seed AAAGUGC)	-1.677	TXNIP	1.918
miR-17-5p (and other miRNAs w/seed AAAGUGC)	-1.677	ULK1	1.292
miR-17-5p (and other miRNAs w/seed AAAGUGC)	-1.677	UNKL	1.007
miR-17-5p (and other miRNAs w/seed AAAGUGC)	-1.677	VLDLR	1.193
miR-17-5p (and other miRNAs w/seed AAAGUGC)	-1.677	ZMAT3	1.827
miR-17-5p (and other miRNAs w/seed AAAGUGC)	-1.677	ZNF652	1.135
miR-17-5p (and other miRNAs w/seed AAAGUGC)	-1.677	ZNFX1	1.146
miR-181a-5p (and other miRNAs w/seed ACAUUCA)	-1.236	ADAMTS1	1.282

miR-181a-5p (and other miRNAs w/seed ACAUUCA)	-1.236	ADM	3.046
miR-181a-5p (and other miRNAs w/seed ACAUUCA)	-1.236	AHNAK	2.181
miR-181a-5p (and other miRNAs w/seed ACAUUCA)	-1.236	AKIRIN1	1.234
miR-181a-5p (and other miRNAs w/seed ACAUUCA)	-1.236	ANKRD44	1.184
miR-181a-5p (and other miRNAs w/seed ACAUUCA)	-1.236	BHLHE40	1.610
miR-181a-5p (and other miRNAs w/seed ACAUUCA)	-1.236	BLOC1S6	1.049
miR-181a-5p (and other miRNAs w/seed ACAUUCA)	-1.236	C12orf68	1.158
miR-181a-5p (and other miRNAs w/seed ACAUUCA)	-1.236	C2orf69	1.023
miR-181a-5p (and other miRNAs w/seed ACAUUCA)	-1.236	CCDC92	1.133
miR-181a-5p (and other miRNAs w/seed ACAUUCA)	-1.236	CEBPA	1.103
miR-181a-5p (and other miRNAs w/seed ACAUUCA)	-1.236	CREB1	1.133
miR-181a-5p (and other miRNAs w/seed ACAUUCA)	-1.236	CYR61	1.894
miR-181a-5p (and other miRNAs w/seed ACAUUCA)	-1.236	DDIT4	1.032
miR-181a-5p (and other miRNAs w/seed ACAUUCA)	-1.236	DUSP5	1.262
miR-181a-5p (and other miRNAs w/seed ACAUUCA)	-1.236	E2F7	1.181
miR-181a-5p (and other miRNAs w/seed ACAUUCA)	-1.236	EGR1	1.452
miR-181a-5p (and other miRNAs w/seed ACAUUCA)	-1.236	FGFR3	1.093
miR-181a-5p (and other miRNAs w/seed ACAUUCA)	-1.236	FOS	1.838
miR-181a-5p (and other miRNAs w/seed ACAUUCA)	-1.236	KIAA1244	1.781
miR-181a-5p (and other miRNAs w/seed ACAUUCA)	-1.236	KIAA1715	1.239
miR-181a-5p (and other miRNAs w/seed ACAUUCA)	-1.236	KLHL3	1.151
miR-181a-5p (and other miRNAs w/seed ACAUUCA)	-1.236	LCOR	1.124
miR-181a-5p (and other miRNAs w/seed ACAUUCA)	-1.236	LOX	2.206
miR-181a-5p (and other miRNAs w/seed ACAUUCA)	-1.236	LRRFIP1	1.351
miR-181a-5p (and other miRNAs w/seed ACAUUCA)	-1.236	MCL1	1.009
miR-181a-5p (and other miRNAs w/seed ACAUUCA)	-1.236	MTURN	1.126
miR-181a-5p (and other miRNAs w/seed ACAUUCA)	-1.236	PAM	1.554
miR-181a-5p (and other miRNAs w/seed ACAUUCA)	-1.236	PDCD4	1.269
miR-181a-5p (and other miRNAs w/seed ACAUUCA)	-1.236	PHLDA1	2.392
miR-181a-5p (and other miRNAs w/seed ACAUUCA)	-1.236	PLAU	1.024
miR-181a-5p (and other miRNAs w/seed ACAUUCA)	-1.236	PTGR2	1.691
miR-181a-5p (and other miRNAs w/seed ACAUUCA)	-1.236	RIMKLA	1.216
miR-181a-5p (and other miRNAs w/seed ACAUUCA)	-1.236	SEMA3B	1.395
miR-181a-5p (and other miRNAs w/seed ACAUUCA)	-1.236	SERTAD2	1.719
miR-181a-5p (and other miRNAs w/seed ACAUUCA)	-1.236	SLC25A36	1.011
miR-181a-5p (and other miRNAs w/seed ACAUUCA)	-1.236	SLC25A4	1.245
miR-181a-5p (and other miRNAs w/seed ACAUUCA)	-1.236	SLC2A3	1.781
miR-181a-5p (and other miRNAs w/seed ACAUUCA)	-1.236	SLC35E1	1.692
miR-181a-5p (and other miRNAs w/seed ACAUUCA)	-1.236	SMAD7	1.135
miR-181a-5p (and other miRNAs w/seed ACAUUCA)	-1.236	STC2	1.551
miR-181a-5p (and other miRNAs w/seed ACAUUCA)	-1.236	TUB	1.001
miR-181a-5p (and other miRNAs w/seed ACAUUCA)	-1.236	UNKL	1.007
miR-181a-5p (and other miRNAs w/seed ACAUUCA)	-1.236	VGLL4	1.395
miR-181a-5p (and other miRNAs w/seed ACAUUCA)	-1.236	WSB1	1.697
miR-181a-5p (and other miRNAs w/seed ACAUUCA)	-1.236	ZNF652	1.135
miR-200b-3p (and other miRNAs w/seed AAUACUG)	-1.790	ABCA1	1.079
miR-200b-3p (and other miRNAs w/seed AAUACUG)	-1.790	AHNAK	2.181
miR-200b-3p (and other miRNAs w/seed AAUACUG)	-1.790	APAF1	1.406
miR-200b-3p (and other miRNAs w/seed AAUACUG)	-1.790	CGGBP1	1.049
miR-200b-3p (and other miRNAs w/seed AAUACUG)	-1.790	CHSY1	1.071
miR-200b-3p (and other miRNAs w/seed AAUACUG)	-1.790	CITED2	1.161
miR-200b-3p (and other miRNAs w/seed AAUACUG)	-1.790	CNTFR	1.302
miR-200b-3p (and other miRNAs w/seed AAUACUG)	-1.790	CREB1	1.133
miR-200b-3p (and other miRNAs w/seed AAUACUG)	-1.790	DDIT4	1.032
miR-200b-3p (and other miRNAs w/seed AAUACUG)	-1.790	DUSP1	1.039
miR-200b-3p (and other miRNAs w/seed AAUACUG)	-1.790	EGLN1	1.478
miR-200b-3p (and other miRNAs w/seed AAUACUG)	-1.790	GATA2	1.639
miR-200b-3p (and other miRNAs w/seed AAUACUG)	-1.790	GLRX	1.667
miR-200b-3p (and other miRNAs w/seed AAUACUG)	-1.790	HNRNPU	1.486

miR-200b-3p (and other miRNAs w/seed AAUACUG)	-1.790	IGSF3	1.003
miR-200b-3p (and other miRNAs w/seed AAUACUG)	-1.790	JAG2	1.112
miR-200b-3p (and other miRNAs w/seed AAUACUG)	-1.790	JUN	2.508
miR-200b-3p (and other miRNAs w/seed AAUACUG)	-1.790	KLHL3	1.151
miR-200b-3p (and other miRNAs w/seed AAUACUG)	-1.790	LCOR	1.124
miR-200b-3p (and other miRNAs w/seed AAUACUG)	-1.790	LIN7B	1.032
miR-200b-3p (and other miRNAs w/seed AAUACUG)	-1.790	LOX	2.206
miR-200b-3p (and other miRNAs w/seed AAUACUG)	-1.790	MAPK7	1.067
miR-200b-3p (and other miRNAs w/seed AAUACUG)	-1.790	MEF2D	1.467
miR-200b-3p (and other miRNAs w/seed AAUACUG)	-1.790	MGAT3	1.248
miR-200b-3p (and other miRNAs w/seed AAUACUG)	-1.790	MXD4	1.829
miR-200b-3p (and other miRNAs w/seed AAUACUG)	-1.790	N4BP2	1.143
miR-200b-3p (and other miRNAs w/seed AAUACUG)	-1.790	NOTCH1	1.667
miR-200b-3p (and other miRNAs w/seed AAUACUG)	-1.790	NRIP3	1.307
miR-200b-3p (and other miRNAs w/seed AAUACUG)	-1.790	PAM	1.554
miR-200b-3p (and other miRNAs w/seed AAUACUG)	-1.790	PRKAR1A	1.012
miR-200b-3p (and other miRNAs w/seed AAUACUG)	-1.790	SESN1	2.178
miR-200b-3p (and other miRNAs w/seed AAUACUG)	-1.790	SNAPC1	1.052
miR-200b-3p (and other miRNAs w/seed AAUACUG)	-1.790	SYDE1	1.791
miR-200b-3p (and other miRNAs w/seed AAUACUG)	-1.790	TP53INP1	2.279
miR-200b-3p (and other miRNAs w/seed AAUACUG)	-1.790	VLDLR	1.193
miR-200b-3p (and other miRNAs w/seed AAUACUG)	-1.790	WDR45B	1.383
miR-200b-3p (and other miRNAs w/seed AAUACUG)	-1.790	ZBTB5	1.316
miR-200b-3p (and other miRNAs w/seed AAUACUG)	-1.790	ZMAT3	1.827
miR-200b-3p (and other miRNAs w/seed AAUACUG)	-1.790	ZNF652	1.135
miR-200b-3p (and other miRNAs w/seed AAUACUG)	-1.790	ZSWIM4	1.474
miR-218-5p (and other miRNAs w/seed UGUGCUU)	-1.231	AK4	1.350
miR-218-5p (and other miRNAs w/seed UGUGCUU)	-1.231	ANKRD44	1.184
miR-218-5p (and other miRNAs w/seed UGUGCUU)	-1.231	ATRN	1.085
miR-218-5p (and other miRNAs w/seed UGUGCUU)	-1.231	BTG2	1.410
miR-218-5p (and other miRNAs w/seed UGUGCUU)	-1.231	CACNA1I	1.662
miR-218-5p (and other miRNAs w/seed UGUGCUU)	-1.231	CCDC24	1.086
miR-218-5p (and other miRNAs w/seed UGUGCUU)	-1.231	CGGBP1	1.049
miR-218-5p (and other miRNAs w/seed UGUGCUU)	-1.231	CREB1	1.133
miR-218-5p (and other miRNAs w/seed UGUGCUU)	-1.231	CTSB	1.121
miR-218-5p (and other miRNAs w/seed UGUGCUU)	-1.231	DUSP5	1.262
miR-218-5p (and other miRNAs w/seed UGUGCUU)	-1.231	FAM13A	1.877
miR-218-5p (and other miRNAs w/seed UGUGCUU)	-1.231	FAM214A	1.164
miR-218-5p (and other miRNAs w/seed UGUGCUU)	-1.231	FLNC	2.818
miR-218-5p (and other miRNAs w/seed UGUGCUU)	-1.231	GALNT3	1.021
miR-218-5p (and other miRNAs w/seed UGUGCUU)	-1.231	JADE1	1.702
miR-218-5p (and other miRNAs w/seed UGUGCUU)	-1.231	LAMP2	1.465
miR-218-5p (and other miRNAs w/seed UGUGCUU)	-1.231	LOX	2.206
miR-218-5p (and other miRNAs w/seed UGUGCUU)	-1.231	LRRFIP1	1.351
miR-218-5p (and other miRNAs w/seed UGUGCUU)	-1.231	MEF2D	1.467
miR-218-5p (and other miRNAs w/seed UGUGCUU)	-1.231	MTURN	1.126
miR-218-5p (and other miRNAs w/seed UGUGCUU)	-1.231	NDRG4	2.087
miR-218-5p (and other miRNAs w/seed UGUGCUU)	-1.231	NFE2L1	1.418
miR-218-5p (and other miRNAs w/seed UGUGCUU)	-1.231	NUDT10	1.052
miR-218-5p (and other miRNAs w/seed UGUGCUU)	-1.231	OTP	1.200
miR-218-5p (and other miRNAs w/seed UGUGCUU)	-1.231	PDZD4	1.115
miR-218-5p (and other miRNAs w/seed UGUGCUU)	-1.231	POLH	1.072
miR-218-5p (and other miRNAs w/seed UGUGCUU)	-1.231	PPME1	1.186
miR-218-5p (and other miRNAs w/seed UGUGCUU)	-1.231	RAP1GAP	1.158
miR-218-5p (and other miRNAs w/seed UGUGCUU)	-1.231	RNF165	1.396
miR-218-5p (and other miRNAs w/seed UGUGCUU)	-1.231	RYBP	1.208
miR-218-5p (and other miRNAs w/seed UGUGCUU)	-1.231	SERTAD2	1.719
miR-218-5p (and other miRNAs w/seed UGUGCUU)	-1.231	SLC25A36	1.011
miR-218-5p (and other miRNAs w/seed UGUGCUU)	-1.231	SNCB	1.427

miR-218-5p (and other miRNAs w/seed UGUGCUU)	-1.231	SSPN	1.003
miR-218-5p (and other miRNAs w/seed UGUGCUU)	-1.231	TPD52	1.015
miR-218-5p (and other miRNAs w/seed UGUGCUU)	-1.231	TRAF5	1.244
miR-218-5p (and other miRNAs w/seed UGUGCUU)	-1.231	TRIM9	2.268
miR-218-5p (and other miRNAs w/seed UGUGCUU)	-1.231	TUB	1.001
miR-218-5p (and other miRNAs w/seed UGUGCUU)	-1.231	UBE2H	1.015
miR-218-5p (and other miRNAs w/seed UGUGCUU)	-1.231	WDR1	1.065
miR-218-5p (and other miRNAs w/seed UGUGCUU)	-1.231	ZMIZ1	1.221
miR-218-5p (and other miRNAs w/seed UGUGCUU)	-1.231	ZNFX1	1.146
miR-224-5p (miRNAs w/seed AAGUCAC)	-1.248	ADAM17	1.081
miR-224-5p (miRNAs w/seed AAGUCAC)	-1.248	AKIRIN1	1.234
miR-224-5p (miRNAs w/seed AAGUCAC)	-1.248	CAST	1.123
miR-224-5p (miRNAs w/seed AAGUCAC)	-1.248	FRMD8	2.070
miR-224-5p (miRNAs w/seed AAGUCAC)	-1.248	HNRNPU	1.486
miR-224-5p (miRNAs w/seed AAGUCAC)	-1.248	KIAA1244	1.781
miR-224-5p (miRNAs w/seed AAGUCAC)	-1.248	LCOR	1.124
miR-224-5p (miRNAs w/seed AAGUCAC)	-1.248	MAFF	1.737
miR-224-5p (miRNAs w/seed AAGUCAC)	-1.248	PAPSS2	1.109
miR-224-5p (miRNAs w/seed AAGUCAC)	-1.248	PFKFB3	2.352
miR-224-5p (miRNAs w/seed AAGUCAC)	-1.248	PPFIA4	1.955
miR-224-5p (miRNAs w/seed AAGUCAC)	-1.248	SEC14L5	1.227
miR-224-5p (miRNAs w/seed AAGUCAC)	-1.248	TRIM9	2.268
miR-224-5p (miRNAs w/seed AAGUCAC)	-1.248	ZMAT3	1.827
miR-24-3p (and other miRNAs w/seed GGCUCAG)	-1.693	ADM	3.046
miR-24-3p (and other miRNAs w/seed GGCUCAG)	-1.693	ANKRD44	1.184
miR-24-3p (and other miRNAs w/seed GGCUCAG)	-1.693	AXL	1.805
miR-24-3p (and other miRNAs w/seed GGCUCAG)	-1.693	BNIP3L	2.633
miR-24-3p (and other miRNAs w/seed GGCUCAG)	-1.693	C8orf58	1.036
miR-24-3p (and other miRNAs w/seed GGCUCAG)	-1.693	CABP7	1.076
miR-24-3p (and other miRNAs w/seed GGCUCAG)	-1.693	CDKN1C	1.095
miR-24-3p (and other miRNAs w/seed GGCUCAG)	-1.693	CITED4	1.154
miR-24-3p (and other miRNAs w/seed GGCUCAG)	-1.693	CSRNP2	1.827
miR-24-3p (and other miRNAs w/seed GGCUCAG)	-1.693	CYTH2	1.322
miR-24-3p (and other miRNAs w/seed GGCUCAG)	-1.693	DENND4B	1.011
miR-24-3p (and other miRNAs w/seed GGCUCAG)	-1.693	DNAJB2	1.439
miR-24-3p (and other miRNAs w/seed GGCUCAG)	-1.693	FGF11	1.348
miR-24-3p (and other miRNAs w/seed GGCUCAG)	-1.693	FGFR3	1.093
miR-24-3p (and other miRNAs w/seed GGCUCAG)	-1.693	IRF1	1.183
miR-24-3p (and other miRNAs w/seed GGCUCAG)	-1.693	KLHL3	1.151
miR-24-3p (and other miRNAs w/seed GGCUCAG)	-1.693	LOX	2.206
miR-24-3p (and other miRNAs w/seed GGCUCAG)	-1.693	MAPK7	1.067
miR-24-3p (and other miRNAs w/seed GGCUCAG)	-1.693	MXI1	1.003
miR-24-3p (and other miRNAs w/seed GGCUCAG)	-1.693	NDRG4	2.087
miR-24-3p (and other miRNAs w/seed GGCUCAG)	-1.693	NOTCH1	1.667
miR-24-3p (and other miRNAs w/seed GGCUCAG)	-1.693	PDXK	1.523
miR-24-3p (and other miRNAs w/seed GGCUCAG)	-1.693	PLOD2	2.106
miR-24-3p (and other miRNAs w/seed GGCUCAG)	-1.693	PPM1D	1.536
miR-24-3p (and other miRNAs w/seed GGCUCAG)	-1.693	PSTPIP2	1.485
miR-24-3p (and other miRNAs w/seed GGCUCAG)	-1.693	PTPRF	1.930
miR-24-3p (and other miRNAs w/seed GGCUCAG)	-1.693	RAB11FIP1	1.382
miR-24-3p (and other miRNAs w/seed GGCUCAG)	-1.693	RAP2A	1.052
miR-24-3p (and other miRNAs w/seed GGCUCAG)	-1.693	RNF165	1.396
miR-24-3p (and other miRNAs w/seed GGCUCAG)	-1.693	SBK1	1.336
miR-24-3p (and other miRNAs w/seed GGCUCAG)	-1.693	SEC14L5	1.227
miR-24-3p (and other miRNAs w/seed GGCUCAG)	-1.693	SERTAD1	1.857
miR-24-3p (and other miRNAs w/seed GGCUCAG)	-1.693	SESN1	2.178
miR-24-3p (and other miRNAs w/seed GGCUCAG)	-1.693	SLC41A1	1.067
miR-24-3p (and other miRNAs w/seed GGCUCAG)	-1.693	SMAD3	1.013
miR-24-3p (and other miRNAs w/seed GGCUCAG)	-1.693	STC2	1.551

miR-24-3p (and other miRNAs w/seed GGCUCAG)	-1.693	STX6	1.220
miR-24-3p (and other miRNAs w/seed GGCUCAG)	-1.693	TMEM194A	1.019
miR-24-3p (and other miRNAs w/seed GGCUCAG)	-1.693	TP53INP1	2.279
miR-24-3p (and other miRNAs w/seed GGCUCAG)	-1.693	VPS37D	1.666
miR-24-3p (and other miRNAs w/seed GGCUCAG)	-1.693	ZMAT3	1.827
miR-27a-3p (and other miRNAs w/seed UCACAGU)	-2.098	ABCA1	1.079
miR-27a-3p (and other miRNAs w/seed UCACAGU)	-2.098	AK4	1.350
miR-27a-3p (and other miRNAs w/seed UCACAGU)	-2.098	AKIRIN1	1.234
miR-27a-3p (and other miRNAs w/seed UCACAGU)	-2.098	APAF1	1.406
miR-27a-3p (and other miRNAs w/seed UCACAGU)	-2.098	ATRN	1.085
miR-27a-3p (and other miRNAs w/seed UCACAGU)	-2.098	BEND7	1.136
miR-27a-3p (and other miRNAs w/seed UCACAGU)	-2.098	BTG2	1.410
miR-27a-3p (and other miRNAs w/seed UCACAGU)	-2.098	CALD1	2.292
miR-27a-3p (and other miRNAs w/seed UCACAGU)	-2.098	CASC10	1.388
miR-27a-3p (and other miRNAs w/seed UCACAGU)	-2.098	CCDC92	1.133
miR-27a-3p (and other miRNAs w/seed UCACAGU)	-2.098	CREB1	1.133
miR-27a-3p (and other miRNAs w/seed UCACAGU)	-2.098	CSRNP1	2.331
miR-27a-3p (and other miRNAs w/seed UCACAGU)	-2.098	CSRP2	1.708
miR-27a-3p (and other miRNAs w/seed UCACAGU)	-2.098	DUSP5	1.262
miR-27a-3p (and other miRNAs w/seed UCACAGU)	-2.098	E2F7	1.181
miR-27a-3p (and other miRNAs w/seed UCACAGU)	-2.098	FAM13A	1.877
miR-27a-3p (and other miRNAs w/seed UCACAGU)	-2.098	FAM84B	2.062
miR-27a-3p (and other miRNAs w/seed UCACAGU)	-2.098	FOXO3	1.169
miR-27a-3p (and other miRNAs w/seed UCACAGU)	-2.098	GALNT3	1.021
miR-27a-3p (and other miRNAs w/seed UCACAGU)	-2.098	GATA2	1.639
miR-27a-3p (and other miRNAs w/seed UCACAGU)	-2.098	GLTP	1.437
miR-27a-3p (and other miRNAs w/seed UCACAGU)	-2.098	IER3	2.569
miR-27a-3p (and other miRNAs w/seed UCACAGU)	-2.098	LCOR	1.124
miR-27a-3p (and other miRNAs w/seed UCACAGU)	-2.098	LEP	1.213
miR-27a-3p (and other miRNAs w/seed UCACAGU)	-2.098	LOX	2.206
miR-27a-3p (and other miRNAs w/seed UCACAGU)	-2.098	MAGT1	1.458
miR-27a-3p (and other miRNAs w/seed UCACAGU)	-2.098	MBTD1	1.374
miR-27a-3p (and other miRNAs w/seed UCACAGU)	-2.098	MTURN	1.126
miR-27a-3p (and other miRNAs w/seed UCACAGU)	-2.098	MXI1	1.003
miR-27a-3p (and other miRNAs w/seed UCACAGU)	-2.098	NOTCH1	1.667
miR-27a-3p (and other miRNAs w/seed UCACAGU)	-2.098	NSD1	1.049
miR-27a-3p (and other miRNAs w/seed UCACAGU)	-2.098	PAPD7	1.062
miR-27a-3p (and other miRNAs w/seed UCACAGU)	-2.098	PAPSS2	1.109
miR-27a-3p (and other miRNAs w/seed UCACAGU)	-2.098	PDK1	1.286
miR-27a-3p (and other miRNAs w/seed UCACAGU)	-2.098	PDXK	1.523
miR-27a-3p (and other miRNAs w/seed UCACAGU)	-2.098	PLEKHA2	2.391
miR-27a-3p (and other miRNAs w/seed UCACAGU)	-2.098	PPME1	1.186
miR-27a-3p (and other miRNAs w/seed UCACAGU)	-2.098	RAB11FIP1	1.382
miR-27a-3p (and other miRNAs w/seed UCACAGU)	-2.098	RYBP	1.208
miR-27a-3p (and other miRNAs w/seed UCACAGU)	-2.098	SAV1	1.055
miR-27a-3p (and other miRNAs w/seed UCACAGU)	-2.098	SBK1	1.336
miR-27a-3p (and other miRNAs w/seed UCACAGU)	-2.098	SEMA3B	1.395
miR-27a-3p (and other miRNAs w/seed UCACAGU)	-2.098	SERTAD2	1.719
miR-27a-3p (and other miRNAs w/seed UCACAGU)	-2.098	SMAD3	1.013
miR-27a-3p (and other miRNAs w/seed UCACAGU)	-2.098	STX6	1.220
miR-27a-3p (and other miRNAs w/seed UCACAGU)	-2.098	SYDE1	1.791
miR-27a-3p (and other miRNAs w/seed UCACAGU)	-2.098	TMSB10/TMSB4X	1.751
miR-27a-3p (and other miRNAs w/seed UCACAGU)	-2.098	TRIM13	1.105
miR-27a-3p (and other miRNAs w/seed UCACAGU)	-2.098	UNKL	1.007
miR-27a-3p (and other miRNAs w/seed UCACAGU)	-2.098	WSB1	1.697
miR-27a-3p (and other miRNAs w/seed UCACAGU)	-2.098	ZMAT3	1.827
miR-292-3p (and other miRNAs w/seed AGUGCCG)	-1.105	GSG1	1.746
miR-292-3p (and other miRNAs w/seed AGUGCCG)	-1.105	SRXN1	1.016
miR-299a-3p (and other miRNAs w/seed AUGUGGG)	-1.159	IKBIP	1.978

miR-299a-3p (and other miRNAs w/seed AUGUGGG)	-1.159	NSD1	1.049
miR-299a-3p (and other miRNAs w/seed AUGUGGG)	-1.159	TRIM9	2.268
miR-299a-3p (and other miRNAs w/seed AUGUGGG)	-1.159	UBE2H	1.015
miR-299a-3p (and other miRNAs w/seed AUGUGGG)	-1.159	ZNFX1	1.146
miR-29b-3p (and other miRNAs w/seed AGCACCA)	-1.548	ABCB6	1.425
miR-29b-3p (and other miRNAs w/seed AGCACCA)	-1.548	ARL4A	1.065
miR-29b-3p (and other miRNAs w/seed AGCACCA)	-1.548	ATRN	1.085
miR-29b-3p (and other miRNAs w/seed AGCACCA)	-1.548	BTG2	1.410
miR-29b-3p (and other miRNAs w/seed AGCACCA)	-1.548	CEACAM1	1.622
miR-29b-3p (and other miRNAs w/seed AGCACCA)	-1.548	CHIC2	1.236
miR-29b-3p (and other miRNAs w/seed AGCACCA)	-1.548	CHSY1	1.071
miR-29b-3p (and other miRNAs w/seed AGCACCA)	-1.548	COL7A1	1.255
miR-29b-3p (and other miRNAs w/seed AGCACCA)	-1.548	CSRNP2	1.827
miR-29b-3p (and other miRNAs w/seed AGCACCA)	-1.548	DNAJB2	1.439
miR-29b-3p (and other miRNAs w/seed AGCACCA)	-1.548	DTWD2	1.156
miR-29b-3p (and other miRNAs w/seed AGCACCA)	-1.548	E2F7	1.181
miR-29b-3p (and other miRNAs w/seed AGCACCA)	-1.548	F11R	1.691
miR-29b-3p (and other miRNAs w/seed AGCACCA)	-1.548	FOS	1.838
miR-29b-3p (and other miRNAs w/seed AGCACCA)	-1.548	FOXO3	1.169
miR-29b-3p (and other miRNAs w/seed AGCACCA)	-1.548	HPCAL4	1.720
miR-29b-3p (and other miRNAs w/seed AGCACCA)	-1.548	IL17RD	1.007
miR-29b-3p (and other miRNAs w/seed AGCACCA)	-1.548	INA	2.100
miR-29b-3p (and other miRNAs w/seed AGCACCA)	-1.548	KDM5B	1.270
miR-29b-3p (and other miRNAs w/seed AGCACCA)	-1.548	KLHL28	1.155
miR-29b-3p (and other miRNAs w/seed AGCACCA)	-1.548	KREMEN2	1.185
miR-29b-3p (and other miRNAs w/seed AGCACCA)	-1.548	LEP	1.213
miR-29b-3p (and other miRNAs w/seed AGCACCA)	-1.548	LOX	2.206
miR-29b-3p (and other miRNAs w/seed AGCACCA)	-1.548	MAP6D1	1.465
miR-29b-3p (and other miRNAs w/seed AGCACCA)	-1.548	MBTD1	1.374
miR-29b-3p (and other miRNAs w/seed AGCACCA)	-1.548	MCL1	1.009
miR-29b-3p (and other miRNAs w/seed AGCACCA)	-1.548	N4BP2	1.143
miR-29b-3p (and other miRNAs w/seed AGCACCA)	-1.548	NSD1	1.049
miR-29b-3p (and other miRNAs w/seed AGCACCA)	-1.548	PLEKHA1	1.476
miR-29b-3p (and other miRNAs w/seed AGCACCA)	-1.548	PPM1D	1.536
miR-29b-3p (and other miRNAs w/seed AGCACCA)	-1.548	PRMT2	1.029
miR-29b-3p (and other miRNAs w/seed AGCACCA)	-1.548	PTRF	1.959
miR-29b-3p (and other miRNAs w/seed AGCACCA)	-1.548	RAPGEFL1	1.031
miR-29b-3p (and other miRNAs w/seed AGCACCA)	-1.548	RIOK3	1.137
miR-29b-3p (and other miRNAs w/seed AGCACCA)	-1.548	RNF165	1.396
miR-29b-3p (and other miRNAs w/seed AGCACCA)	-1.548	RYBP	1.208
miR-29b-3p (and other miRNAs w/seed AGCACCA)	-1.548	SHROOM4	1.366
miR-29b-3p (and other miRNAs w/seed AGCACCA)	-1.548	SIDT2	1.420
miR-29b-3p (and other miRNAs w/seed AGCACCA)	-1.548	SLC5A8	1.751
miR-29b-3p (and other miRNAs w/seed AGCACCA)	-1.548	STAT3	2.118
miR-29b-3p (and other miRNAs w/seed AGCACCA)	-1.548	SUN1	1.178
miR-29b-3p (and other miRNAs w/seed AGCACCA)	-1.548	TP53INP1	2.279
miR-29b-3p (and other miRNAs w/seed AGCACCA)	-1.548	TPM1	1.385
miR-29b-3p (and other miRNAs w/seed AGCACCA)	-1.548	TRAF5	1.244
miR-29b-3p (and other miRNAs w/seed AGCACCA)	-1.548	TRIM9	2.268
miR-29b-3p (and other miRNAs w/seed AGCACCA)	-1.548	TUBB2A	1.697
miR-29b-3p (and other miRNAs w/seed AGCACCA)	-1.548	TUBB2B	1.046
miR-29b-3p (and other miRNAs w/seed AGCACCA)	-1.548	UBE2H	1.015
miR-29b-3p (and other miRNAs w/seed AGCACCA)	-1.548	UNKL	1.007
miR-29b-3p (and other miRNAs w/seed AGCACCA)	-1.548	WDR26	1.935
miR-29b-3p (and other miRNAs w/seed AGCACCA)	-1.548	ZBTB5	1.316
miR-29b-3p (and other miRNAs w/seed AGCACCA)	-1.548	ZMIZ1	1.221
miR-30a-3p (and other miRNAs w/seed UUUCAGU)	-1.489	CYR61	1.894
miR-30c-5p (and other miRNAs w/seed GUAAACA)	-2.645	AHNAK	2.181
miR-30c-5p (and other miRNAs w/seed GUAAACA)	-2.645	ARL4A	1.065

miR-30c-5p (and other miRNAs w/seed GUAAACA)	-2.645	ATRN	1.085
miR-30c-5p (and other miRNAs w/seed GUAAACA)	-2.645	BNIP3L	2.633
miR-30c-5p (and other miRNAs w/seed GUAAACA)	-2.645	C3orf58	1.041
miR-30c-5p (and other miRNAs w/seed GUAAACA)	-2.645	CALD1	2.292
miR-30c-5p (and other miRNAs w/seed GUAAACA)	-2.645	CAPN5	1.295
miR-30c-5p (and other miRNAs w/seed GUAAACA)	-2.645	CEACAM1	1.622
miR-30c-5p (and other miRNAs w/seed GUAAACA)	-2.645	CTGF	2.896
miR-30c-5p (and other miRNAs w/seed GUAAACA)	-2.645	DDIT4	1.032
miR-30c-5p (and other miRNAs w/seed GUAAACA)	-2.645	E2F7	1.181
miR-30c-5p (and other miRNAs w/seed GUAAACA)	-2.645	ELAVL3	2.393
miR-30c-5p (and other miRNAs w/seed GUAAACA)	-2.645	FAM13A	1.877
miR-30c-5p (and other miRNAs w/seed GUAAACA)	-2.645	FAM214A	1.164
miR-30c-5p (and other miRNAs w/seed GUAAACA)	-2.645	FAM43A	1.004
miR-30c-5p (and other miRNAs w/seed GUAAACA)	-2.645	FOXD1	2.072
miR-30c-5p (and other miRNAs w/seed GUAAACA)	-2.645	FOXO3	1.169
miR-30c-5p (and other miRNAs w/seed GUAAACA)	-2.645	GALNT3	1.021
miR-30c-5p (and other miRNAs w/seed GUAAACA)	-2.645	GPT2	1.076
miR-30c-5p (and other miRNAs w/seed GUAAACA)	-2.645	INSIG2	1.733
miR-30c-5p (and other miRNAs w/seed GUAAACA)	-2.645	JAG2	1.112
miR-30c-5p (and other miRNAs w/seed GUAAACA)	-2.645	JUN	2.508
miR-30c-5p (and other miRNAs w/seed GUAAACA)	-2.645	JUNB	1.051
miR-30c-5p (and other miRNAs w/seed GUAAACA)	-2.645	KDM3A	2.191
miR-30c-5p (and other miRNAs w/seed GUAAACA)	-2.645	KIAA0408	1.050
miR-30c-5p (and other miRNAs w/seed GUAAACA)	-2.645	KIAA1244	1.781
miR-30c-5p (and other miRNAs w/seed GUAAACA)	-2.645	KIAA1715	1.239
miR-30c-5p (and other miRNAs w/seed GUAAACA)	-2.645	KLHL28	1.155
miR-30c-5p (and other miRNAs w/seed GUAAACA)	-2.645	LCOR	1.124
miR-30c-5p (and other miRNAs w/seed GUAAACA)	-2.645	LOX	2.206
miR-30c-5p (and other miRNAs w/seed GUAAACA)	-2.645	MEF2D	1.467
miR-30c-5p (and other miRNAs w/seed GUAAACA)	-2.645	MFSD11	1.416
miR-30c-5p (and other miRNAs w/seed GUAAACA)	-2.645	N4BP2	1.143
miR-30c-5p (and other miRNAs w/seed GUAAACA)	-2.645	NOTCH1	1.667
miR-30c-5p (and other miRNAs w/seed GUAAACA)	-2.645	NSD1	1.049
miR-30c-5p (and other miRNAs w/seed GUAAACA)	-2.645	P4HA1	1.654
miR-30c-5p (and other miRNAs w/seed GUAAACA)	-2.645	P4HA2	2.360
miR-30c-5p (and other miRNAs w/seed GUAAACA)	-2.645	PRKAR1A	1.012
miR-30c-5p (and other miRNAs w/seed GUAAACA)	-2.645	RALGDS	1.613
miR-30c-5p (and other miRNAs w/seed GUAAACA)	-2.645	RASD1	1.248
miR-30c-5p (and other miRNAs w/seed GUAAACA)	-2.645	RHOB	2.088
miR-30c-5p (and other miRNAs w/seed GUAAACA)	-2.645	RIOK3	1.137
miR-30c-5p (and other miRNAs w/seed GUAAACA)	-2.645	RNF165	1.396
miR-30c-5p (and other miRNAs w/seed GUAAACA)	-2.645	SBK1	1.336
miR-30c-5p (and other miRNAs w/seed GUAAACA)	-2.645	SCN2A	1.391
miR-30c-5p (and other miRNAs w/seed GUAAACA)	-2.645	SIDT2	1.420
miR-30c-5p (and other miRNAs w/seed GUAAACA)	-2.645	SLC25A36	1.011
miR-30c-5p (and other miRNAs w/seed GUAAACA)	-2.645	SLC7A10	1.476
miR-30c-5p (and other miRNAs w/seed GUAAACA)	-2.645	STX6	1.220
miR-30c-5p (and other miRNAs w/seed GUAAACA)	-2.645	TMEM41B	1.076
miR-30c-5p (and other miRNAs w/seed GUAAACA)	-2.645	TNFRSF10B	1.602
miR-30c-5p (and other miRNAs w/seed GUAAACA)	-2.645	TNIP1	1.267
miR-30c-5p (and other miRNAs w/seed GUAAACA)	-2.645	TP53INP1	2.279
miR-30c-5p (and other miRNAs w/seed GUAAACA)	-2.645	TRIM9	2.268
miR-30c-5p (and other miRNAs w/seed GUAAACA)	-2.645	UBE2O	1.028
miR-30c-5p (and other miRNAs w/seed GUAAACA)	-2.645	UNKL	1.007
miR-30c-5p (and other miRNAs w/seed GUAAACA)	-2.645	WDR1	1.065
miR-30c-5p (and other miRNAs w/seed GUAAACA)	-2.645	WDR26	1.935
miR-30c-5p (and other miRNAs w/seed GUAAACA)	-2.645	YPEL5	1.866
miR-30c-5p (and other miRNAs w/seed GUAAACA)	-2.645	ZNF652	1.135
miR-31-5p (and other miRNAs w/seed GGCAAGA)	-1.969	ADAMTS1	1.282

miR-31-5p (and other miRNAs w/seed GGCAAGA)	-1.969	AK4	1.350
miR-31-5p (and other miRNAs w/seed GGCAAGA)	-1.969	CEBPA	1.103
miR-31-5p (and other miRNAs w/seed GGCAAGA)	-1.969	CSRNP1	2.331
miR-31-5p (and other miRNAs w/seed GGCAAGA)	-1.969	GCLM	1.134
miR-31-5p (and other miRNAs w/seed GGCAAGA)	-1.969	KIAA1244	1.781
miR-31-5p (and other miRNAs w/seed GGCAAGA)	-1.969	LRP10	1.022
miR-31-5p (and other miRNAs w/seed GGCAAGA)	-1.969	PAM	1.554
miR-31-5p (and other miRNAs w/seed GGCAAGA)	-1.969	PDZD4	1.115
miR-31-5p (and other miRNAs w/seed GGCAAGA)	-1.969	SCN2A	1.391
miR-31-5p (and other miRNAs w/seed GGCAAGA)	-1.969	SERTAD2	1.719
miR-31-5p (and other miRNAs w/seed GGCAAGA)	-1.969	SYDE1	1.791
miR-31-5p (and other miRNAs w/seed GGCAAGA)	-1.969	TMEM145	1.243
miR-31-5p (and other miRNAs w/seed GGCAAGA)	-1.969	UBE2H	1.015
miR-31-5p (and other miRNAs w/seed GGCAAGA)	-1.969	ZNF652	1.135
miR-362-5p (and other miRNAs w/seed AUCCUUG)	-1.410	CHSY1	1.071
miR-486-5p (and other miRNAs w/seed CCUGUAC)	-1.158	CLIP3	1.258
miR-486-5p (and other miRNAs w/seed CCUGUAC)	-1.158	MXI1	1.003
miR-486-5p (and other miRNAs w/seed CCUGUAC)	-1.158	NFE2L1	1.418
miR-486-5p (and other miRNAs w/seed CCUGUAC)	-1.158	RAPGEFL1	1.031
miR-5107-3p (and other miRNAs w/seed AACCUGU)	-1.321	SUN1	1.178
miR-515-3p (and other miRNAs w/seed AGUGCCU)	-1.137	AXL	1.805
miR-515-3p (and other miRNAs w/seed AGUGCCU)	-1.137	FAM13A	1.877
miR-515-3p (and other miRNAs w/seed AGUGCCU)	-1.137	HPCAL4	1.720
miR-515-3p (and other miRNAs w/seed AGUGCCU)	-1.137	PTGR2	1.691
miR-515-3p (and other miRNAs w/seed AGUGCCU)	-1.137	RIMKLA	1.216
miR-516a-3p (and other miRNAs w/seed GCUUCCU)	-1.193	JAG2	1.112
miR-516a-3p (and other miRNAs w/seed GCUUCCU)	-1.193	KIAA1244	1.781
miR-516a-3p (and other miRNAs w/seed GCUUCCU)	-1.193	PCDH7	1.417
miR-516a-3p (and other miRNAs w/seed GCUUCCU)	-1.193	SYAP1	1.464
miR-516a-3p (and other miRNAs w/seed GCUUCCU)	-1.193	TNFRSF10B	1.602
miR-518a-3p (and other miRNAs w/seed AAAGCGC)	-1.330	EGR1	1.452
miR-518a-3p (and other miRNAs w/seed AAAGCGC)	-1.330	TEAD3	1.352
miR-518a-3p (and other miRNAs w/seed AAAGCGC)	-1.330	WDR1	1.065
miR-520g-3p (and other miRNAs w/seed CAAAGUG)	-1.767	TRIM13	1.105
miR-542-5p (miRNAs w/seed CGGGGAU)	-1.775	OSBPL2	1.401
miR-542-5p (miRNAs w/seed CGGGGAU)	-1.775	RGS16	1.133
miR-551b-3p (and other miRNAs w/seed CGACCCA)	-1.222	ANGPTL4	3.123

RNA samples from the previously discussed bevacizumab-treated A2780 tumors showed reduced E-cadherin expression and increased vimentin expression, consistent with our *in vitro* observations **(Figure 17a)**. To elucidate the roles of Drosha and Dicer in the EMT process, we silenced Drosha and Dicer in A2780 and MCF7 cells, after which we observed significantly decreased E-cadherin and increased vimentin expression **(Figure 17b, c)**. There was significant increase in migration and invasion of the A2780 cells after silencing of Dicer, Drosha, or both **(Figure 17d)**. Correlative analysis of E-cadherin and CA9 in samples from patients with ovarian cancer showed a significant inverse correlation between E-cadherin and CA9 expression ($r = -0.69$, $p = 0.0007$). Vimentin expression, however, was positively correlated with CA9 expression ($r = 0.66$, $p = 0.0013$; **Figure 17e**).

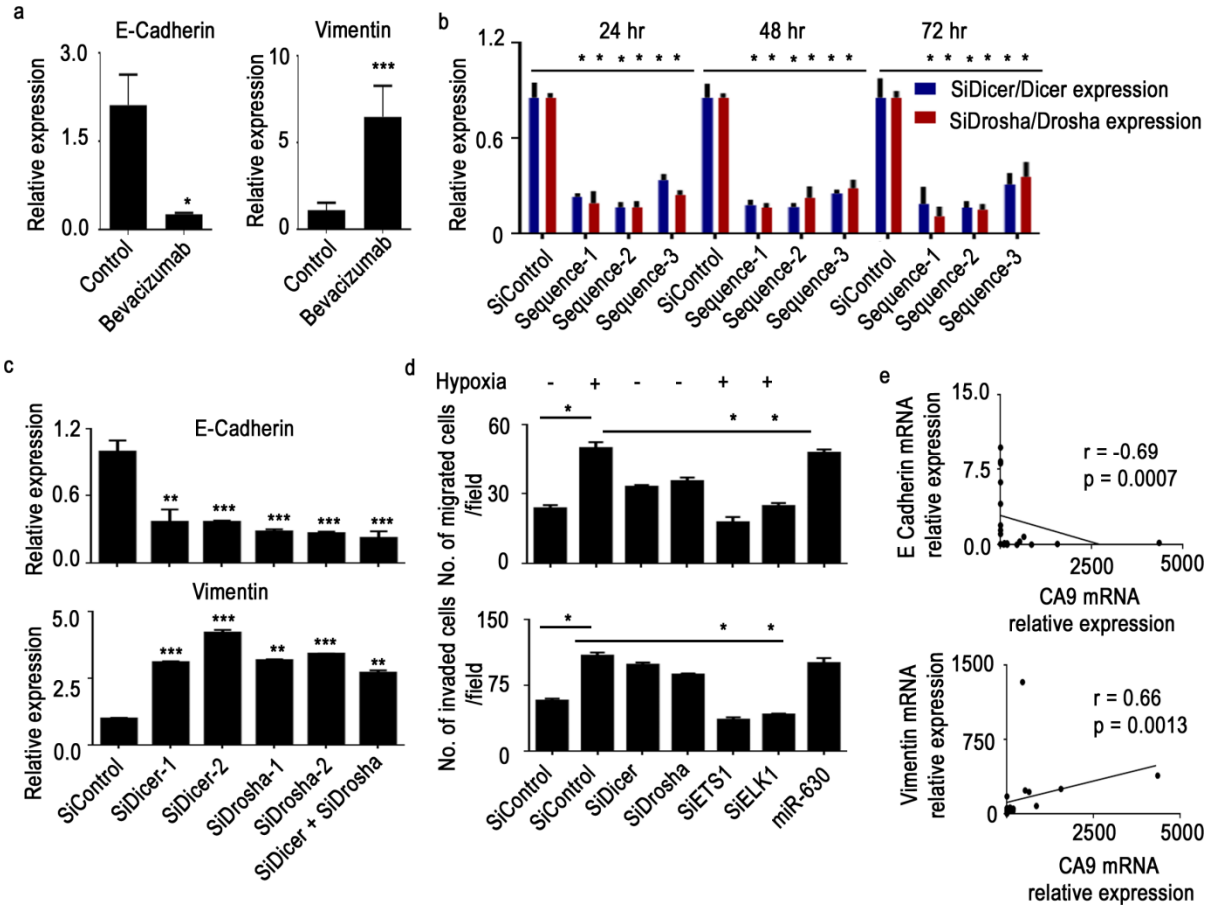

Figure 17: (a) mRNA levels of E-cadherin and vimentin in A2780 mouse tumor samples treated with bevacizumab. (b) Drosha and Dicer relative mRNA expression levels after knockdown using 3 independent siRNA sequences across 3 different time points in A2780 cells (c) E-cadherin (top) and vimentin (bottom) expression after knockdown of Dicer, Drosha, or both using siRNAs in A2780 cells. (d) Effect of Drosha and Dicer on cell migration and invasion in A2780 cells. Drosha and Dicer levels were downregulated using siRNAs under normoxic conditions. Rescue of Drosha was achieved using siRNAs against ETS1 and ELK1 under hypoxic conditions. Dicer expression in cells under normoxia exposure was decreased by transfecting cell with miR-630. (e) Pearson correlation between E-cadherin or vimentin and hypoxia marker carbonic anhydrase 9 (CA9) expression in clinical ovarian tumor samples (n=30). All images shown are representative and data are presented as mean ± standard error of the mean of n ≥ 3 experimental groups. *p < 0.05, **p < 0.01, ***p < 0.001 (Student t test).

We created stable cell lines ectopically expressing Dicer and/or Drosha in HeyA8 ovarian cancer cells that have low basal Drosha/Dicer expression levels, and exposed the cells to hypoxia **(Figure 18a, b)**. There was a significant reduction in EMT phenotype, including increased E-cadherin and decreased vimentin expression in HeyA8-control cells under hypoxia exposure. We observed disruption of hypoxia mediated induction of EMT phenotype upon rescue of Drosha and Dicer in these cells **(Figure 18c, d)**. In addition, a reduction in migration and invasion was observed in all three cell line variants compared to control cells exposed to hypoxia **(Figure 18e, f)**. Next, we ectopically expressed Drosha and Dicer in A2780 cells and tested their effects after hypoxia exposure **(Figure 18g).** There was significant reduction in the EMT phenotype in Drosha, Dicer or Drosha + Dicer expressing cells compared to control cells exposed to hypoxia **(Figure 18g)**.

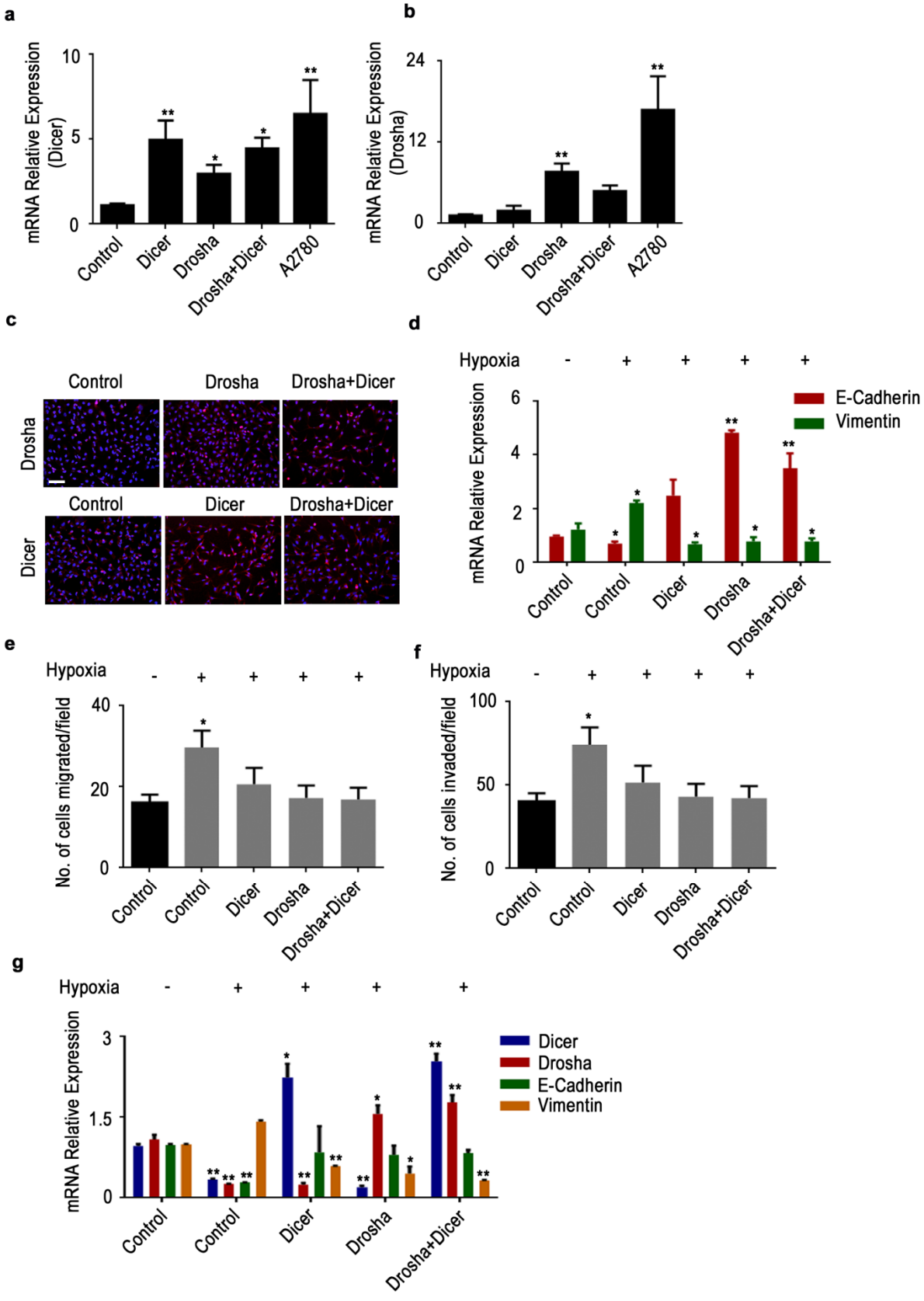
a
mRNA Relative Expression (Dicer)
10
5
0
Control
Dicer
Drosha
Drosha+Dicer
A2780
b
mRNA Relative Expression (Drosha)
24
12
0
c
Control
Drosha
Drosha+Dicer
Dicer
d
Hypoxia
E-Cadherin
Vimentin
mRNA Relative Expression
e
No. of cells migrated/field
40
20
f
No. of cells invaded/field
100
50
g
Dicer
Drosha
E-Cadherin
Vimentin
3
1.5

Figure 18: (a and b) Dicer and Drosha mRNA expression levels in HeyA8 cell line variants ectopically expressing Dicer, Drosha, Drosha + Dicer, compared to relative levels in A2780 cells. (c) Protein levels of Drosha and Dicer in HeyA8 cells ectopically expressing Drosha, Dicer or both, analyzed using immunofluorescence microscopy. Scale bar: 200 µm. (d) Expression of E-Cadherin and Vimentin in the HeyA8 cells expressing Dicer, Drosha, or both and treated with hypoxia. Data were normalized to normoxic cells. (e and f) Migration and invasion assay data showing number of cells migrated or invaded in the respective groups of cells ectopically expressing Drosha, Dicer, or both and exposed to hypoxia. (g) Expression of Dicer, Drosha, and EMT markers in A2780 cells exposed normoxia and hypoxia or in cells exposed to hypoxia while ectopically expressing Dicer, Drosha and Drosha + Dicer. Data are presented as mean ± standard error of the mean of $n \geq 3$ independent experimental groups. *$p<0.05$, **$p < 0.01$ (Student t test).

Next, to understand the biological roles that Drosha and Dicer play in tumor progression, we used an orthotopic model of ovarian cancer with luciferase-labeled A2780 cells implanted in the ovary. Upon knockdown of Drosha and Dicer using siRNAs encapsulated in DOPC nanoliposomes, we observed significant increases in aggregate tumor weight **(Figure 19)** and number and incidence of distant metastatic nodules **(Figure 19b)** in the treatment groups compared with the control group. These findings are consistent with the increase in luciferase intensity observed in treatment groups **(Figure 19c)**. The tumor metastasis rate was significantly higher including rare sites such as liver in the siDicer-DOPC, siDrosha-DOPC, and combination treatment groups compared with the control group **(Figure 19d)**, which showed metastatic lesions only in the mesentery. Reduction in Dicer or Drosha expression in respective treatment groups was also observed **(Figure 19e)**. Decreased E-cadherin and increased vimentin protein levels were observed in the siDicer, siDrosha, and combination treatment groups compared with the control group **(Figure 19f)**. Treatment with siDicer + siDrosha also produced a similar pattern as A2780 model in the MCF7 mouse model of breast cancer with significant increases in tumor growth and metastatic rate being observed **(Figure 20a-d)**. In the HeyA8 *in vivo* model of ovarian cancer, ectopically expression of Drosha, Dicer, or Drosha + Dicer resulted in significant reduction in tumor weight **(Figure 20e)** and number of distant metastatic nodules **(Figure 20g)**.

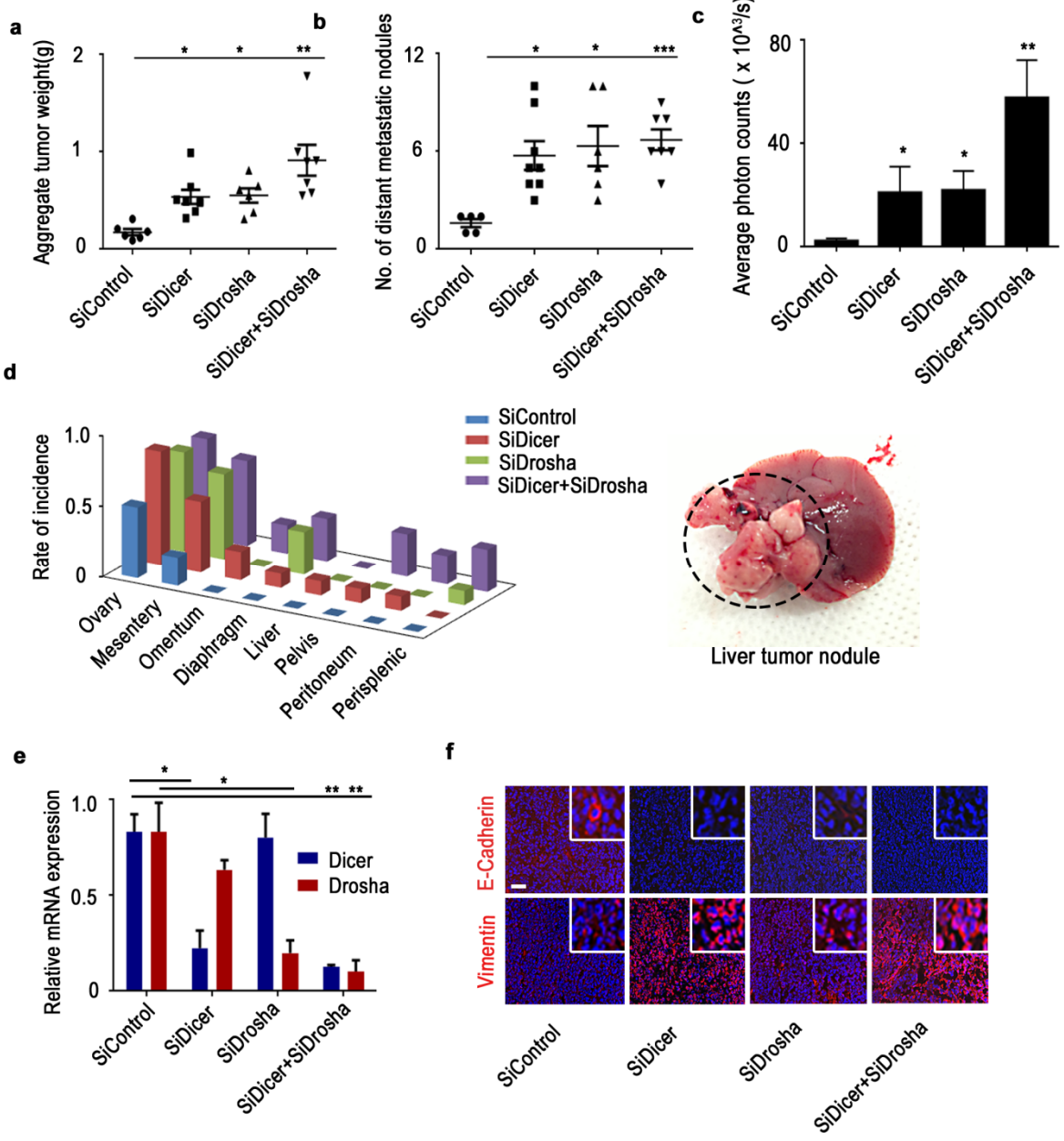
a
Aggregate tumor weight(g)
2
1
0
* * **
SiControl
SiDicer
SiDrosha
SiDicer+SiDrosha
b
No. of distant metastatic nodules
12
6
0
* * ***
SiControl
SiDicer
SiDrosha
SiDicer+SiDrosha
c
Average photon counts (x 10^3/s)
80
40
0
* * **
SiControl
SiDicer
SiDrosha
SiDicer+SiDrosha
d
Rate of incidence
1.0
0.5
0
Ovary
Mesentery
Omentum
Diaphragm
Liver
Pelvis
Peritoneum
Perisplenic
SiControl
SiDicer
SiDrosha
SiDicer+SiDrosha
Liver tumor nodule
e
Relative mRNA expression
1.0
0.5
0
* * ** **
Dicer
Drosha
SiControl
SiDicer
SiDrosha
SiDicer+SiDrosha
f
E-Cadherin
Vimentin
SiControl
SiDicer
SiDrosha
SiDicer+SiDrosha

Figure 19: Aggregate tumor weight (a) and number of distant metastatic nodules (b) in mice treated with siRNA against Dicer, Drosha, or both compared with the control siRNA group (n = 10 per group). (c) Average photon counts from each group of mice treated with siRNA against Dicer, Drosha, or both compared to controls. Representative bioluminescence images are shown below the respective groups. (d) Distant metastatic nodule incidence rate in an orthotopic mouse model of ovarian cancer. Metastatic liver nodule representative picture is shown. (e) Drosha and Dicer mRNA expression in mouse tumor samples treated with siRNA against Dicer or Drosha. (f) Expression of epithelial-to-mesenchymal transition markers (E-cadherin-Red, vimentin-Red, Nucleus-Blue) in tumor samples from the in vivo experiment groups. Scale bar: 200 µm. Aggregate tumor weight (g) and number of distant metastatic nodules (h) in mice implanted with HeyA8 cells ectopically expressing Dicer, Drosha and Dicer + Drosha. *$p < 0.05$, **$p < 0.01$, ***$p < 0.001$ (Student t test).

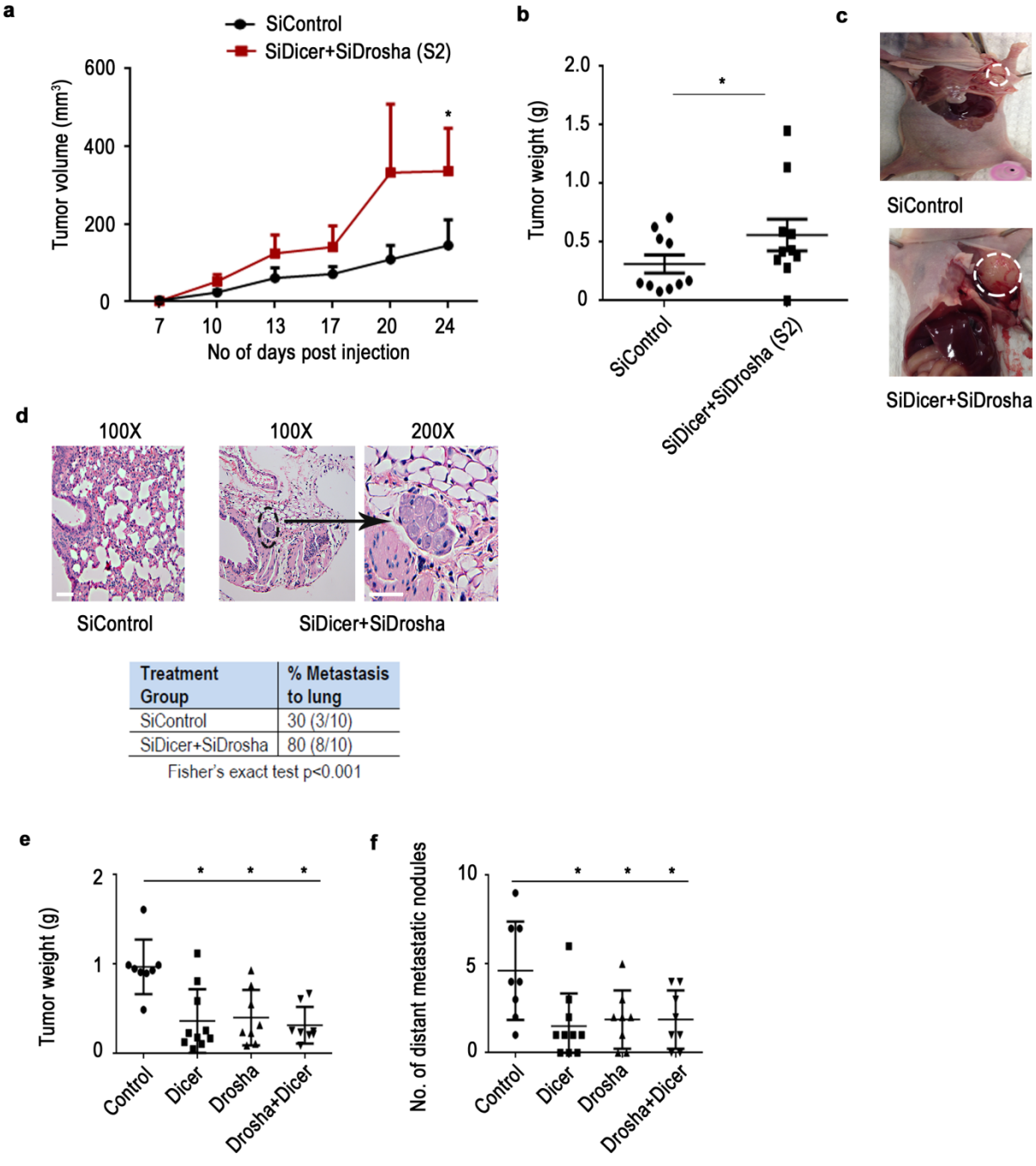

Treatment Group	% Metastasis to lung
SiControl	30 (3/10)
SiDicer+SiDrosha	80 (8/10)

Fisher's exact test p<0.001

Figure 20: (a-d) Effect of silencing Dicer and Drosha using siRNAs (seq 2) in the MCF7 mouse model of breast cancer. Tumor volume (a) and aggregate tumor weight (b) across 2 groups. (c) Representative pictures showing tumor burden (white dotted circles) in all the groups. (d) Representative hematoxylin and eosin staining of lungs from the in vivo MCF7 mouse model depicting micrometastases in the siDicer + Drosha group (top) and quantification of the micrometastases in the control and siDicer + siDrosha groups (bottom; n = 10 per group). Scale bar: 200 µm. (e-f) Aggregate tumor weight (e) and number of distant metastatic nodules (f) in mice implanted with HeyA8 cells ectopically expressing Dicer, Drosha and Dicer + Drosha. *$p < 0.05$, **$p < 0.01$, ***$p < 0.001$ (Student t test).

We next sought to determine whether treatment with siETS1/siELK1 could reverse the hypoxia-induced downregulation of miRNA biogenesis machinery following treatment with bevacizumab. Mice were treated with bevacizumab 2 weeks after tumor establishment. There was a significant increase in tumor weight and number of metastatic nodules in the bevacizumab treatment group **(Figure 21a)**. In mice treated with siETS1/siELK1 and anti-miR-630, we observed significant reductions in tumor weight and number of metastatic nodules compared with mice treated with bevacizumab alone **(Figure 21b, c)**. A significant increase in CA9 expression was observed in mice that received anti-VEGF therapy compared with control mice **(Figure 21d)**. Importantly, we noted rescue of Drosha expression in the siETS/ELK1 treatment group, and rescue of Dicer in anti-miR-630 treatment group **(Figure 21e)**. Taken together, these data demonstrate the importance of Drosha in tumor progression, as well as the role of ETS1/ELK1 in its regulation.

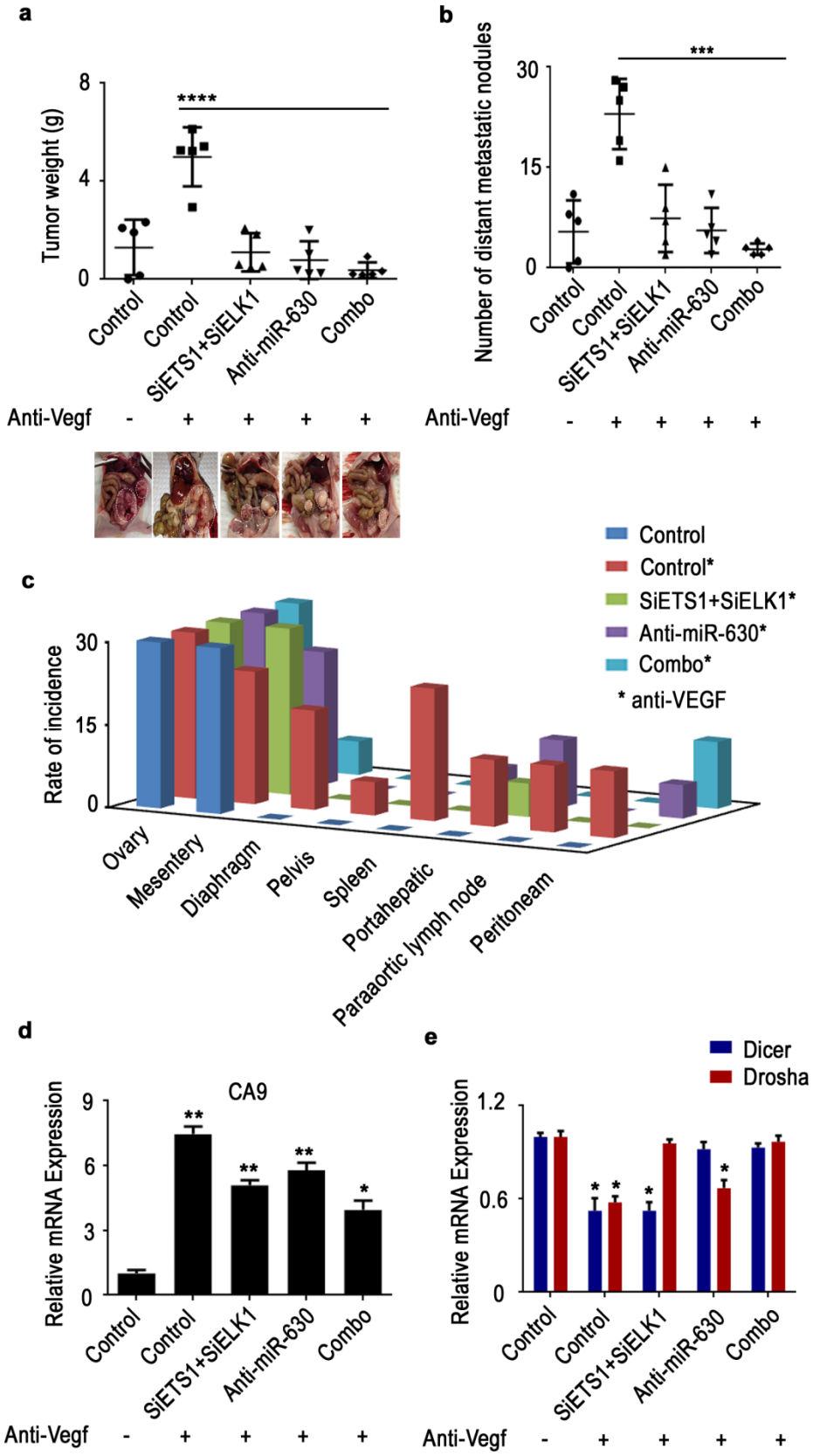
a
Tumor weight (g)
8
4
0
****
Control
Control
SiETS1+SiELK1
Anti-miR-630
Combo
Anti-Vegf - + + + +
b
Number of distant metastatic nodules
30
15
0
***
Control
Control
SiETS1+SiELK1
Anti-miR-630
Combo
Anti-Vegf - + + + +
c
Control
Control*
SiETS1+SiELK1*
Anti-miR-630*
Combo*
* anti-VEGF
Rate of incidence
30
15
0
Ovary
Mesentery
Diaphragm
Pelvis
Spleen
Portahepatic
Paraaortic lymph node
Peritoneam
d
CA9
Relative mRNA Expression
9
6
3
0
**
**
**
*
Control
Control
SiETS1+SiELK1
Anti-miR-630
Combo
Anti-Vegf - + + + +
e
Dicer
Drosha
Relative mRNA Expression
1.2
0.6
0
Control
Control
SiETS1+SiELK1
Anti-miR-630
Combo
Anti-Vegf - + + + +

Figure 21: Effect of rescue of Drosha after anti–vascular endothelial growth factor (VEGF) therapy in A2780 model. Aggregate tumor weight is shown (a) and number of distant metastatic nodules (b) in mice treated with bevacizumab and mice treated with siRNAs against ETS+ELK1. Also shown are representative pictures of tumor burden (a, bottom) in all treatment groups (n = 5 per group). (c) Distribution of metastatic nodules in individual mice groups treated with siDicer, siDrosha and siDicer + siDrosha. Hypoxia marker CA9 (d) and Dicer and Drosha (e) mRNA expression levels in the tumor samples from the mouse model. All images shown are representative and data are presented as mean ± standard error of the mean of n ≥ 3 experimental groups. *p < 0.05, **p < 0.01, ***p < 0.001 (Student t test).

Chapter 7: Discussion

MicroRNAs (miRNAs) are evolutionarily conserved small RNA molecules intricately involved in gene regulation [1, 2]. Considering the broad functional involvement of miRNAs in cellular homeostasis, it is not surprising that cancer cells have altered miRNA levels [2, 84] and that miRNAs are extensively involved in cancer progression [85, 86]. Although global miRNA downregulation in cancer has been reported [2, 87, 88], the mechanism of this downregulation is not fully understood. Drosha and Dicer are key enzymes involved in miRNA biogenesis. We and others have previously shown that downregulation of Drosha and Dicer in ovarian, lung, and breast cancer is associated with poor patient outcomes [33, 34, 38, 40, 88]. Although individual regulators of Dicer (e.g., let7) [40, 42, 43, 46, 64] have been implicated, the underlying mechanisms are poorly defined. During cancer growth, tumors develop significant hypoxia and have been attributed to tumor promoting effects and even cancer resistance to therapy [60, 61]. Direct assessment of tumor hypoxia in clinical patient samples have showed worst patient out come in the cohort with higher hypoxia in the tumors[62]. Cancer cells evolve to grow under hypoxia conditions by modifying their key cellular metabolisms and gene alterations [60, 61]. Anti-VEGF therapies shown to induce hypoxia and cancers post treatment have aggressive tumor recurrence and increased invasiveness but the mechanisms are not clear. A previous study showed downregulation of Dicer in hypoxia leading to downregulated miRNA in endothelial cells [64]. In addition, EGFR dependent Argonaute2 deficiency under hypoxia was shown to lead to downregulated miRNAs [46]. However a comprehensive study understanding the impact of hypoxia on

cancer cells with regard to miRNA biogenesis has not addressed. My thesis project directly addressed this question.

7.1: Role of hypoxia deregulated miRNAs

Using breast cancer cell lines cultured under normoxia or hypoxia, a hypoxia signature of miRNAs was identified [89]. One of the miRNA in this group is miR-210, a transcriptional target of HIF1-α [90]. By use of Ago2 immunoprecipitation and RNA sequencing analysis, more than 50 potential gene targets of miR-210 have been identified and these targets are involved in hypoxia response, towards better cell survival. In orthotopic mouse models of head and neck or pancreatic cancer, loss of miR-210 resulted in decreased tumor initiation or growth [90]. The role of miR-210 in mitochondrial alteration under hypoxia has been reported. MiR-210 was one among the highly upregulated miRNAs in late lung cancer patients samples [91]. In the cell line overexpression miR-210, microarray based mRNA signature pathway analysis suggested increase in apoptosis. However, target analysis showed miR-210 targets SDHD, leading to stabilization of HIF1-α and survival under hypoxia [91]. However, another study showed cytoprotective roles of miR-210 by targeting apoptosis-inducing factor, mitochondrion-associated 3 (AIFM3), known to induce cell death [92]. Negative regulation of NF-κB1 in murine macrophages by miR-210 resulting in decreased cytokines has been observed, suggesting that miR-210 role is not limited to cancer cell signaling [93]. Increased miR-210 in the placenta results in decreased IL6/STAT signaling [94]. MiR-210 is also involved in TH17 differentiation. HIF1-α is reported as a target of miR-210 in T-cells and, under hypoxia deletion of mir-210 promoted TH17 differentiation [95]. Considering controversies that exist on role of

TH17 differentiation acting as either pro-tumor or anti-tumor, role of miR-210 under hypoxia in Th17 differentiation is an important question to be answered.

MiR-34 is another important miRNA downregulated under hypoxia conditions and is involved in influencing cancer cells and tumor microenvironment [96]. Notch1 and Jagged1 as the target of miR-34a, and also transfection of miR-34a resulted in reversal of EMT [96]. In prostate cancer, miR-34 was involved in cancer stem cells signaling by direct targeting of CD44 [97]. In colorectal cancer, downregulation in miR-34 results in increased IL6 signaling, leading to EMT and cancer metastasis [98]. Altogether, these data suggest a mechanism for hypoxia induced increased cancer metastasis.

Another miRNA proven to have important roles in hypoxia response is MiR-199a. Downregulation of miR-199a under hypoxia exposure results in derepression of Hif-1α and Sirtuin 1, resulting in the preconditioning of myocardiocytes [99]. Targeting of mTOR and c-met by miR-199a resulted in increased sensitivity to doxorubicin [100]. Targeting of PPARδ by miR-199a under cardiac hypoxia resulted in metabolic shift toward glycolysis. Treatment with antagomir-199a resulted in mice displaying improved cardiac function and restored mitochondrial fatty acid oxidation [101]. Eventhough this study is not on cancer mouse model, it stresses on importance of miR-199a in modulating hypoxia metabolism. Recently, role of miR-199 in regulation of HIF signaling in ovarian cancer has been reported [102]. Decreased miR-199a expression in the hypoxic condition resulted in increased HIFs levels. Exogenous expression of miR-199a decreased HIFs, cell migration, and

metastasis of ovarian cancer cells [102], suggesting potential therapeutic strategy to target cancer metastasis.

Eventhough these studies have stressed the importance of hypoxia on miRNA alterations, a comprehensive study understanding the impact of hypoxia on cancer cells with regard to miRNA biogenesis remains obscure while considering significant roles played by the tumor microenvironment on tumor growth.

7.2: Significance

Our data shows that tumor hypoxia plays a critical role in the downregulation of Drosha and Dicer, leading to downregulated miRNA biogenesis in cancer. Drosha is downregulated by ETS1 and ELK1 recruitment of HDAC1 and ARID4B onto the promoter, and Dicer is downregulated by miR-630. Using efficient DOPC nanoparticles, we delivered siRNAs against ETS1/ELK1 or anti-miR-630 under hypoxic conditions *in vivo*, which in-turn rescued expression of Drosha and Dicer and led to significant reductions in tumor growth and metastasis **(Figure 22)**.

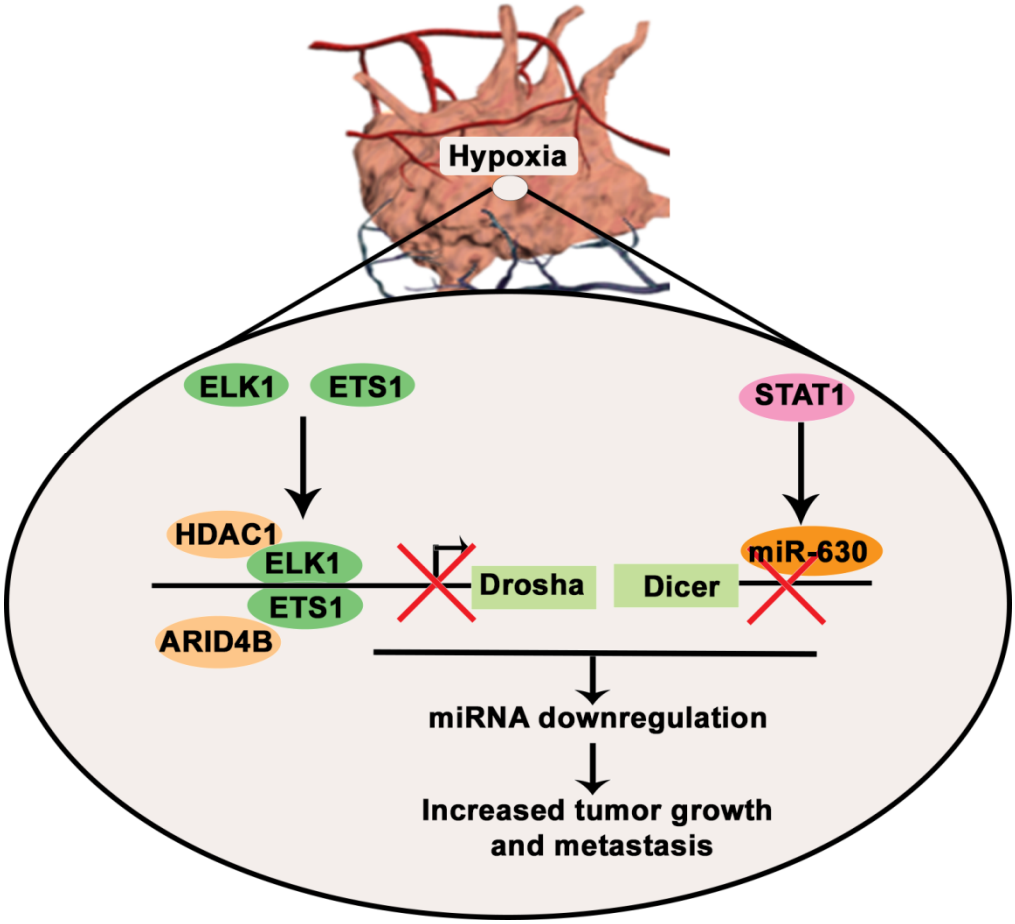

Figure 22: Overall model of the study showing the mechanistic understanding and biological implications of downregulation of Drosha and Dicer under hypoxic conditions.

During progression, tumors encounter significant hypoxia owing to abnormal vasculature [60]. Emerging studies have shown that hypoxia is involved in promoting tumor progression and resistance to therapy [60, 61]. Direct assessment of tumor hypoxia in patient samples has demonstrated worse clinical outcomes in patients whose tumors had high levels of hypoxia [62]. In addition, emerging data suggest that anti-VEGF therapies currently in use in the clinic induce significant hypoxia in tumors [103, 104]. We observed that short-term anti-VEGF therapy results in potential “angiogenesis rebound,” resulting in increased cancer metastasis. Recent report showed hypoxia mediating Ago2 downregulation [46], leading to downregulation in group of miRNAs which further strengthens importance of hypoxia and miRNA biogenesis link.

Our laboratory and several others have shown that decreased expression of Drosha and Dicer in cancer is associated with poor clinical outcome [33, 34, 38, 40, 46]. This study sheds light on this clinical observation and provides logical molecular understanding of the role of hypoxia in regulating Drosha and Dicer. Use of RNAi-based gene targeting is an upcoming strategy to develop therapies that target non-druggable genes using classic chemical agents or antibodies [54, 105, 106]. As demonstrated in this study, DOPC liposome-coated siRNA or an anti-miRNA system for *in vivo* delivery acts as a promising therapeutic approach to rescue expression of Drosha and Dicer in cancer. In summary, this study provides a clear mechanistic link between hypoxia-miRNA biogenesis-tumor progression. These findings could translate into the development of new translational approaches that target dysregulated miRNA biogenesis.

7.3: Future directions

MiRNAs have a unique advantage in targeted therapy because single miRNAs can target multiple genes. As highlighted in earlier reviews, miRNA or siRNA delivery to tumors is an attractive, yet challenging approach to improve cancer therapy [105, 107-109]. Some of the major challenges are identifying clinically feasible delivery approaches for these nucleotides, and designing stable synthetic miRNA or siRNA molecules [105, 110]. One of the early miRNA therapeutic strategies that showed a significant impact on tumor growth was the delivery of miR-34a and Let-7 in lung cancer models [111]. Encouraging results from preclinical studies involving miR-34a in several types of cancer have accelerated efforts to move miR-34a into clinical trials [112]. Delivery of miR-200 in ovarian, lung, breast, and renal cancer preclinical models significantly reduced tumor metastasis and angiogenesis and induced vascular normalization by targeting IL-8 and CXCL1 [54]. We also showed that combining miRNA with siRNA was another viable approach for targeting cancer. Combined systemic delivery of miR-520d-3p with EphA2 siRNA using the DOPC nanoliposomal system resulted in significant reduction in tumor growth and metastasis [113]. We provide evidence in this study, use of siRNA/miRNA in combination with anti-VEGF therapy shows promising anti-tumor effects.

Apart from therapeutic implications, my study answered several questions which advances knowledge of the role of miRNAs in tumor biology and the current role of hypoxia in other disease settings. Considering the significant relationship between the role of hypoxia in Dicer and Drosha downregulation, we can hypothesize other

stress factors such reactive oxygen species in the tumor microenvironment might play role in ncRNA modulation as well. To my knowledge, no studies exist to support the role of these factors on miRNA biogenesis pathways in cancer.

With advances in genomic and proteomic approaches, it is of great interest to study the role of miRNA-mRNA targets that are deregulated in hypoxia, despite low levels of Dicer and Drosha under these conditions. Using a systems-based approach, a study of miRNAs upregulated in hypoxia and their mRNA targets will further our understanding of hypoxia biology and the molecular mechanisms involved in hypoxia promoting tumor progression.

I further speculate that there are miRNAs that are independent of Dicer and Drosha. My study further strengthens this phenomenon and opens up avenues to study miRNA biogenesis in this context. Using cell specific knockouts and genomic sequencing approaches, we can study miRNAs, which are not influenced by either hypoxia or loss of Dicer and Drosha in various disease settings.

Translational implications: Hypoxia is an integral microenvironment factor aiding tumor progression. Ever rising shortage of angiogenesis and improperly developed tortuous blood vessels in the tumor lead to the development of hypoxia during tumor growth. Interestingly, anti-angiogenesis therapeutic agents targeting VEGF or VEGFR are shown to induce hypoxia in tumors, while showing modest therapeutic benefits as single agents. There is an increasing need for understanding complex biological signaling arising due to hypoxia and cancer cell interactions and for developing better therapeutic strategies. MiRNAs are known to regulate key cellular

signaling *via* mRNA modulations. Several miRNAs have previously been reported to be altered in the tumor microenvironment; however, clear understandings on regulatory mechanisms are not clear. In this study, we elucidate the mechanisms governing the downregulation of miRNAs in hypoxic tumors. We demonstrate that hypoxia leads to decreased biogenesis enzymes, Drosha and Dicer. Additionally, downstream effector mRNAs were found to be upregulated due to loss of repression by miRNAs, which ultimately led to tumor progression. As shown in the study, use of siRNAs or anti-miRNAs targeting the deregulatory mechanisms show a great promise for rescue of miRNA biogenesis in hypoxic tumors. Overall, we provide significant conceptual advancement in understanding the key microenvrionmental influences on tumor progression.

Bibliography

1. Bartel, D.P., *MicroRNAs: genomics, biogenesis, mechanism, and function.* Cell, 2004. **116**(2): p. 281-97.
2. Lee, Y.S. and A. Dutta, *MicroRNAs in cancer.* Annu Rev Pathol, 2009. **4**: p. 199-227.
3. Esteller, M., *Non-coding RNAs in human disease.* Nat Rev Genet, 2011. **12**(12): p. 861-74.
4. Lee, R.C., R.L. Feinbaum, and V. Ambros, *The C. elegans heterochronic gene lin-4 encodes small RNAs with antisense complementarity to lin-14.* Cell, 1993. **75**(5): p. 843-54.
5. Wightman, B., I. Ha, and G. Ruvkun, *Posttranscriptional regulation of the heterochronic gene lin-14 by lin-4 mediates temporal pattern formation in C. elegans.* Cell, 1993. **75**(5): p. 855-62.
6. Spizzo, R., M.S. Nicoloso, C.M. Croce, and G.A. Calin, *SnapShot: MicroRNAs in Cancer.* Cell, 2009. **137**(3): p. 586-586 e1.
7. Boehm, M. and F.J. Slack, *MicroRNA control of lifespan and metabolism.* Cell Cycle, 2006. **5**(8): p. 837-40.
8. Pasquinelli, A.E., S. Hunter, and J. Bracht, *MicroRNAs: a developing story.* Current Opinion in Genetics & Development., 2005. **15**: p. 200-205.
9. Bartel, D.P., *MicroRNAs: genomics, biogenesis, mechanism, and function.* Cell, 2004. **116**(2): p. 281-97.

10. Lee, Y., M. Kim, J. Han, K.H. Yeom, S. Lee, S.H. Baek, and V.N. Kim, *MicroRNA genes are transcribed by RNA polymerase II.* EMBO J, 2004. **23**(20): p. 4051-60.

11. Lee, Y., C. Ahn, J. Han, H. Choi, J. Kim, J. Yim, J. Lee, P. Provost, O. Radmark, S. Kim, and V.N. Kim, *The nuclear RNase III Drosha initiates microRNA processing.* Nature, 2003. **425**(6956): p. 415-9.

12. Han, J., Y. Lee, K.H. Yeom, J.W. Nam, I. Heo, J.K. Rhee, S.Y. Sohn, Y. Cho, B.T. Zhang, and V.N. Kim, *Molecular basis for the recognition of primary microRNAs by the Drosha-DGCR8 complex.* Cell, 2006. **125**(5): p. 887-901.

13. Yi, R., Y. Qin, I.G. Macara, and B.R. Cullen, *Exportin-5 mediates the nuclear export of pre-microRNAs and short hairpin RNAs.* Genes Dev, 2003. **17**(24): p. 3011-6.

14. Gregory, R.I., *The Microprocessor complex mediates the genesis of microRNAs.* Nature, 2004. **432**: p. 235-240.

15. Gregory, R.I., T.P. Chendrimada, N. Cooch, and R. Shiekhattar, *Human RISC couples microRNA biogenesis and posttranscriptional gene silencing.* Cell, 2005. **123**: p. 631-640.

16. Haase, A.D., L. Jaskiewicz, H. Zhang, S. Laine, R. Sack, A. Gatignol, and W. Filipowicz, *TRBP, a regulator of cellular PKR and HIV-1 virus expression, interacts with Dicer and functions in RNA silencing.* EMBO Rep, 2005. **6**(10): p. 961-7.

17. Chendrimada, T.P., *TRBP recruits the Dicer complex to Ago2 for microRNA processing and gene silencing.* Nature, 2005. **436**: p. 740-744.

18. Gregory, R.I., T.P. Chendrimada, N. Cooch, and R. Shiekhattar, *Human RISC couples microRNA biogenesis and posttranscriptional gene silencing.* Cell, 2005. **123**(4): p. 631-40.

19. Haase, A.D., *TRBP, a regulator of cellular PKR and HIV-1 virus expression, interacts with Dicer and functions in RNA silencing.* EMBO Rep., 2005. **6**: p. 961-967.

20. Bernstein, E., A.A. Caudy, S.M. Hammond, and G.J. Hannon, *Role for a bidentate ribonuclease in the initiation step of RNA interference.* Nature, 2001. **409**(6818): p. 363-6.

21. Bernstein, E., *Dicer is essential for mouse development.* Nature Genet., 2003. **35**: p. 215-217.

22. Tomari, Y., C. Matranga, B. Haley, N. Martinez, and P.D. Zamore, *A protein sensor for siRNA asymmetry.* Science, 2004. **306**(5700): p. 1377-80.

23. Matranga, C., Y. Tomari, C. Shin, D.P. Bartel, and P.D. Zamore, *Passenger-strand cleavage facilitates assembly of siRNA into Ago2-containing RNAi enzyme complexes.* Cell, 2005. **123**: p. 607-620.

24. Zamilpa, R., R. Rupaimoole, C.F. Phelix, M. Somaraki-Cormier, W. Haskins, R. Asmis, and R.G. LeBaron, *C-terminal fragment of transforming growth factor beta-induced protein (TGFBIp) is required for apoptosis in human osteosarcoma cells.* Matrix Biol, 2009. **28**(6): p. 347-53.

25. Reinhart, B.J., F.J. Slack, M. Basson, A.E. Pasquinelli, J.C. Bettinger, A.E. Rougvie, H.R. Horvitz, and G. Ruvkun, *The 21-nucleotide let-7 RNA regulates*

developmental timing in Caenorhabditis elegans. Nature, 2000. **403**(6772): p. 901-6.

26. Horvitz, H.R. and J.E. Sulston, *Isolation and genetic characterization of cell-lineage mutants of the nematode Caenorhabditis elegans.* Genetics, 1980. **96**(2): p. 435-54.
27. Bernstein, E., S.Y. Kim, M.A. Carmell, E.P. Murchison, H. Alcorn, M.Z. Li, A.A. Mills, S.J. Elledge, K.V. Anderson, and G.J. Hannon, *Dicer is essential for mouse development.* Nat Genet, 2003. **35**(3): p. 215-7.
28. Giraldez, A.J., R.M. Cinalli, M.E. Glasner, A.J. Enright, J.M. Thomson, S. Baskerville, S.M. Hammond, D.P. Bartel, and A.F. Schier, *MicroRNAs regulate brain morphogenesis in zebrafish.* Science, 2005. **308**(5723): p. 833-8.
29. Chen, C.Z., L. Li, H.F. Lodish, and D.P. Bartel, *MicroRNAs modulate hematopoietic lineage differentiation.* Science, 2004. **303**(5654): p. 83-6.
30. Naguibneva, I., M. Ameyar-Zazoua, A. Polesskaya, S. Ait-Si-Ali, R. Groisman, M. Souidi, S. Cuvellier, and A. Harel-Bellan, *The microRNA miR-181 targets the homeobox protein Hox-A11 during mammalian myoblast differentiation.* Nat Cell Biol, 2006. **8**(3): p. 278-84.
31. Lagos-Quintana, M., R. Rauhut, A. Yalcin, J. Meyer, W. Lendeckel, and T. Tuschl, *Identification of tissue-specific microRNAs from mouse.* Curr Biol, 2002. **12**(9): p. 735-9.
32. Chen, J.F., E.M. Mandel, J.M. Thomson, Q. Wu, T.E. Callis, S.M. Hammond, F.L. Conlon, and D.Z. Wang, *The role of microRNA-1 and microRNA-133 in*

skeletal muscle proliferation and differentiation. Nat Genet, 2006. **38**(2): p. 228-33.

33. Karube, Y., H. Tanaka, H. Osada, S. Tomida, Y. Tatematsu, K. Yanagisawa, Y. Yatabe, J. Takamizawa, S. Miyoshi, T. Mitsudomi, and T. Takahashi, *Reduced expression of Dicer associated with poor prognosis in lung cancer patients.* Cancer Sci, 2005. **96**(2): p. 111-5.

34. Merritt, W.M., Y.G. Lin, L.Y. Han, A.A. Kamat, W.A. Spannuth, R. Schmandt, D. Urbauer, L.A. Pennacchio, J.F. Cheng, A.M. Nick, M.T. Deavers, A. Mourad-Zeidan, H. Wang, P. Mueller, M.E. Lenburg, J.W. Gray, S. Mok, M.J. Birrer, G. Lopez-Berestein, R.L. Coleman, M. Bar-Eli, and A.K. Sood, *Dicer, Drosha, and outcomes in patients with ovarian cancer.* N Engl J Med, 2008. **359**(25): p. 2641-50.

35. Wang, X., X. Zhao, P. Gao, and M. Wu, *c-Myc modulates microRNA processing via the transcriptional regulation of Drosha.* Sci Rep, 2013. **3**: p. 1942.

36. Allegra, D., V. Bilan, A. Garding, H. Dohner, S. Stilgenbauer, F. Kuchenbauer, and D. Mertens, *Defective DROSHA processing contributes to downregulation of MiR-15/-16 in chronic lymphocytic leukemia.* Leukemia, 2014. **28**(1): p. 98-107.

37. Torres, A., K. Torres, T. Paszkowski, B. Jodlowska-Jedrych, T. Radomanski, A. Ksiazek, and R. Maciejewski, *Major regulators of microRNAs biogenesis Dicer and Drosha are down-regulated in endometrial cancer.* Tumour Biol, 2011. **32**(4): p. 769-76.

38. Dedes, K.J., R. Natrajan, M.B. Lambros, F.C. Geyer, M.A. Lopez-Garcia, K. Savage, R.L. Jones, and J.S. Reis-Filho, *Down-regulation of the miRNA master regulators Drosha and Dicer is associated with specific subgroups of breast cancer.* Eur J Cancer, 2011. **47**(1): p. 138-50.

39. Guo, X., Q. Liao, P. Chen, X. Li, W. Xiong, J. Ma, X. Li, Z. Luo, H. Tang, M. Deng, Y. Zheng, R. Wang, W. Zhang, and G. Li, *The microRNA-processing enzymes: Drosha and Dicer can predict prognosis of nasopharyngeal carcinoma.* J Cancer Res Clin Oncol, 2012. **138**(1): p. 49-56.

40. Su, X., D. Chakravarti, M.S. Cho, L. Liu, Y.J. Gi, Y.L. Lin, M.L. Leung, A. El-Naggar, C.J. Creighton, M.B. Suraokar, I. Wistuba, and E.R. Flores, *TAp63 suppresses metastasis through coordinate regulation of Dicer and miRNAs.* Nature, 2010. **467**(7318): p. 986-90.

41. Muller, P.A., A.G. Trinidad, P.T. Caswell, J.C. Norman, and K.H. Vousden, *Mutant p53 regulates Dicer through p63-dependent and -independent mechanisms to promote an invasive phenotype.* J Biol Chem, 2014. **289**(1): p. 122-32.

42. Martello, G., A. Rosato, F. Ferrari, A. Manfrin, M. Cordenonsi, S. Dupont, E. Enzo, V. Guzzardo, M. Rondina, T. Spruce, A.R. Parenti, M.G. Daidone, S. Bicciato, and S. Piccolo, *A MicroRNA targeting dicer for metastasis control.* Cell, 2010. **141**(7): p. 1195-207.

43. Tokumaru, S., M. Suzuki, H. Yamada, M. Nagino, and T. Takahashi, *let-7 regulates Dicer expression and constitutes a negative feedback loop.* Carcinogenesis, 2008. **29**(11): p. 2073-7.

44. Melo, S.A., S. Ropero, C. Moutinho, L.A. Aaltonen, H. Yamamoto, G.A. Calin, S. Rossi, A.F. Fernandez, F. Carneiro, C. Oliveira, B. Ferreira, C.G. Liu, A. Villanueva, G. Capella, S. Schwartz, Jr., R. Shiekhattar, and M. Esteller, *A TARBP2 mutation in human cancer impairs microRNA processing and DICER1 function.* Nat Genet, 2009. **41**(3): p. 365-70.

45. De Vito, C., N. Riggi, S. Cornaz, M.L. Suva, K. Baumer, P. Provero, and I. Stamenkovic, *A TARBP2-dependent miRNA expression profile underlies cancer stem cell properties and provides candidate therapeutic reagents in Ewing sarcoma.* Cancer Cell, 2012. **21**(6): p. 807-21.

46. Shen, J., W. Xia, Y.B. Khotskaya, L. Huo, K. Nakanishi, S.O. Lim, Y. Du, Y. Wang, W.C. Chang, C.H. Chen, J.L. Hsu, Y. Wu, Y.C. Lam, B.P. James, X. Liu, C.G. Liu, D.J. Patel, and M.C. Hung, *EGFR modulates microRNA maturation in response to hypoxia through phosphorylation of AGO2.* Nature, 2013. **497**(7449): p. 383-7.

47. Zhang, X., G. Wan, F.G. Berger, X. He, and X. Lu, *The ATM kinase induces microRNA biogenesis in the DNA damage response.* Mol Cell, 2011. **41**(4): p. 371-83.

48. Mori, M., R. Triboulet, M. Mohseni, K. Schlegelmilch, K. Shrestha, F.D. Camargo, and R.I. Gregory, *Hippo signaling regulates microprocessor and links cell-density-dependent miRNA biogenesis to cancer.* Cell, 2014. **156**(5): p. 893-906.

49. Melo, S.A., C. Moutinho, S. Ropero, G.A. Calin, S. Rossi, R. Spizzo, A.F. Fernandez, V. Davalos, A. Villanueva, G. Montoya, H. Yamamoto, S.

Schwartz, Jr., and M. Esteller, *A genetic defect in exportin-5 traps precursor microRNAs in the nucleus of cancer cells.* Cancer Cell, 2010. **18**(4): p. 303-15.

50. Gregory, P.A., A.G. Bert, E.L. Paterson, S.C. Barry, A. Tsykin, G. Farshid, M.A. Vadas, Y. Khew-Goodall, and G.J. Goodall, *The miR-200 family and miR-205 regulate epithelial to mesenchymal transition by targeting ZEB1 and SIP1.* Nat Cell Biol, 2008. **10**(5): p. 593-601.

51. Korpal, M., E.S. Lee, G. Hu, and Y. Kang, *The miR-200 family inhibits epithelial-mesenchymal transition and cancer cell migration by direct targeting of E-cadherin transcriptional repressors ZEB1 and ZEB2.* J Biol Chem, 2008. **283**(22): p. 14910-4.

52. Park, S.M., A.B. Gaur, E. Lengyel, and M.E. Peter, *The miR-200 family determines the epithelial phenotype of cancer cells by targeting the E-cadherin repressors ZEB1 and ZEB2.* Genes Dev, 2008. **22**(7): p. 894-907.

53. Chan, Y.C., S. Khanna, S. Roy, and C.K. Sen, *miR-200b targets Ets-1 and is down-regulated by hypoxia to induce angiogenic response of endothelial cells.* J Biol Chem, 2011. **286**(3): p. 2047-56.

54. Pecot, C.V., R. Rupaimoole, D. Yang, R. Akbani, C. Ivan, C. Lu, S. Wu, H.D. Han, M.Y. Shah, C. Rodriguez-Aguayo, J. Bottsford-Miller, Y. Liu, S.B. Kim, A. Unruh, V. Gonzalez-Villasana, L. Huang, B. Zand, M. Moreno-Smith, L.S. Mangala, M. Taylor, H.J. Dalton, V. Sehgal, Y. Wen, Y. Kang, K.A. Baggerly, J.S. Lee, P.T. Ram, M.K. Ravoori, V. Kundra, X. Zhang, R. Ali-Fehmi, A.M. Gonzalez-Angulo, P.P. Massion, G.A. Calin, G. Lopez-Berestein, W. Zhang,

and A.K. Sood, *Tumour angiogenesis regulation by the miR-200 family.* Nat Commun, 2013. **4**: p. 2427.

55. Yu, F., H. Yao, P. Zhu, X. Zhang, Q. Pan, C. Gong, Y. Huang, X. Hu, F. Su, J. Lieberman, and E. Song, *let-7 regulates self renewal and tumorigenicity of breast cancer cells.* Cell, 2007. **131**(6): p. 1109-23.

56. Sung, S.Y., C.H. Liao, H.P. Wu, W.C. Hsiao, I.H. Wu, Jinpu, Yu, S.H. Lin, and C.L. Hsieh, *Loss of let-7 microRNA upregulates IL-6 in bone marrow-derived mesenchymal stem cells triggering a reactive stromal response to prostate cancer.* PLoS One, 2013. **8**(8): p. e71637.

57. Johnson, C.D., A. Esquela-Kerscher, G. Stefani, M. Byrom, K. Kelnar, D. Ovcharenko, M. Wilson, X. Wang, J. Shelton, J. Shingara, L. Chin, D. Brown, and F.J. Slack, *The let-7 microRNA represses cell proliferation pathways in human cells.* Cancer Res, 2007. **67**(16): p. 7713-22.

58. Yang, D., Y. Sun, L. Hu, H. Zheng, P. Ji, C.V. Pecot, Y. Zhao, S. Reynolds, H. Cheng, R. Rupaimoole, D. Cogdell, M. Nykter, R. Broaddus, C. Rodriguez-Aguayo, G. Lopez-Berestein, J. Liu, I. Shmulevich, A.K. Sood, K. Chen, and W. Zhang, *Integrated analyses identify a master microRNA regulatory network for the mesenchymal subtype in serous ovarian cancer.* Cancer Cell, 2013. **23**(2): p. 186-99.

59. Ma, L., J. Teruya-Feldstein, and R.A. Weinberg, *Tumour invasion and metastasis initiated by microRNA-10b in breast cancer.* Nature, 2007. **449**(7163): p. 682-8.

60. Harris, A.L., *Hypoxia--a key regulatory factor in tumour growth.* Nat Rev Cancer, 2002. **2**(1): p. 38-47.

61. Shannon, A.M., D.J. Bouchier-Hayes, C.M. Condron, and D. Toomey, *Tumour hypoxia, chemotherapeutic resistance and hypoxia-related therapies.* Cancer Treat Rev, 2003. **29**(4): p. 297-307.

62. Vaupel, P. and A. Mayer, *Hypoxia in cancer: significance and impact on clinical outcome.* Cancer Metastasis Rev, 2007. **26**(2): p. 225-39.

63. Keith, B. and M.C. Simon, *Hypoxia-inducible factors, stem cells, and cancer.* Cell, 2007. **129**(3): p. 465-72.

64. Ho, J.J., J.L. Metcalf, M.S. Yan, P.J. Turgeon, J.J. Wang, M. Chalsev, T.N. Petruzziello-Pellegrini, A.K. Tsui, J.Z. He, H. Dhamko, H.S. Man, G.B. Robb, B.T. Teh, M. Ohh, and P.A. Marsden, *Functional importance of Dicer protein in the adaptive cellular response to hypoxia.* J Biol Chem, 2012. **287**(34): p. 29003-20.

65. Chen, S., Y. Xue, X. Wu, C. Le, A. Bhutkar, E.L. Bell, F. Zhang, R. Langer, and P.A. Sharp, *Global microRNA depletion suppresses tumor angiogenesis.* Genes Dev, 2014. **28**(10): p. 1054-67.

66. Wu, C., J. So, B.N. Davis-Dusenbery, H.H. Qi, D.B. Bloch, Y. Shi, G. Lagna, and A. Hata, *Hypoxia potentiates microRNA-mediated gene silencing through posttranslational modification of Argonaute2.* Mol Cell Biol, 2011. **31**(23): p. 4760-74.

67. Kalluri, R. and R.A. Weinberg, *The basics of epithelial-mesenchymal transition.* J Clin Invest, 2009. **119**(6): p. 1420-8.

68. Thiery, J.P., *Epithelial-mesenchymal transitions in tumour progression.* Nat Rev Cancer, 2002. **2**(6): p. 442-54.

69. Armaiz-Pena, G.N., J.K. Allen, A. Cruz, R.L. Stone, A.M. Nick, Y.G. Lin, L.Y. Han, L.S. Mangala, G.J. Villares, P. Vivas-Mejia, C. Rodriguez-Aguayo, A.S. Nagaraja, K.M. Gharpure, Z. Wu, R.D. English, K.V. Soman, M.M. Shahzad, M. Zigler, M.T. Deavers, A. Zien, T.G. Soldatos, D.B. Jackson, J.E. Wiktorowicz, M. Torres-Lugo, T. Young, K. De Geest, G.E. Gallick, M. Bar-Eli, G. Lopez-Berestein, S.W. Cole, G.E. Lopez, S.K. Lutgendorf, and A.K. Sood, *Src activation by beta-adrenoreceptors is a key switch for tumour metastasis.* Nat Commun, 2013. **4**: p. 1403.

70. Wu, S.Y., X. Yang, K.M. Gharpure, H. Hatakeyama, M. Egli, M.H. McGuire, A.S. Nagaraja, T.M. Miyake, R. Rupaimoole, C.V. Pecot, M. Taylor, S. Pradeep, M. Sierant, C. Rodriguez-Aguayo, H.J. Choi, R.A. Previs, G.N. Armaiz-Pena, L. Huang, C. Martinez, T. Hassell, C. Ivan, V. Sehgal, R. Singhania, H.D. Han, C. Su, J.H. Kim, H.J. Dalton, C. Kovvali, K. Keyomarsi, N.A. McMillan, W.W. Overwijk, J. Liu, J.S. Lee, K.A. Baggerly, G. Lopez-Berestein, P.T. Ram, B. Nawrot, and A.K. Sood, *2'-OMe-phosphorodithioate-modified siRNAs show increased loading into the RISC complex and enhanced anti-tumour activity.* Nat Commun, 2014. **5**: p. 3459.

71. Landen, C.N., Jr., A. Chavez-Reyes, C. Bucana, R. Schmandt, M.T. Deavers, G. Lopez-Berestein, and A.K. Sood, *Therapeutic EphA2 gene targeting in vivo using neutral liposomal small interfering RNA delivery.* Cancer Res, 2005. **65**(15): p. 6910-8.

72. Winter, S.C., F.M. Buffa, P. Silva, C. Miller, H.R. Valentine, H. Turley, K.A. Shah, G.J. Cox, R.J. Corbridge, J.J. Homer, B. Musgrove, N. Slevin, P. Sloan, P. Price, C.M. West, and A.L. Harris, *Relation of a hypoxia metagene derived from head and neck cancer to prognosis of multiple cancers.* Cancer Res, 2007. **67**(7): p. 3441-9.

73. Kim, S.W., Z. Li, P.S. Moore, A.P. Monaghan, Y. Chang, M. Nichols, and B. John, *A sensitive non-radioactive northern blot method to detect small RNAs.* Nucleic Acids Res, 2010. **38**(7): p. e98.

74. Lu, C., H.D. Han, L.S. Mangala, R. Ali-Fehmi, C.S. Newton, L. Ozbun, G.N. Armaiz-Pena, W. Hu, R.L. Stone, A. Munkarah, M.K. Ravoori, M.M. Shahzad, J.W. Lee, E. Mora, R.R. Langley, A.R. Carroll, K. Matsuo, W.A. Spannuth, R. Schmandt, N.B. Jennings, B.W. Goodman, R.B. Jaffe, A.M. Nick, H.S. Kim, E.O. Guven, Y.H. Chen, L.Y. Li, M.C. Hsu, R.L. Coleman, G.A. Calin, E.B. Denkbas, J.Y. Lim, J.S. Lee, V. Kundra, M.J. Birrer, M.C. Hung, G. Lopez-Berestein, and A.K. Sood, *Regulation of tumor angiogenesis by EZH2.* Cancer Cell, 2010. **18**(2): p. 185-97.

75. Loges, S., M. Mazzone, P. Hohensinner, and P. Carmeliet, *Silencing or fueling metastasis with VEGF inhibitors: antiangiogenesis revisited.* Cancer Cell, 2009. **15**(3): p. 167-70.

76. Wang, B.D., C.L. Kline, D.M. Pastor, T.L. Olson, B. Frank, T. Luu, A.K. Sharma, G. Robertson, M.T. Weirauch, S.R. Patierno, J.M. Stuart, R.B. Irby, and N.H. Lee, *Prostate apoptosis response protein 4 sensitizes human colon*

cancer cells to chemotherapeutic 5-FU through mediation of an NF kappaB and microRNA network. Mol Cancer, 2010. **9**: p. 98.

77. Ren, M., D. Qin, K. Li, J. Qu, L. Wang, Z. Wang, A. Huang, and H. Tang, *Correlation between hepatitis B virus protein and microRNA processor Drosha in cells expressing HBV.* Antiviral Res, 2012. **94**(3): p. 225-31.

78. Gupta, M., R. Zak, T.A. Libermann, and M.P. Gupta, *Tissue-restricted expression of the cardiac alpha-myosin heavy chain gene is controlled by a downstream repressor element containing a palindrome of two ets-binding sites.* Mol Cell Biol, 1998. **18**(12): p. 7243-58.

79. Oikawa, M., M. Abe, H. Kurosawa, W. Hida, K. Shirato, and Y. Sato, *Hypoxia induces transcription factor ETS-1 via the activity of hypoxia-inducible factor-1.* Biochem Biophys Res Commun, 2001. **289**(1): p. 39-43.

80. Yan, S.F., J. Lu, Y.S. Zou, J. Soh-Won, D.M. Cohen, P.M. Buttrick, D.R. Cooper, S.F. Steinberg, N. Mackman, D.J. Pinsky, and D.M. Stern, *Hypoxia-associated induction of early growth response-1 gene expression.* J Biol Chem, 1999. **274**(21): p. 15030-40.

81. Yang, S.H., E. Vickers, A. Brehm, T. Kouzarides, and A.D. Sharrocks, *Temporal recruitment of the mSin3A-histone deacetylase corepressor complex to the ETS domain transcription factor Elk-1.* Mol Cell Biol, 2001. **21**(8): p. 2802-14.

82. Miyamoto-Sato, E., S. Fujimori, M. Ishizaka, N. Hirai, K. Masuoka, R. Saito, Y. Ozawa, K. Hino, T. Washio, M. Tomita, T. Yamashita, T. Oshikubo, H. Akasaka, J. Sugiyama, Y. Matsumoto, and H. Yanagawa, *A comprehensive*

resource of interacting protein regions for refining human transcription factor networks. PLoS One, 2010. **5**(2): p. e9289.

83. Merritt, W.M., C.G. Danes, M.M. Shahzad, Y.G. Lin, A.A. Kamat, L.Y. Han, W.A. Spannuth, A.M. Nick, L.S. Mangala, R.L. Stone, H.S. Kim, D.M. Gershenson, R.B. Jaffe, R.L. Coleman, J. Chandra, and A.K. Sood, *Anti-angiogenic properties of metronomic topotecan in ovarian carcinoma.* Cancer Biol Ther, 2009. **8**(16): p. 1596-603.

84. Calin, G.A., M. Ferracin, A. Cimmino, G. Di Leva, M. Shimizu, S.E. Wojcik, M.V. Iorio, R. Visone, N.I. Sever, M. Fabbri, R. Iuliano, T. Palumbo, F. Pichiorri, C. Roldo, R. Garzon, C. Sevignani, L. Rassenti, H. Alder, S. Volinia, C.G. Liu, T.J. Kipps, M. Negrini, and C.M. Croce, *A MicroRNA signature associated with prognosis and progression in chronic lymphocytic leukemia.* N Engl J Med, 2005. **353**(17): p. 1793-801.

85. Croce, C.M. and G.A. Calin, *miRNAs, cancer, and stem cell division.* Cell, 2005. **122**(1): p. 6-7.

86. Hwang, H.W. and J.T. Mendell, *MicroRNAs in cell proliferation, cell death, and tumorigenesis.* Br J Cancer, 2006. **94**(6): p. 776-80.

87. Porkka, K.P., M.J. Pfeiffer, K.K. Waltering, R.L. Vessella, T.L. Tammela, and T. Visakorpi, *MicroRNA expression profiling in prostate cancer.* Cancer Res, 2007. **67**(13): p. 6130-5.

88. Lu, J., G. Getz, E.A. Miska, E. Alvarez-Saavedra, J. Lamb, D. Peck, A. Sweet-Cordero, B.L. Ebert, R.H. Mak, A.A. Ferrando, J.R. Downing, T. Jacks,

H.R. Horvitz, and T.R. Golub, *MicroRNA expression profiles classify human cancers.* Nature, 2005. **435**(7043): p. 834-8.

89. Kulshreshtha, R., M. Ferracin, S.E. Wojcik, R. Garzon, H. Alder, F.J. Agosto-Perez, R. Davuluri, C.G. Liu, C.M. Croce, M. Negrini, G.A. Calin, and M. Ivan, *A microRNA signature of hypoxia.* Mol Cell Biol, 2007. **27**(5): p. 1859-67.

90. Huang, X., L. Ding, K.L. Bennewith, R.T. Tong, S.M. Welford, K.K. Ang, M. Story, Q.T. Le, and A.J. Giaccia, *Hypoxia-inducible mir-210 regulates normoxic gene expression involved in tumor initiation.* Mol Cell, 2009. **35**(6): p. 856-67.

91. Puissegur, M.P., N.M. Mazure, T. Bertero, L. Pradelli, S. Grosso, K. Robbe-Sermesant, T. Maurin, K. Lebrigand, B. Cardinaud, V. Hofman, S. Fourre, V. Magnone, J.E. Ricci, J. Pouyssegur, P. Gounon, P. Hofman, P. Barbry, and B. Mari, *miR-210 is overexpressed in late stages of lung cancer and mediates mitochondrial alterations associated with modulation of HIF-1 activity.* Cell Death Differ, 2011. **18**(3): p. 465-78.

92. Mutharasan, R.K., V. Nagpal, Y. Ichikawa, and H. Ardehali, *microRNA-210 is upregulated in hypoxic cardiomyocytes through Akt- and p53-dependent pathways and exerts cytoprotective effects.* Am J Physiol Heart Circ Physiol, 2011. **301**(4): p. H1519-30.

93. Qi, J., Y. Qiao, P. Wang, S. Li, W. Zhao, and C. Gao, *microRNA-210 negatively regulates LPS-induced production of proinflammatory cytokines by targeting NF-kappaB1 in murine macrophages.* FEBS Lett, 2012. **586**(8): p. 1201-7.

94. Kopriva, S.E., V.L. Chiasson, B.M. Mitchell, and P. Chatterjee, *TLR3-induced placental miR-210 down-regulates the STAT6/interleukin-4 pathway.* PLoS One, 2013. **8**(7): p. e67760.

95. Wang, H., H. Flach, M. Onizawa, L. Wei, M.T. McManus, and A. Weiss, *Negative regulation of Hif1a expression and TH17 differentiation by the hypoxia-regulated microRNA miR-210.* Nat Immunol, 2014. **15**(4): p. 393-401.

96. Du, R., W. Sun, L. Xia, A. Zhao, Y. Yu, L. Zhao, H. Wang, C. Huang, and S. Sun, *Hypoxia-induced down-regulation of microRNA-34a promotes EMT by targeting the Notch signaling pathway in tubular epithelial cells.* PLoS One, 2012. **7**(2): p. e30771.

97. Liu, C., K. Kelnar, B. Liu, X. Chen, T. Calhoun-Davis, H. Li, L. Patrawala, H. Yan, C. Jeter, S. Honorio, J.F. Wiggins, A.G. Bader, R. Fagin, D. Brown, and D.G. Tang, *The microRNA miR-34a inhibits prostate cancer stem cells and metastasis by directly repressing CD44.* Nat Med, 2011. **17**(2): p. 211-5.

98. Rokavec, M., M.G. Oner, H. Li, R. Jackstadt, L. Jiang, D. Lodygin, M. Kaller, D. Horst, P.K. Ziegler, S. Schwitalla, J. Slotta-Huspenina, F.G. Bader, F.R. Greten, and H. Hermeking, *IL-6R/STAT3/miR-34a feedback loop promotes EMT-mediated colorectal cancer invasion and metastasis.* J Clin Invest, 2014. **124**(4): p. 1853-67.

99. Rane, S., M. He, D. Sayed, H. Vashistha, A. Malhotra, J. Sadoshima, D.E. Vatner, S.F. Vatner, and M. Abdellatif, *Downregulation of miR-199a derepresses hypoxia-inducible factor-1alpha and Sirtuin 1 and recapitulates*

hypoxia preconditioning in cardiac myocytes. Circ Res, 2009. **104**(7): p. 879-86.

100. Fornari, F., M. Milazzo, P. Chieco, M. Negrini, G.A. Calin, G.L. Grazi, D. Pollutri, C.M. Croce, L. Bolondi, and L. Gramantieri, *MiR-199a-3p regulates mTOR and c-Met to influence the doxorubicin sensitivity of human hepatocarcinoma cells.* Cancer Res, 2010. **70**(12): p. 5184-93.

101. el Azzouzi, H., S. Leptidis, E. Dirkx, J. Hoeks, B. van Bree, K. Brand, E.A. McClellan, E. Poels, J.C. Sluimer, M.M. van den Hoogenhof, A.S. Armand, X. Yin, S. Langley, M. Bourajjaj, S. Olieslagers, J. Krishnan, M. Vooijs, H. Kurihara, A. Stubbs, Y.M. Pinto, W. Krek, M. Mayr, P.A. da Costa Martins, P. Schrauwen, and L.J. De Windt, *The hypoxia-inducible microRNA cluster miR-199a approximately 214 targets myocardial PPARdelta and impairs mitochondrial fatty acid oxidation.* Cell Metab, 2013. **18**(3): p. 341-54.

102. Joshi, H.P., I.V. Subramanian, E.K. Schnettler, G. Ghosh, R. Rupaimoole, C. Evans, M. Saluja, Y. Jing, I. Cristina, S. Roy, Y. Zeng, V.H. Shah, A.K. Sood, and S. Ramakrishnan, *Dynamin 2 along with microRNA-199a reciprocally regulate hypoxia-inducible factors and ovarian cancer metastasis.* Proc Natl Acad Sci U S A, 2014. **111**(14): p. 5331-6.

103. Mancuso, M.R., R. Davis, S.M. Norberg, S. O'Brien, B. Sennino, T. Nakahara, V.J. Yao, T. Inai, P. Brooks, B. Freimark, D.R. Shalinsky, D.D. Hu-Lowe, and D.M. McDonald, *Rapid vascular regrowth in tumors after reversal of VEGF inhibition.* J Clin Invest, 2006. **116**(10): p. 2610-21.

104. Yamagishi, N., S. Teshima-Kondo, K. Masuda, K. Nishida, Y. Kuwano, D.T. Dang, L.H. Dang, T. Nikawa, and K. Rokutan, *Chronic inhibition of tumor cell-derived VEGF enhances the malignant phenotype of colorectal cancer cells.* BMC Cancer, 2013. **13**: p. 229.

105. Pecot, C.V., G.A. Calin, R.L. Coleman, G. Lopez-Berestein, and A.K. Sood, *RNA interference in the clinic: challenges and future directions.* Nat Rev Cancer, 2011. **11**(1): p. 59-67.

106. Nishimura, M., E.J. Jung, M.Y. Shah, C. Lu, R. Spizzo, M. Shimizu, H.D. Han, C. Ivan, S. Rossi, X. Zhang, M.S. Nicoloso, S.Y. Wu, M.I. Almeida, J. Bottsford-Miller, C.V. Pecot, B. Zand, K. Matsuo, M.M. Shahzad, N.B. Jennings, C. Rodriguez-Aguayo, G. Lopez-Berestein, A.K. Sood, and G.A. Calin, *Therapeutic synergy between microRNA and siRNA in ovarian cancer treatment.* Cancer Discov, 2013.

107. Cheng, C.J., W.M. Saltzman, and F.J. Slack, *Canonical and non-canonical barriers facing antimiR cancer therapeutics.* Curr Med Chem, 2013. **20**(29): p. 3582-93.

108. Rupaimoole, R., H.D. Han, G. Lopez-Berestein, and A.K. Sood, *MicroRNA therapeutics: principles, expectations, and challenges.* Chin J Cancer, 2011. **30**(6): p. 368-70.

109. Ling, H., M. Fabbri, and G.A. Calin, *MicroRNAs and other non-coding RNAs as targets for anticancer drug development.* Nat Rev Drug Discov, 2013. **12**(11): p. 847-65.

110. Wu, S.Y., G. Lopez-Berestein, G.A. Calin, and A.K. Sood, *RNAi therapies: drugging the undruggable.* Sci Transl Med, 2014. **6**(240): p. 240ps7.

111. Trang, P., J.F. Wiggins, C.L. Daige, C. Cho, M. Omotola, D. Brown, J.B. Weidhaas, A.G. Bader, and F.J. Slack, *Systemic delivery of tumor suppressor microRNA mimics using a neutral lipid emulsion inhibits lung tumors in mice.* Mol Ther, 2011. **19**(6): p. 1116-22.

112. Bader, A.G., *miR-34 - a microRNA replacement therapy is headed to the clinic.* Front Genet, 2012. **3**: p. 120.

113. Nishimura, M., E.J. Jung, M.Y. Shah, C. Lu, R. Spizzo, M. Shimizu, H.D. Han, C. Ivan, S. Rossi, X. Zhang, M.S. Nicoloso, S.Y. Wu, M.I. Almeida, J. Bottsford-Miller, C.V. Pecot, B. Zand, K. Matsuo, M.M. Shahzad, N.B. Jennings, C. Rodriguez-Aguayo, G. Lopez-Berestein, A.K. Sood, and G.A. Calin, *Therapeutic synergy between microRNA and siRNA in ovarian cancer treatment.* Cancer Discov, 2013. **3**(11): p. 1302-15.

Vita

Rajesha Rupaimoole was born in small village called Manila in Karnataka State of India on 05-05-1986. He attended Visvesvaraya Technological University, Belgaum from 2003 to 2007 and received a Bachelor of Engineering in Biotechnology in 2007. Upon completion of bachelor degree, he moved to the United States of America and pursued Master of Science degree in Biotechnology in the Department of Biology at University of Texas at San Antonio (UTSA). After successful completion of MS degree in Biotechnology in the summer of 2009, Rajesha joined the PhD program in Cancer Biology at The Graduate school of Biomedical Sciences, a joint venture of University of Texas Health Science Center at Houston and University of Texas MD Anderson Cancer Research Center. He joined the laboratory of Dr. Anil Sood and is currently studying the role of hypoxia in miRNA alterations in cancer and biological consequences.